e-Zine for meteor observers meteornews.net

MeteorNews

ISSN 2570-4745 VOL 8 / ISSUE 4 / JULY 2023

2023 April 22, 17h00m-18h00m UT – 4 Lyrids and 3 Sporadics with a Pentax KP camera and 8.5 mm lens, without guiding (Courtesy: Mikhail Maslov).

- New meteor shower
- Crew-5 trunk reentry
- GMN results
- Photographic Lyrids
- CAMS reports
- Radio meteor work

Contents

© eMeteorNews

Major meteor showers based on Global Meteor Network data

Masahiro Koseki

The Nippon Meteor Society, 4-3-5 Annaka Annaka-shi, Gunma-ken, 379-0116 Japan
geh04301@nifty.ne.jp

We confirm the validity of video observations to get the magnitude ratio of meteor showers by calculating the ratio of shower meteors to sporadic meteors. The magnitude ratios obtained from the Global Meteor Network are a little bit higher than those of SonotaCo net. The difference in cameras and in photometry may explain the difference, but the sequences of the magnitude ratios are well matched in each group. The research on the property of a meteor shower should be done carefully by a reclassification of meteors.

1 Introduction

We studied 14 major meteor showers (Koseki, 2023) using SonotaCo net data[1] (SonotaCo, 2009 and SonotaCo et al, 2021). It is very interesting and important to compare them with Global Meteor Network data[2] (Vida et al., 2019; 2020; 2021). We can get similar results of course but recognize interesting differences. It does not seem to be meaningful to repeat the common points. We will focus on the differences, limiting the similarities only to some examples.

2 General view

This study intends to compare the results obtained by the Global Meteor Network data with SonotaCo net. The method of the analysis should be the same and the readers interested in this are requested to refer to previous publication (Koseki, 2023). We showed three types of graphs: the distribution of the relative number of shower meteors to sporadic meteors, the activity graph with the change of the mean magnitude, and the beginning height comparison (Koseki, 2023). The observations of GMN cover a rather short period of 2018–2023 (used data downloaded 2023 February 25) and, therefore, this dataset does not include the enhanced activity of the Orionids. The Southern Taurids (SE component) showed enhanced activity in 2022 while GMN data has been rapidly increasing, so that STA data are biased. There are minor differences due to different conditions like this, but basically, the results are very similar.

Here, we will only compare the GMN results with the previous example (*Figure 1~3*, Quadrantids). *Figure 1* shows the distribution of the relative number of shower meteors to sporadic meteors; at top the result for GMN and at bottom for the SonotaCo net. The slopes of the graphs seem somewhat different, but we see these might change when we select a different range for determining them. *Figure 2* gives the activity graph with the change in the mean magnitude. The activity and the mean magnitude differ a little bit; the causes will be discussed later. *Figure 3* shows the beginning height comparisons; they are very similar, though the Quadrantids by the Global Meteor Network appear concentrated in narrower magnitude range.

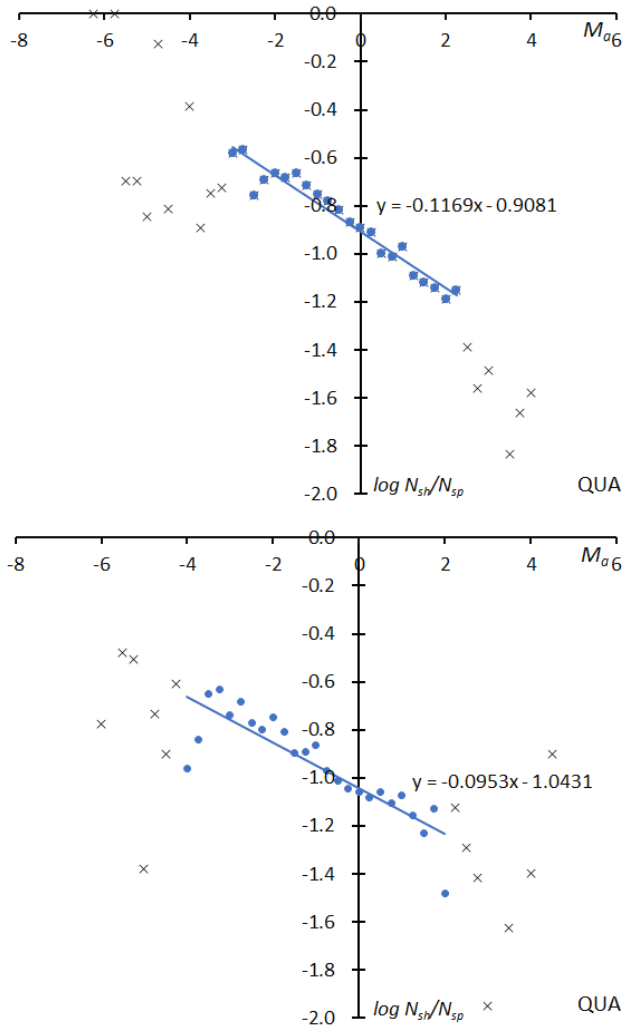

Figure 1 – The distribution of the logarithm of the relative number of Quadrantid meteors to sporadic meteors. GMN (top), SonotaCo net (bottom).

[1] SonotaCo Network Simultaneously Observed Meteor Data Sets SNM20xxx, https://sonotaco.jp/doc/SNM/Catalog

[2] Global Meteor Network. https://globalmeteornetwork.org/

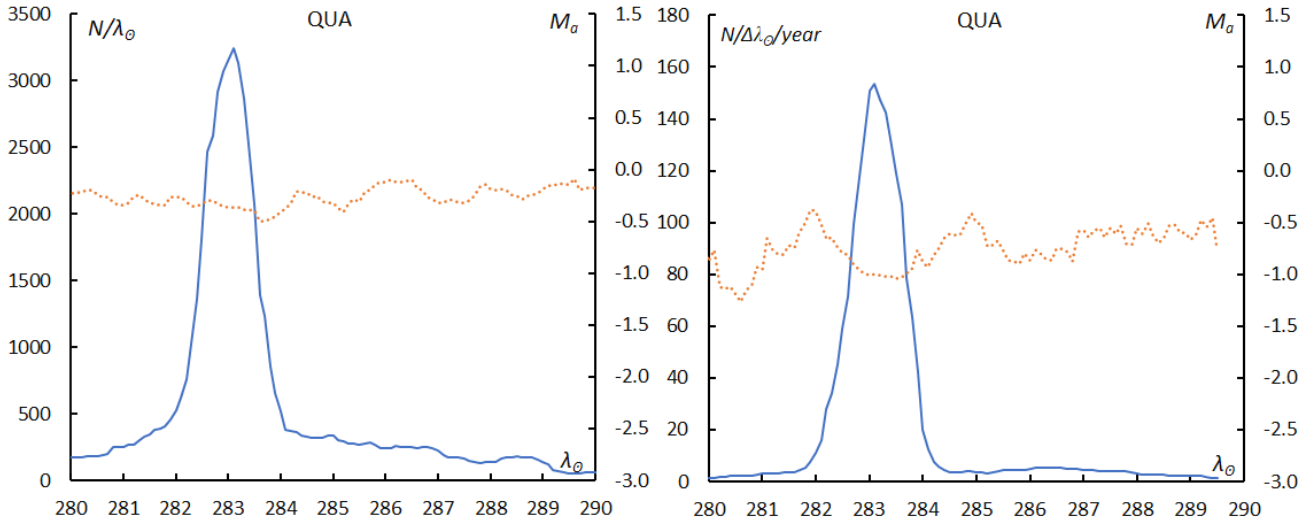

Figure 2 – The sliding mean of the number of Quadrantids (solid blue line) and of the absolute magnitude (dotted orange line) using a 1 solar longitude bin. left: GMN and right: SonotaCo net; the number is divided by the number of years of observations.

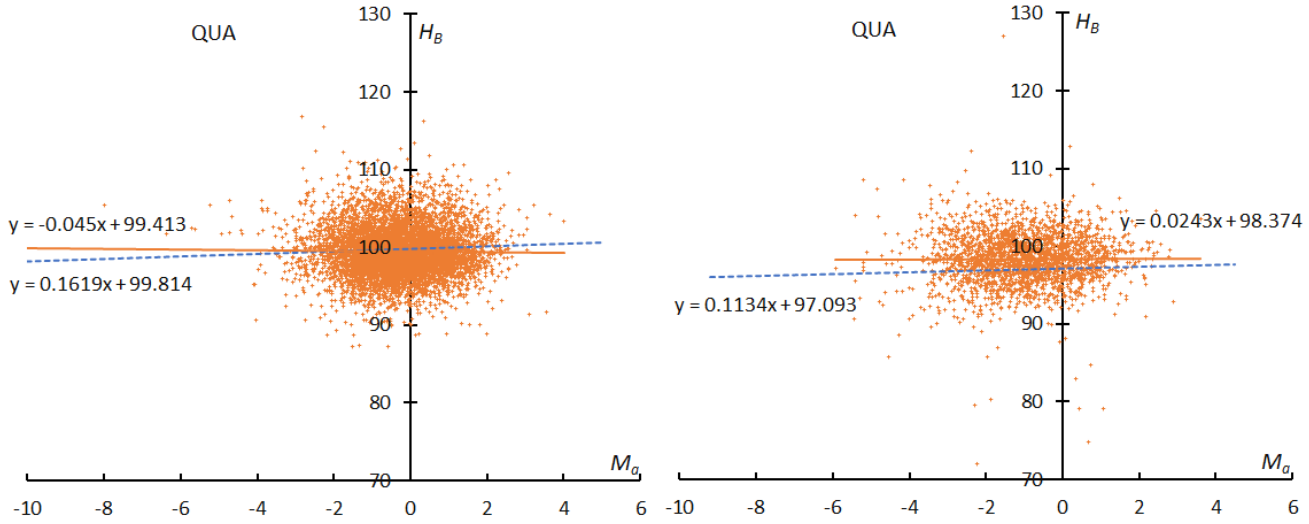

Figure 3 – The result of the linear regression for sporadic meteors is shown as a dashed line, that of the Quadrantids as a solid line. At left: GMN, right: SonotaCo net.

Table 1 – Comparison of the magnitude ratio obtained by this study with SonotaCo net results. Slope and *r*-values are shown each upper row for GMN and lower SonotaCo net, and the bottom is the magnitude ratio from the meteor calendar 2023 of IMO (Rendtel, 2022).

Shower	QUA	LYR	ETA	SDA	CAP	PER	ORI	_SE	_SF	NTA	LEO	HYD	GEM	COM
slope	-0.117	-0.149	0.084	-0.112	-0.159	-0.216	-0.03	0.074	-0.245	-0.055	-0.151	-0.094	-0.226	-0.175
	-0.095	-0.161	-0.007	-0.076	-0.161	-0.196	-0.036	0.076	-0.146	-0.063	-0.167	-0.06	-0.1	-0.083
r	3.09	2.98	5.69	3.12	2.53	2.73	4.36	4.48	2.15	3.32	3.38	3.63	2.32	3.08
	2.81	2.51	4	2.93	2.17	2.49	3.75	3.89	2.33	2.81	2.84	3.42	2.68	3.31
IMO	2.1	2.1	2.4	2.5	2.5	2.2	2.5	2.3		2.3	2.5	3	2.6	3

In the following sections, we will discuss some small but interesting differences.

3 Magnitude ratio

We studied the ratio of shower meteors to sporadic meteors instead of the perception coefficient and showed we could calculate the magnitude ratio using the ratio of shower meteors relative to sporadic ones (Koseki, 2023). It is necessary to investigate how the magnitude ratio of sporadic meteors changes with the geocentric velocity. We divided sporadic meteors into 14 groups with 10 km/s bins in geocentric velocity overlapping 5 km/s each, $v_g < 15$, $10 < v_g < 20$, $15 < v_g < 25$, and so on.

Figure 4 shows changes in the slopes of the logarithm distribution in the different magnitude ranges along with the geocentric velocity. We select the slope of the range $M_a = -6 \sim -3$ as we did in the case of SonotaCo net data; there is some question as to whether the range can be fixed, which we will discuss in more detail later. *Table 1* compares the results of this study with the former results of SonotaCo net data. We use the shower classification listed in the GMN database except for Taurids (STA and NTA).

 © eMeteorNews

Southern Taurids should be divided into two components, that is, 'Steady Expression' (_SE) and 'Sharply Fluctuating' (_SF); *Table 1* shows the clear difference between them. We, therefore, classified three components of Taurids by ourselves; We realized then that there was a big problem with the classification of Taurids in GMN, which we will discuss later.

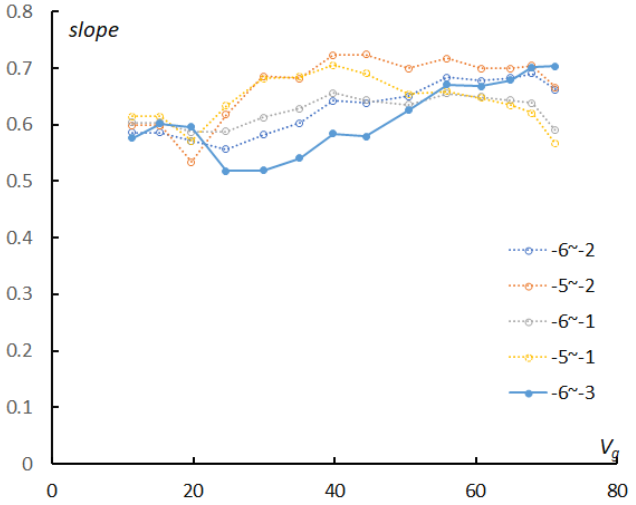

Figure 4 – Changes in the slopes in function of the geocentric velocity. The values of the slopes for the most plausible range $-6 < M_a < -3$ are connected with a bold line.

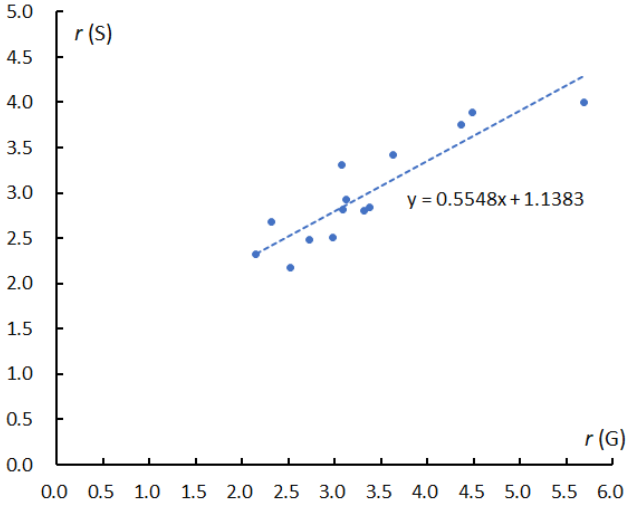

Figure 5 – The relation between the magnitude ratios obtained by GMN and by SonotaCo net (*Table 1*).

The slopes of the logarithm distribution as shown in *Figure 1* for example are listed in *Table 1* upper row for GMN and lower row for SonotaCo, and the same for the estimated magnitude ratios. Though GMN estimates are higher than SonotaCo net's, the magnitude relation of the magnitude ratio of each group is almost the same (*Figure 5*).

The tendency for the GMN results to increase will be discussed in more detail later, but here we give some notes on the differences seen in *Table 1*.

The magnitude ratio and the mean magnitude become lower around the shower maximum. GMN observations used here are shorter periods than those of SonotaCo net and GMN data are rapidly increasing. If GMN observers missed the shower maximum in 2022 the most fruitful year or had the maximum, the magnitude ratio obtained here might be biased not only in the case of STA but also other showers.

3.1. Discrepancy of observational time zone and maximum

Figure 6 shows the numbers of shower meteors in function of the solar longitude separately per year. GMN missed the Quadrantids maximum in 2022 (*Figure 6*, top) and covered the Geminids in 2022 (*Figure 6*, bottom). The magnitude ratio of the Quadrantids (*Table 1*) might be biased by meteors observed in 2022 before and after the maximum. On the contrary the Geminid maximum was covered in 2022 and, therefore, the magnitude ratio of the Geminids (*Table 1*) might be underestimated by meteors which have a lower magnitude ratio at the maximum. This causes the magnitude ratio of Geminids obtained by GMN to be lower than that of SonotaCo net.

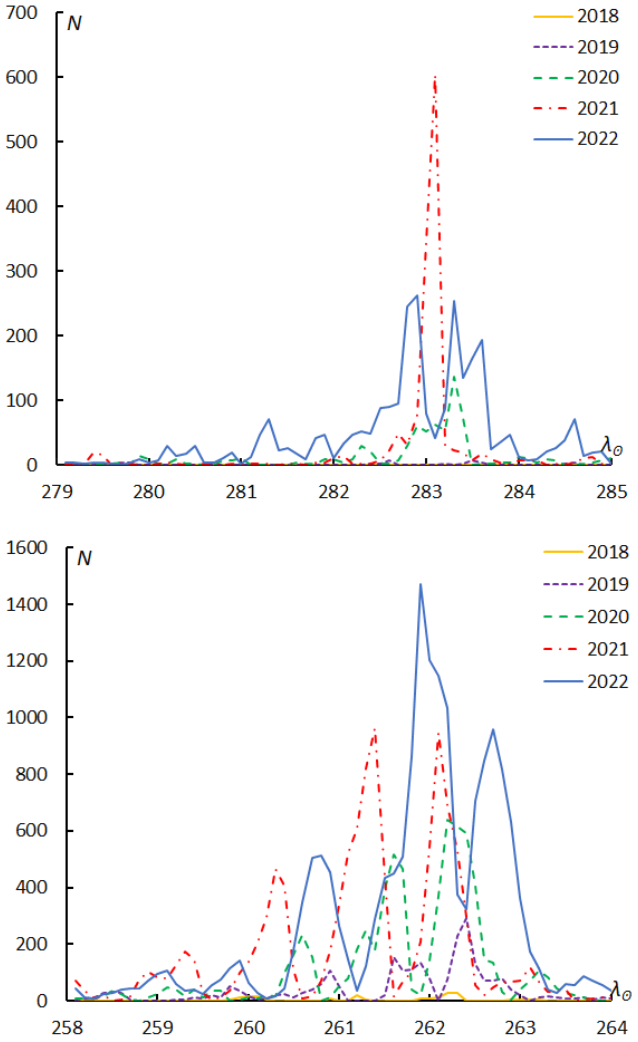

Figure 6 – Changes in the observed shower meteors by year. Quadrantids (top), Geminids (bottom) according to GMN.

The magnitude ratio of STA_SF is also lower than that of SonotaCo net. The reason is similar to the Geminids case because GMN covered the enhanced activity of STA_SF in 2022; *Table 1* lists the magnitude ratio of the regular year of STA_SF for the SonotaCo net and the GMN result is lower than that for the SonotaCo net.

2.2. Shower classification

Figure 7 (top) Quadrantids and (bottom) Geminids are the radiant distribution compensated for their radiant drift: each figure includes the period of each classified shower member recognized. Quadrantids (*Figure 7*, top) are contaminated by DAD and BBO. DAD interferes with one-third of the Quadrantids in the case of SonotaCo net, but SonotaCo net changed their definition of the shower table recently and this overlap has been resolved.

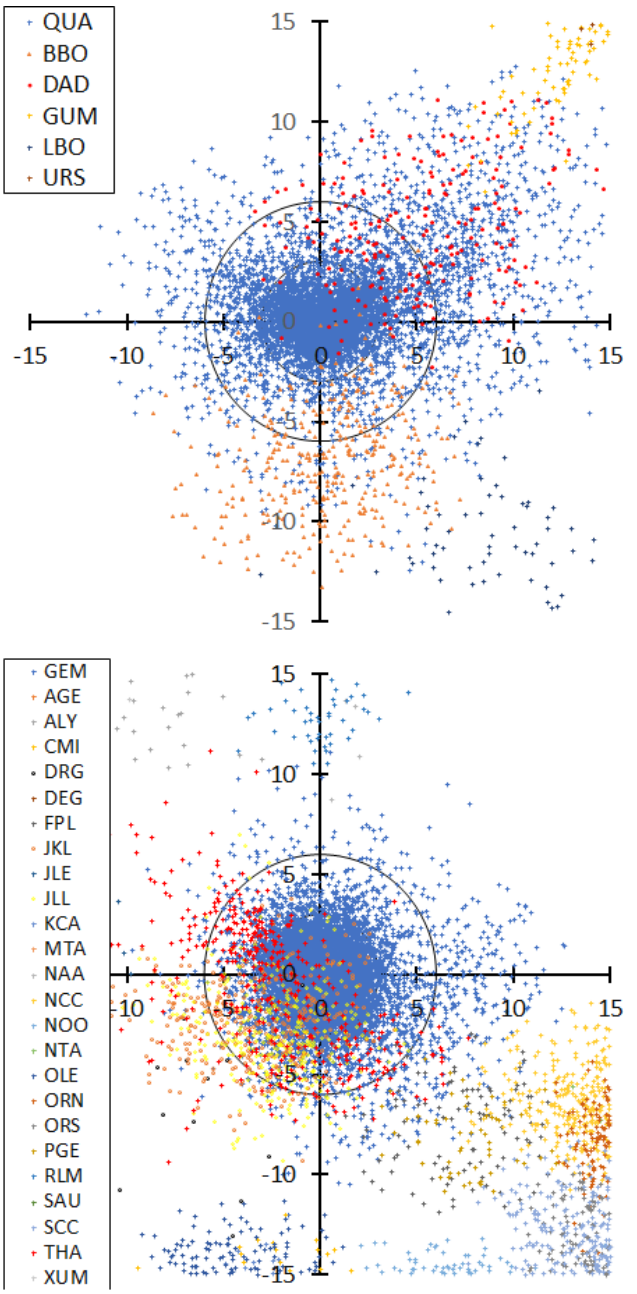

Figure 7 – Radiant distribution centered at the result of the regression analysis for the radiant drift according to GMN. Quadrantids (top), Geminids (bottom). The periods of the figures drawn here are selected between their earliest classified meteor and the last one, that is, $264.69° < \lambda_\odot < 298.41°$ for the Quadrantids and $239.7° < \lambda_\odot < 295.88°$ for the Geminids.

The radiant distribution of the Geminids (*Figure 7*, bottom) is complex; four minor showers overlap it (DRG, JKL, JLL, and THA). We pointed out already that DRG is at the outskirt of the velocity distribution of the Geminids and THA might be the early activity of the Geminids (Koseki, 2018). JKL and JLL seem to be sporadic activities, or the outskirt of the Geminids as seen on the opposite side of the radiant distribution.

We use unique classification for the three Taurid activities; there are confusing situations, and we will return to the shower classification problems later.

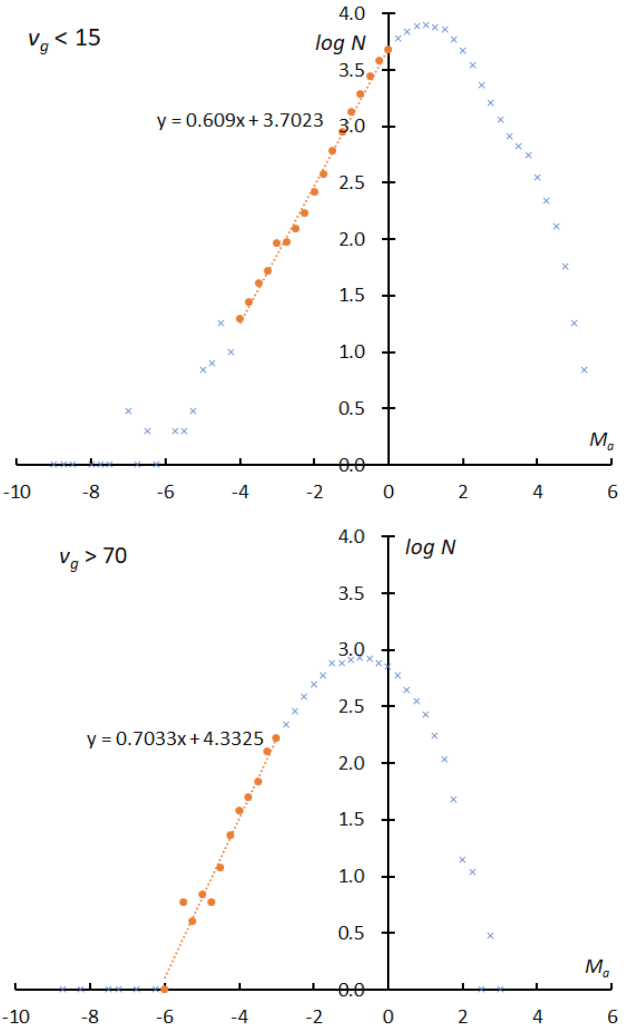

Figure 8 – The logarithm distribution of the number of sporadic meteors against absolute magnitude M_a. $v_g < 15$ km/s (top), $v_g > 70$ km/s (bottom) according to GMN.

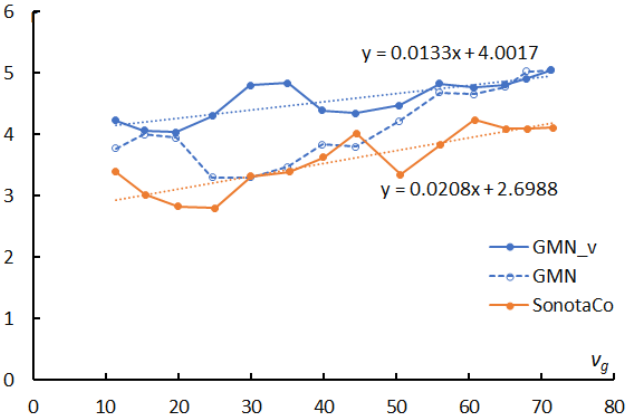

Figure 9 – Changes in the slopes in function of the geocentric velocity. The line 'GMN_v' (blue solid) is obtained by the varied range of magnitude according to the change of perception.

© eMeteorNews

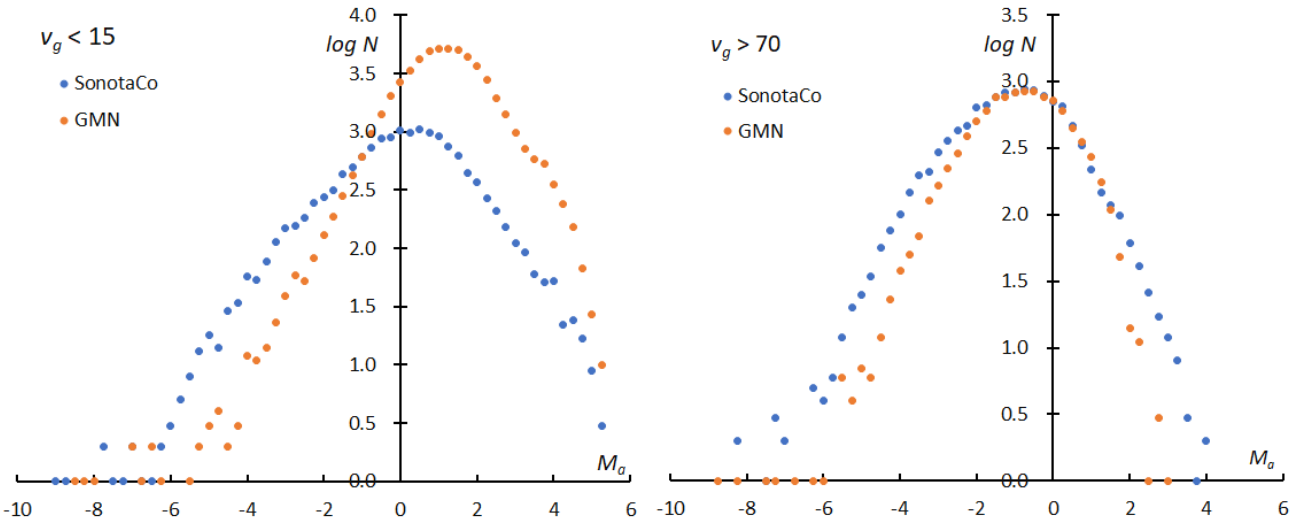

Figure 10 – The logarithm distribution of the number of sporadic meteors against the absolute magnitude M_a; SonotaCo net results (blue filled circle) are added to *Figure 7*. left: v_g < 15 km/s, right: v_g > 70 km/s.

4 Discussions

4.1. Perception with velocity

If observations can catch all meteors, the logarithmic distribution would become a straight line. *Figure 8* clearly shows the perception changes with velocity as the perception in the slower range is higher than in the faster range. Almost all meteors of the –2nd magnitude could be recorded in *Figure 8* (top) but is missing several percentages in *Figure 8* (bottom). We selected the slope of the range as M_a = –6~–3 and calculated the magnitude ratio (*Table 1*). If we changed the range for calculating the sporadic magnitude ratio as shown in *Figure 8* in every velocity range, the results would become higher than the former ratio for M_a = –6~–3 (*Figure 9*).

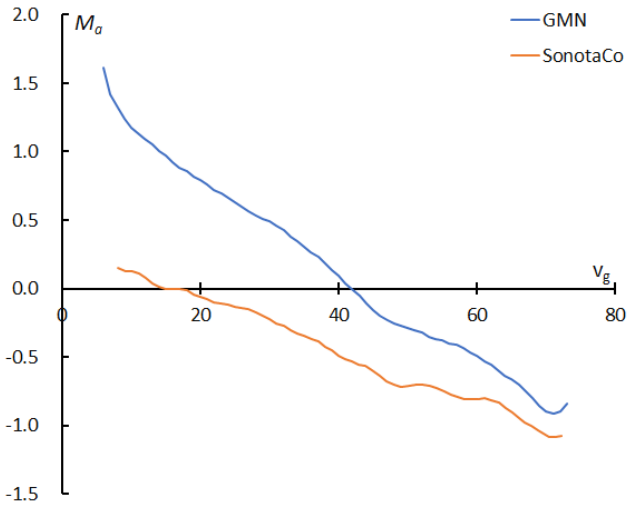

Figure 11 – Moving means of the magnitude of sporadic meteors against velocity (km/s).

It seems too high for the sporadic magnitude ratio which we have known, the ratios are over 4 in all velocity ranges and reach 5 at the highest velocity. *Figure 9* compares with SonotaCo net results also, and this comparison might give clues to answer the question. Both results show the increase of the magnitude ratio with velocity; this may be true because the higher velocity meteors belong to the apex source, the middle range the Toroidal, and the slower the ANT source. But the magnitude ratios themselves are different; GMN results are always higher than those of SonotaCo net.

Figure 10 (left) and (right) compares the magnitude distribution of GMN with the one of SonotaCo net for v_g < 15(km/s) and v_g > 70(km/s) respectively. GMN catches fainter meteors than SonotaCo net especially for slower meteors because they use larger lenses (*Figure 11*). The magnitude ratio of the latter in the range of slower meteors might be biased and seems to be underestimated. On the other hand, the mean magnitude of GMN rapidly decreases because they use longer focus lenses than SonotaCo net; the apparent angular velocity of the meteors on a CCD is higher, and the collected light per pixel decreases.

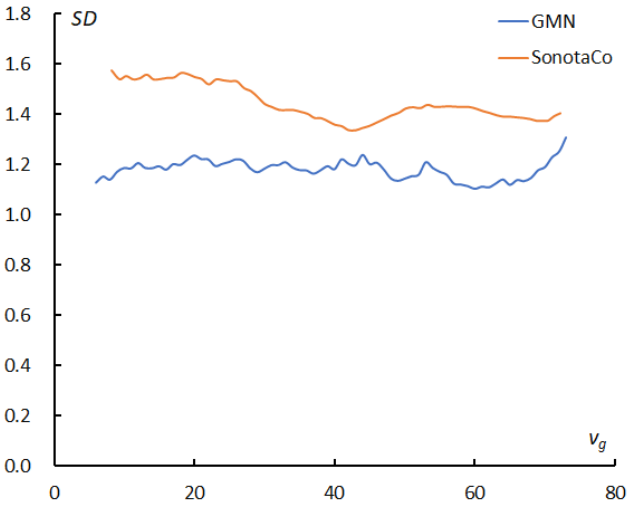

Figure 12 – Moving means of the standard deviation of the magnitude distribution in *Figure 11* against velocity (km/s).

Figure 10 shows one more important suggestion for the question; both magnitude distributions of GMN are narrower than those of SonotaCo net. *Figure 12* gives the standard deviations for the mean magnitude in *Figure 11*.

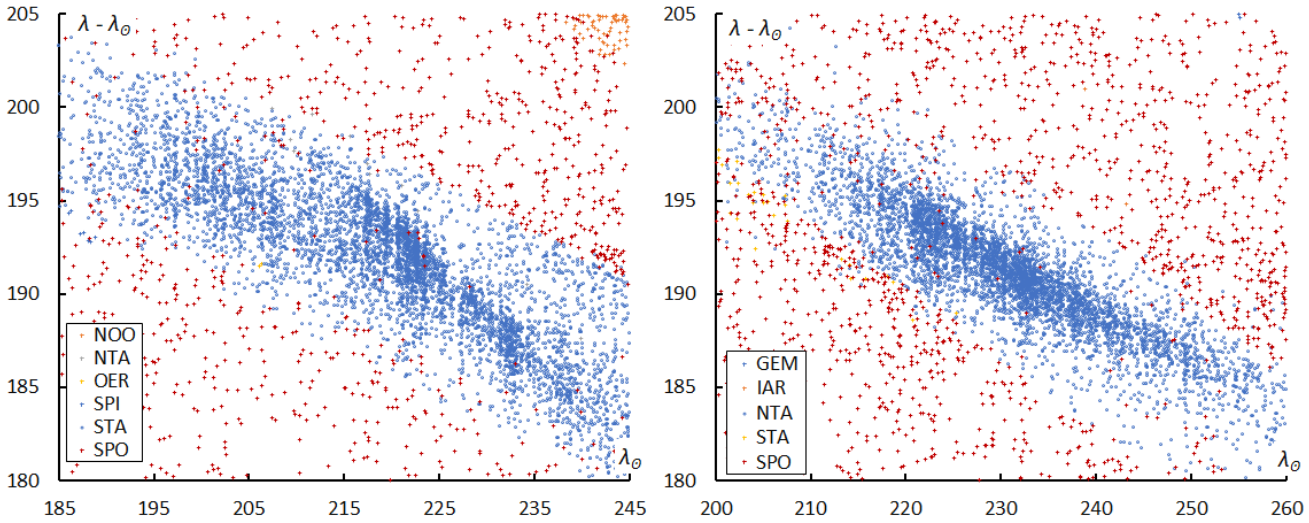

Figure 13 – The distribution of the radiants by SonotaCo net. left: STA, 180° < λ–$\lambda_\odot$ < 205°, −8° < β < −2°, between 185° < $\lambda_\odot$ < 245°, right: NTA, 180° < λ–$\lambda_\odot$ < 205°, 0° < β < +6°, between 200° < $\lambda_\odot$ < 260°.

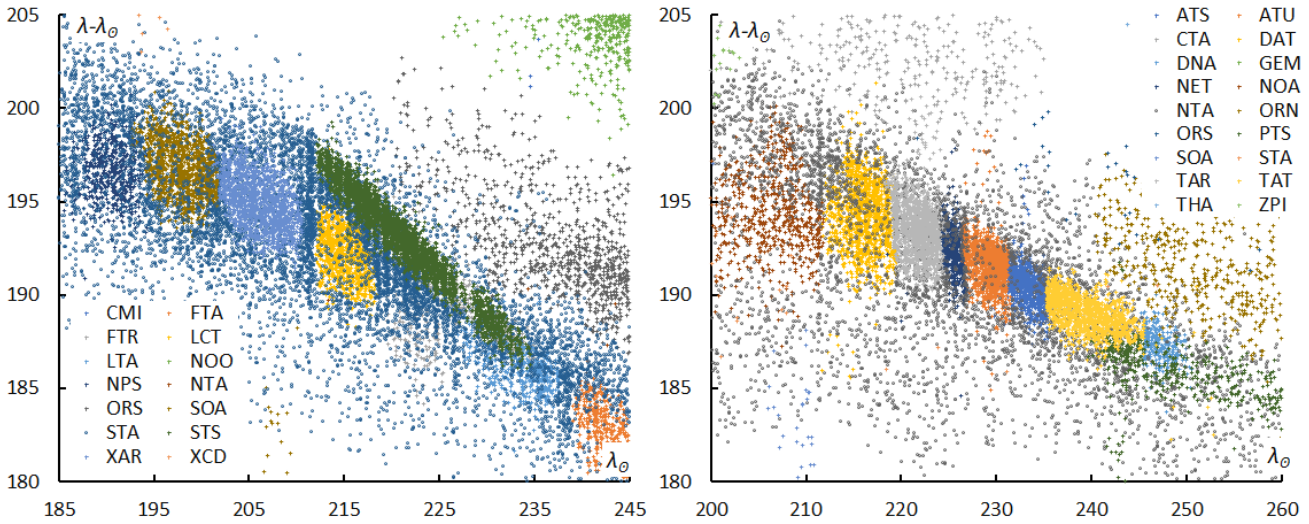

Figure 14 – The distribution of the radiants by the Global Meteor Network. left: STA, 180° < λ–$\lambda_\odot$ < 205°, −8° < β < −2°, between 185° < $\lambda_\odot$ < 245°, right: NTA, 180° < λ–$\lambda_\odot$ < 205°, 0° < β < +6°, between 200° < $\lambda_\odot$ < 260°.

It is clear that the standard deviation, which is the width of the magnitude distribution, of the Global Meteor Network is always narrower than those of SonotaCo net. Therefore, it is suggested that the magnitude difference between the Global Meteor Network and SonotaCo net is apparent because they use different cameras and different photometry. It is difficult to obtain an absolute magnitude ratio by video observations at present, though this is also true for other observation techniques. The magnitude ratios or similar indexes are different for visual, radio, and other observing techniques.

4.2. Shower classification in the case of Taurids

We already mentioned the contamination by sporadic or minor shower meteors within the Quadrantids and Geminids. There are many more important problems with the shower classification for the Taurids. *Figure 13* shows the sun-centered longitude (λ–$\lambda_\odot$) with the longitude of the sun for classified STA (*Figure 13* left) and NTA (*Figure 13*, right) by SonotaCo net. Both STA and NTA are simply expressed as a single broad group. On the contrary, Global Meteor Network divided both STA and NTA into several sub streams (*Figure 14*). It seems that the IAU classification was taken very strictly. We noted that such subdivisions should not apply to complex showers such as the Taurids (Koseki, 2018). These subdivisions were introduced by Jenniskens et al. (2016) but they themselves listed these subdivisions ranked as a lower category. The working status in the IAU shower database (IAUSD) means they are under research and not confirmed. There are questionable entries even in the ‘established status’ in IAUSD (Koseki, 2020). We should be careful to study the properties of a meteor shower, if someone does this the shower identification should be redone.

Figure 15 and *Figure 16* represent the difference in the magnitude distribution before and after the reclassification. *Figure 15 (top)* shows the distribution of STA according to the GMN shower classification and it is curiously curved. *Figure 15* shows the result after being divided into _SE (middle) and _SF (bottom) components and reclassified. The distributions are just as valid as those for SonotaCo net data (Koseki, 2023). *Figure 16* is a similar comparison for NTA; after the reclassification (bottom) the distribution

 © eMeteorNews

becomes similar like the one shown in the previous result (Koseki, 2023).

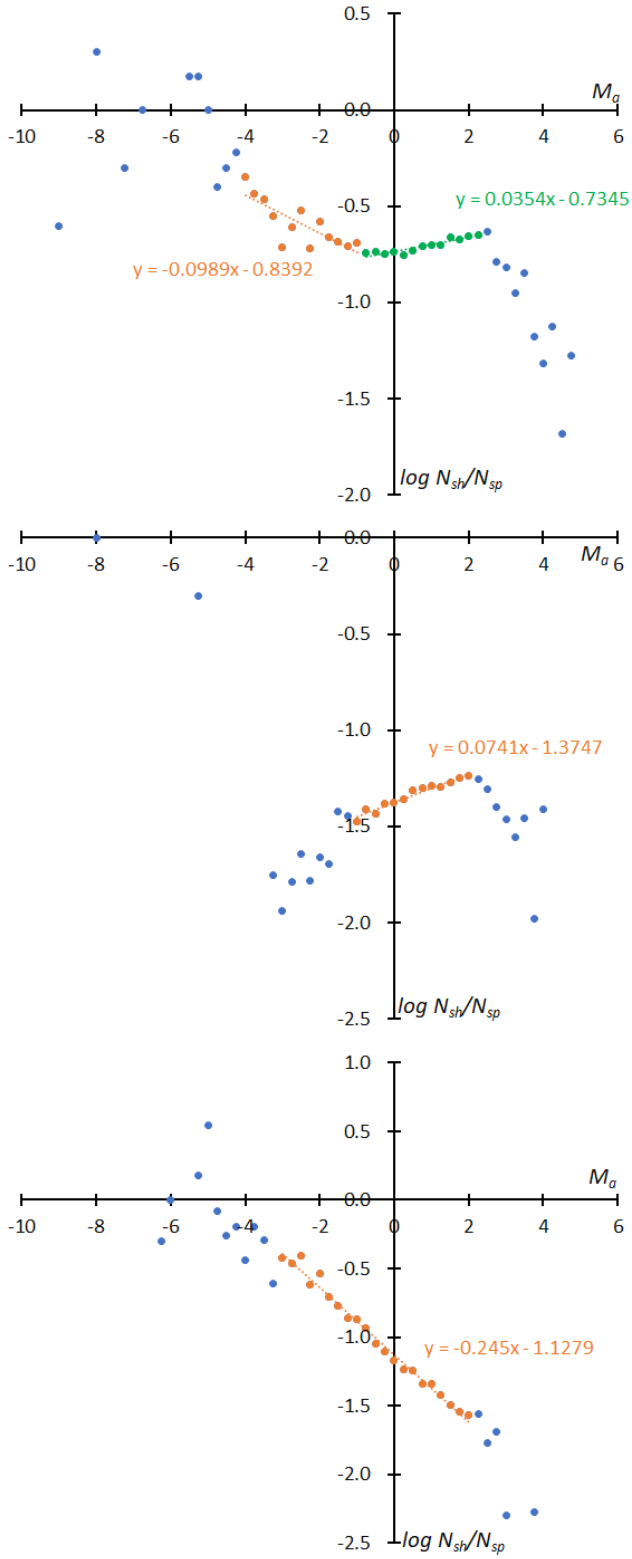

Figure 15 – The distribution of the logarithm of the number of shower meteors relative to sporadic meteors. (Top): GMN originally classified STA meteors, (middle): reclassified results of STA_SE, (bottom): reclassified results of STA_SF.

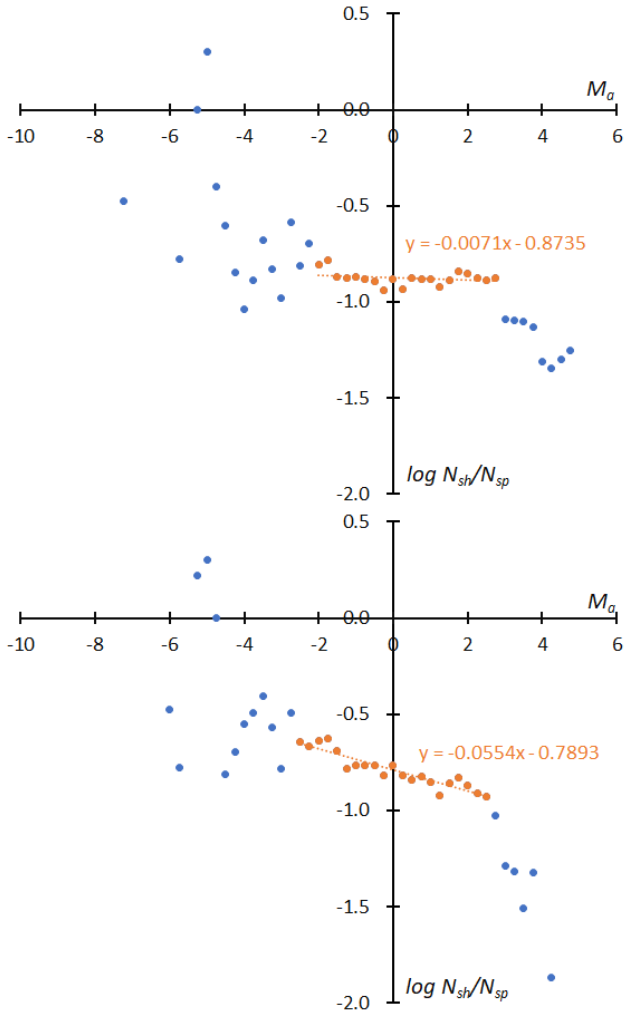

Figure 16 – The distribution of the logarithm of the number of shower meteors relative to sporadic meteors. (Top): GMN originally classified NTA meteors, (bottom): reclassified results of NTA.

5 Properties discussed by shower

The following meteor shower characteristics obtained from Global Meteor Network data can be compared to the corresponding results obtained from SonotaCo data (Koseki, 2023).

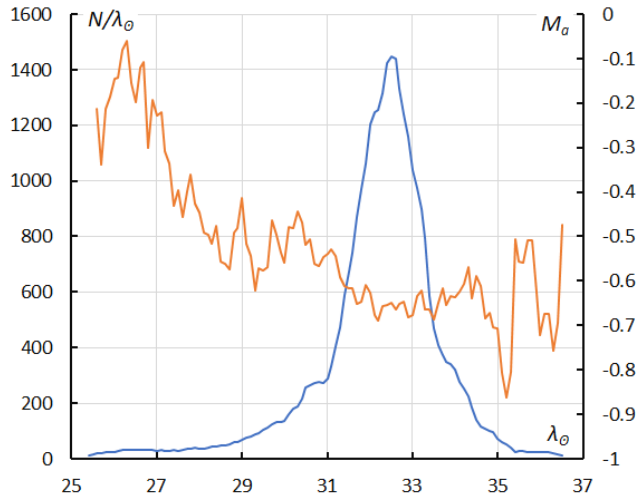

Figure 17 – The sliding mean of the number of Lyrids (solid line, blue) and of the absolute magnitude (solid line, orange) using with 1 solar longitude bin; the number is the total number of orbits collected (see Koseki, 2023, page 156).

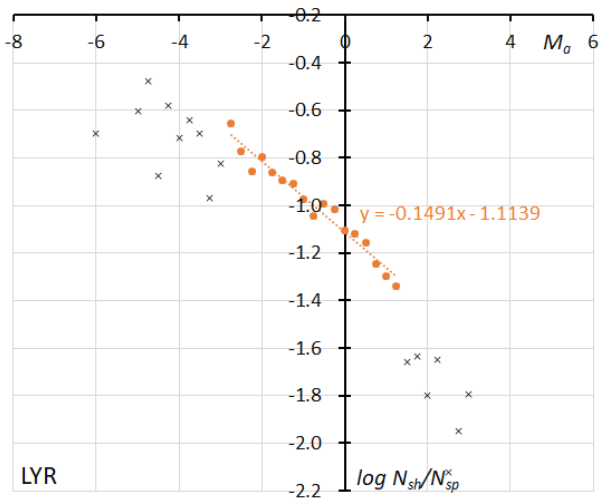

Figure 18 – The dotted line indicates the result of the linear regression analysis for the Lyrids between M_a = –2.75~+1.25, crosses on both sides are excluded from the analysis because of the scarcity of the data (see Koseki, 2023, page 156).

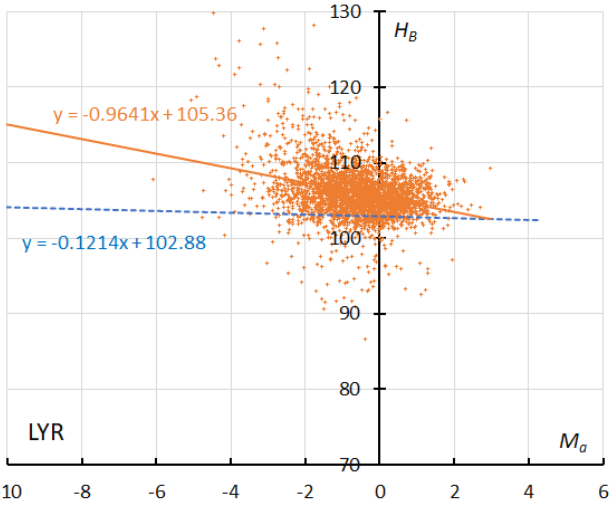

Figure 19 – The result of the linear regression for sporadic meteors is shown as a dashed line, that of the Lyrids as a solid line (see Koseki, 2023, page 156).

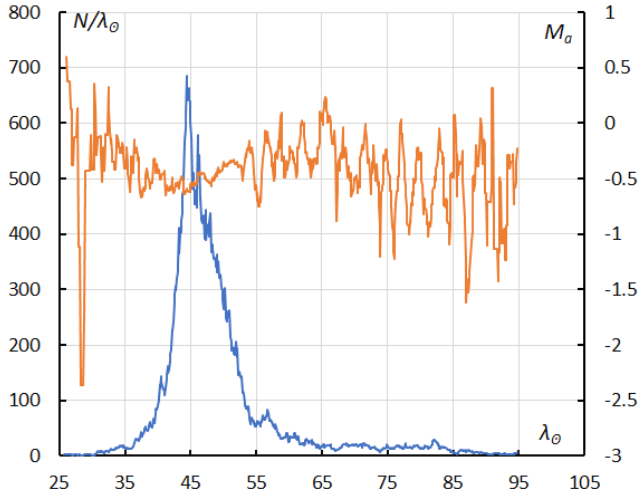

Figure 20 – The sliding mean of the number of eta Aquariids (solid line, blue) and of the absolute magnitude (solid line, orange) using with 1 solar longitude bin; the number is the total number of orbits collected (see Koseki, 2023, page 157).

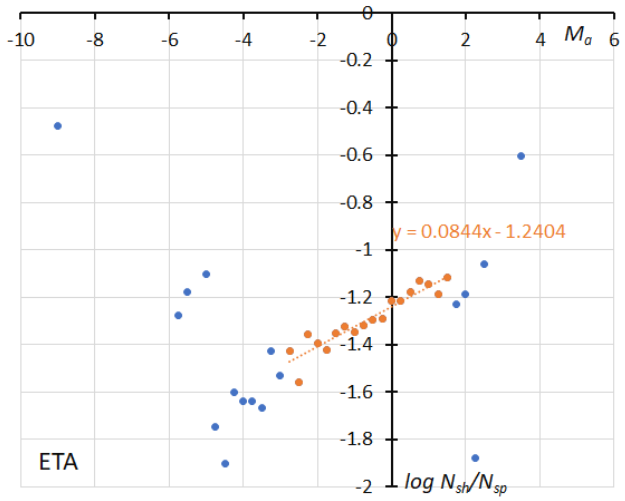

Figure 21 – The dotted line indicates the result of the linear regression analysis for the eta Aquariids between M_a = –2.75~+1.5, dots on both sides are excluded from the analysis because of the scarcity of the data observations (see Koseki, 2023, page 157).

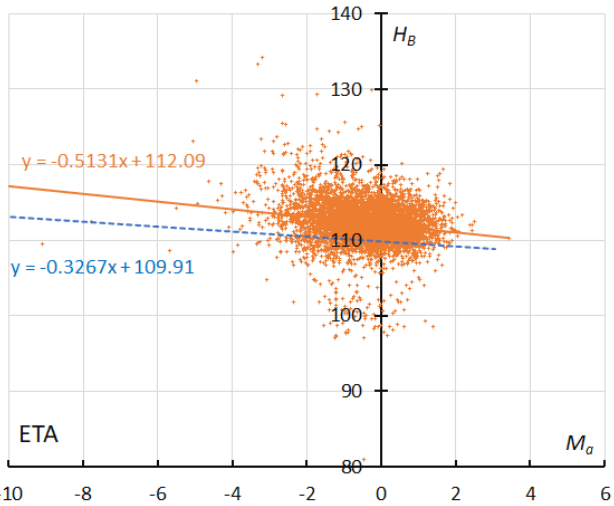

Figure 22 – The result of the linear regression for sporadic meteors is shown as a dashed line, that of the eta Aquariids as a solid line observations (see Koseki, 2023, page 157).

© eMeteorNews

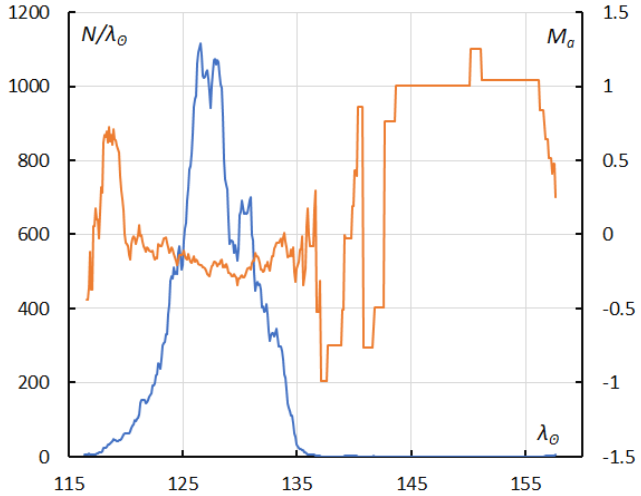

Figure 23 – The sliding mean of the number of Southern delta Aquariids (solid line, blue) and of the absolute magnitude (solid line, orange) using with 1 solar longitude bin; the number is the total number of orbits collected (see Koseki, 2023, page 157).

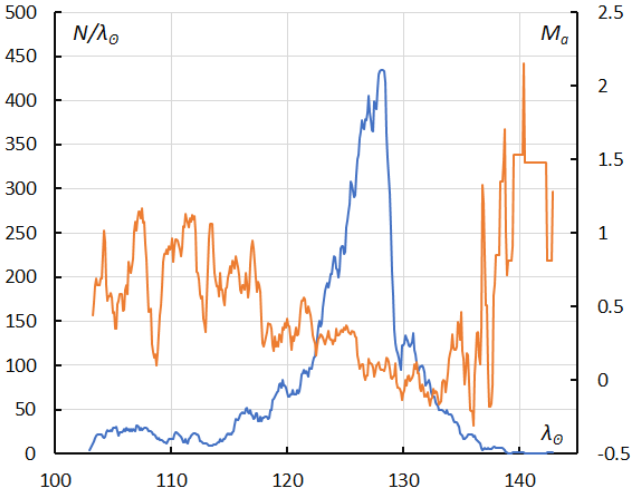

Figure 26 – The sliding mean of the number of Capricornids (solid line, blue) and of the absolute magnitude (solid line, orange) using with 1 solar longitude bin; the number is the total number of orbits collected (see Koseki, 2023, page 158).

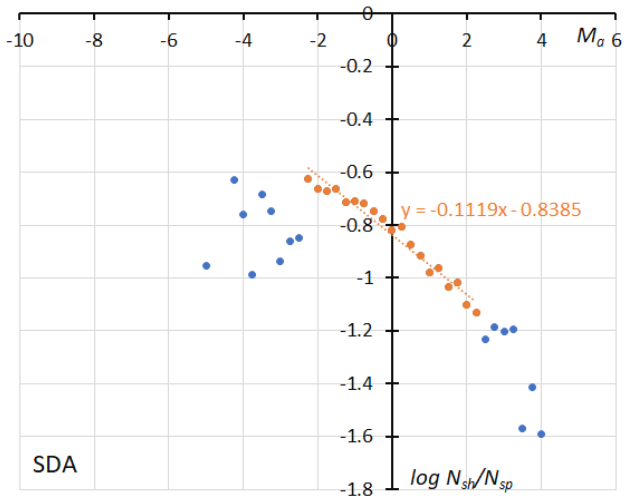

Figure 24 – The dotted line indicates the result of the linear regression analysis for the Southern delta Aquariids between M_a = –2.25~+2.25, dots on both sides are excluded from the analysis because of the scarcity of the data (see Koseki, 2023, page 157).

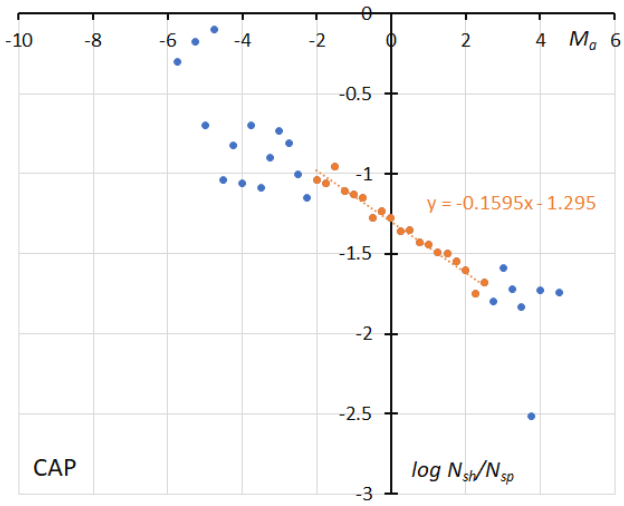

Figure 27 – The dotted line indicates the result of the linear regression analysis for the Capricornids between M_a = –2~+2.5, dots on both sides are excluded from the analysis because of the scarcity of the data (see Koseki, 2023, page 158).

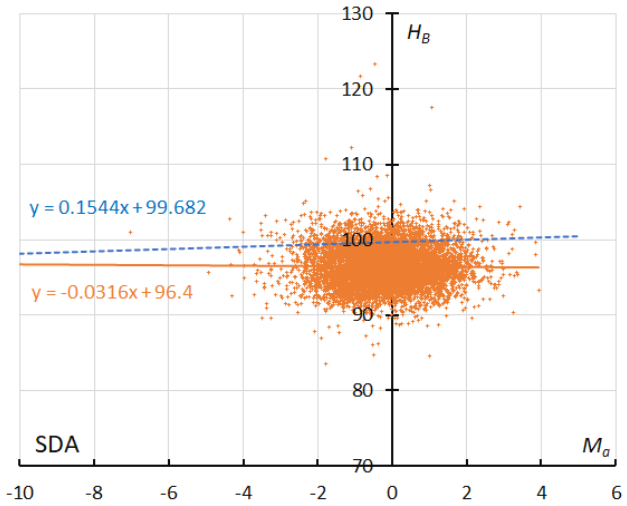

Figure 25 – The result of the linear regression for sporadic meteors is shown as a dashed line, that of the Southern delta Aquariids as a solid line (see Koseki, 2023, page 158).

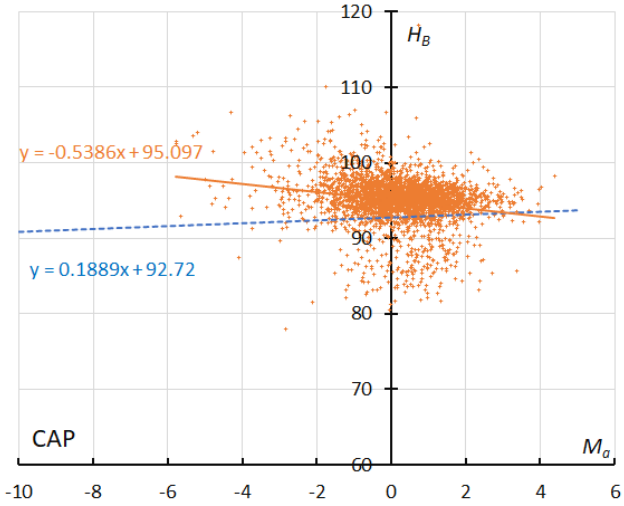

Figure 28 – The result of the linear regression for sporadic meteors is shown as a dashed line, that of the Capricornids as a solid line (see Koseki, 2023, page 158).

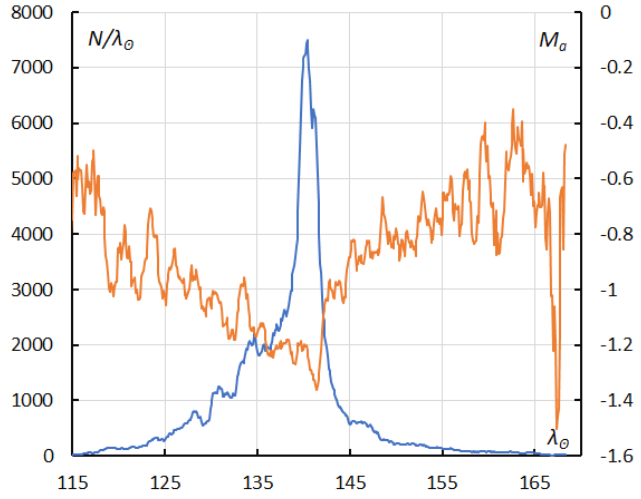

Figure 29 – The sliding mean of the number of Perseids (solid line, blue) and of the absolute magnitude (solid line, orange) using with 1 solar longitude bin; the number is the total number of orbits collected (see Koseki, 2023, page 159).

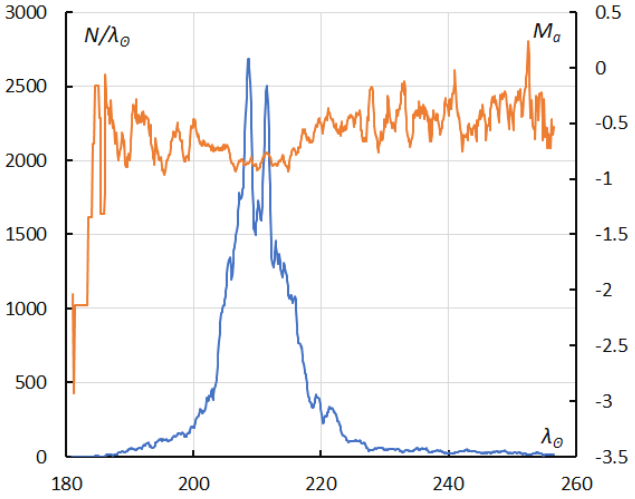

Figure 32 – The sliding mean of the number of Orionids regular activity (solid line, blue) and of the absolute magnitude (solid line, orange) using with 1 solar longitude bin; the number is the total number of orbits collected (see Koseki, 2023, page 159).

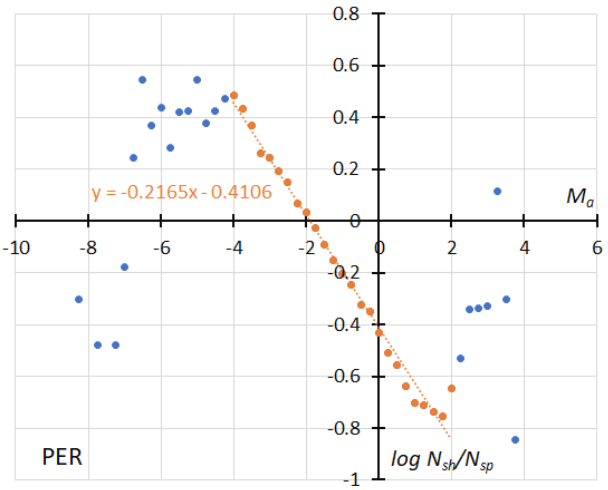

Figure 30 – The dotted line indicates the result of the linear regression analysis for the Perseids between M_a = –4~+2, dots on both sides are excluded from the analysis because of the scarcity of the data (see Koseki, 2023, page 159).

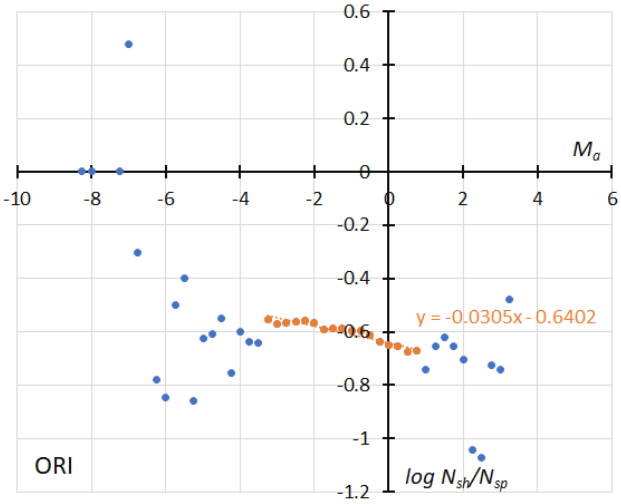

Figure 33 – The dotted line indicates the result of the linear regression analysis for the Orionids during the regular activity, between M_a = –3.25~+0.75, dots on both sides are excluded from the analysis because of the scarcity of the data (see Koseki, 2023, page 160).

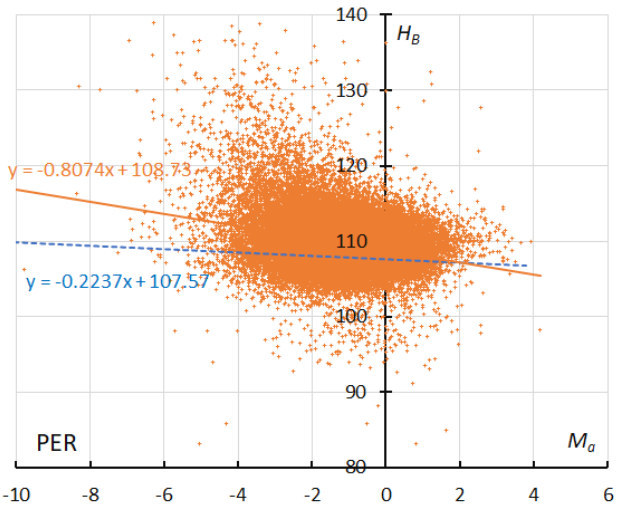

Figure 31 – The result of the linear regression for sporadic meteors is shown as a dashed line, that of the Perseids as a solid line (see Koseki, 2023, page 159).

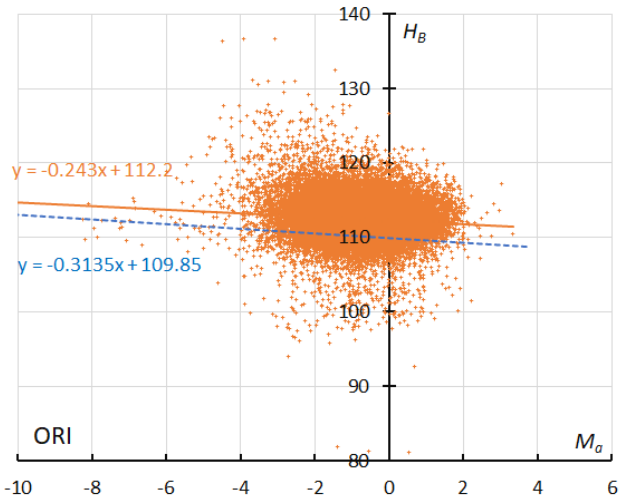

Figure 34 – The result of the linear regression for sporadic meteors is shown as a dashed line, that of the Orionids during regular activity as a solid line (see Koseki, 2023, page 160).

© eMeteorNews

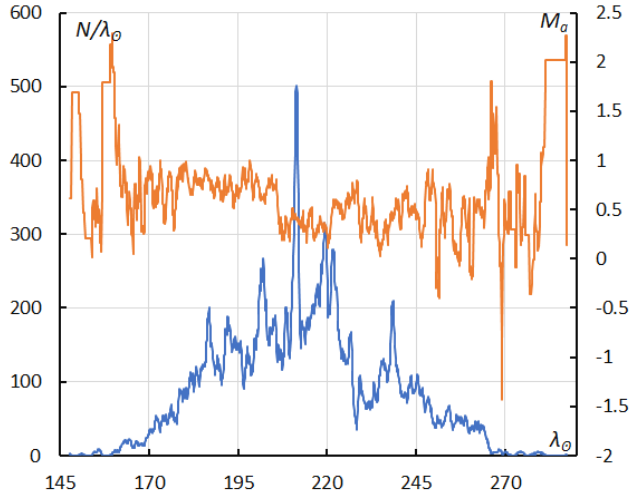

Figure 35 – GMN originally classified STA meteors, sliding mean of the number of Southern Taurids activity (solid line, blue) and of the absolute magnitude (solid line, orange) using with 1 solar longitude bin; the number is the total number of orbits collected.

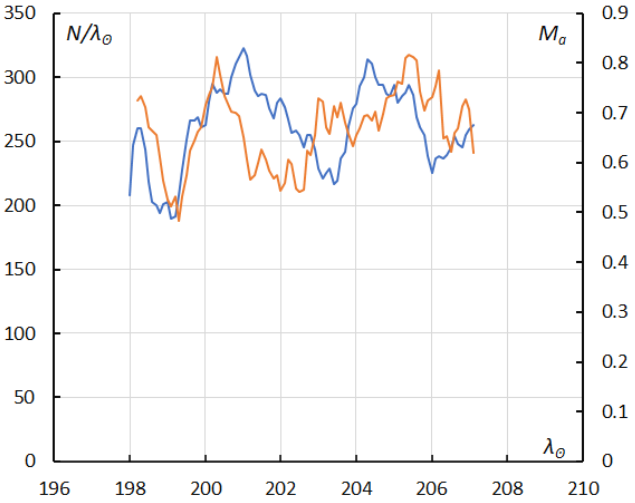

Figure 38 – The sliding mean of the number of Southern Taurids SE activity (solid line, blue) and of the absolute magnitude (solid line, orange) using with 1 solar longitude bin; the number is the total number of orbits collected (see Koseki, 2023, page 160).

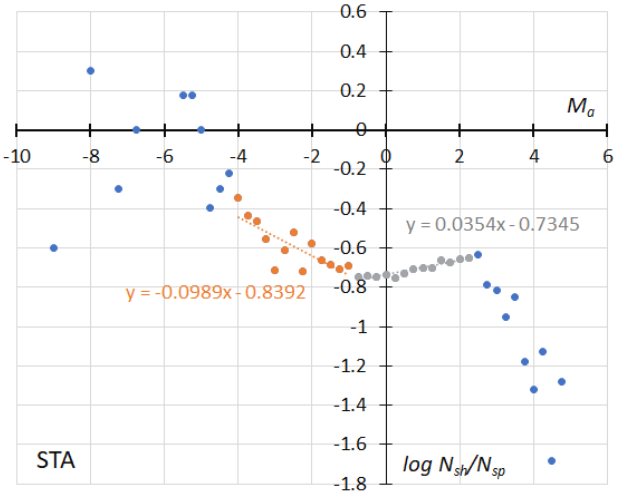

Figure 36 – GMN originally classified STA meteors, the dotted line indicates the result of the linear regression analysis for the Southern Taurids, between M_a = –4~–1 and M_a = –0.75~+2.25, dots on both sides are excluded from the analysis because of the scarcity of the data.

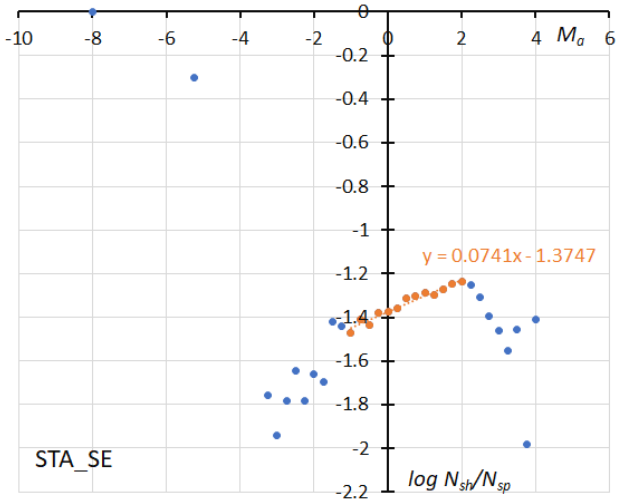

Figure 39 – The solid line indicates the result of the linear regression analysis for the Southern Taurids SE, between M_a = –1~+2, dots on both sides are excluded from the analysis because of the scarcity of the data (see Koseki, 2023, page 160).

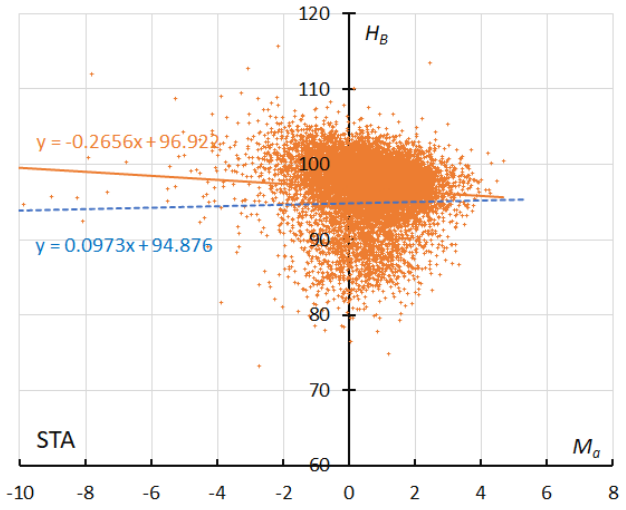

Figure 37 – GMN originally classified STA meteors. The result of the linear regression for sporadic meteors is shown as a dashed line, that of the Southern Taurids as a solid line.

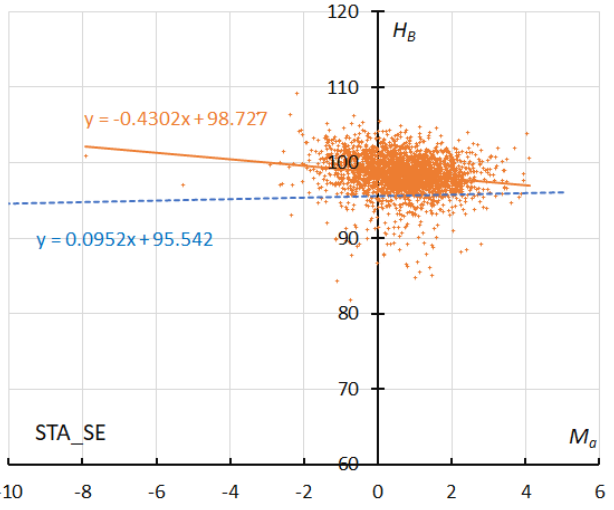

Figure 40 – The result of the linear regression for sporadic meteors is shown as a dashed line, that of the Southern Taurids SE as a solid line (see Koseki, 2023, page 161).

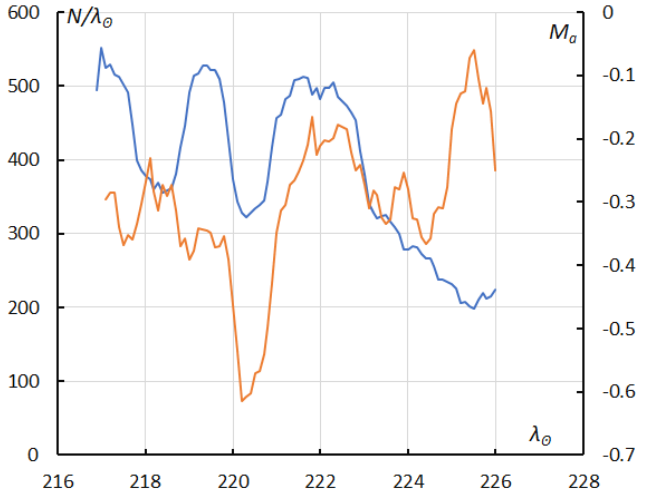

Figure 41 – The sliding mean of the number of Southern Taurids SF regular activity (solid line, blue) and of the absolute magnitude (solid line, orange) using with 1 solar longitude bin; the number is the total number of orbits collected (see Koseki, 2023, page 161).

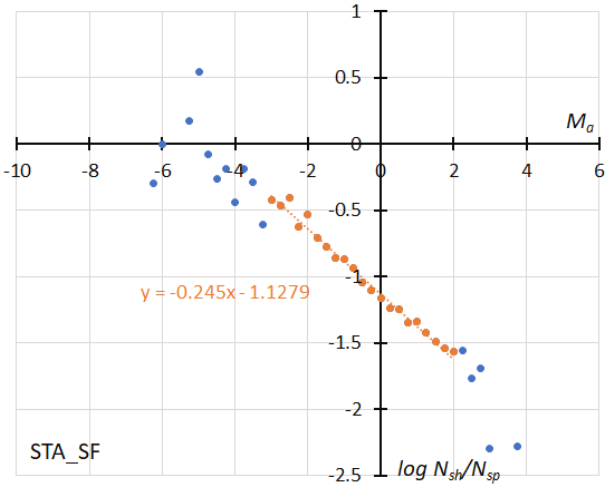

Figure 42 – The dotted line indicates the result of the linear regression analysis for the Southern Taurids SF during the regular activity, between M_a = –3~+2, dots on both sides are excluded from the analysis because of the scarcity of the data (see Koseki, 2023, page 161).

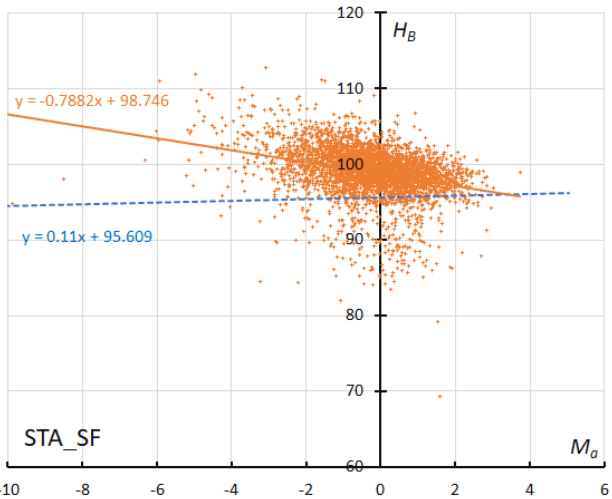

Figure 43 – The result of the linear regression for sporadic meteors is shown as a dashed line, that of the Southern Taurids SF during regular activity as a solid line (see Koseki, 2023, page 162).

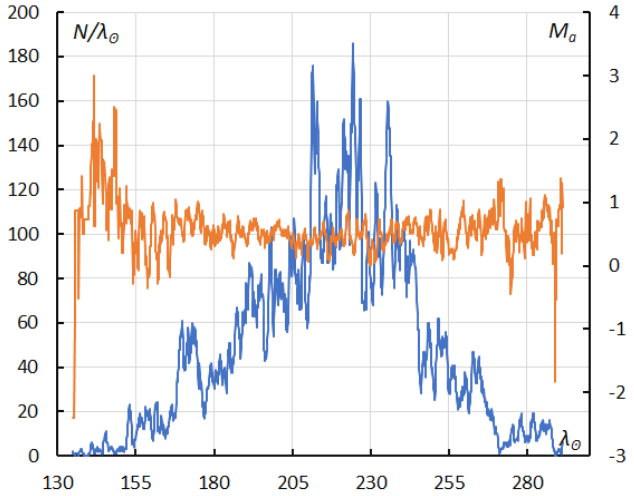

Figure 44 – GMN originally classified NTA meteors. The sliding mean of the number of Northern Taurids (solid line, blue) and of the absolute magnitude (solid line, orange) using with 1 solar longitude bin; the number is the total number of orbits collected (see Koseki, 2023, page 162).

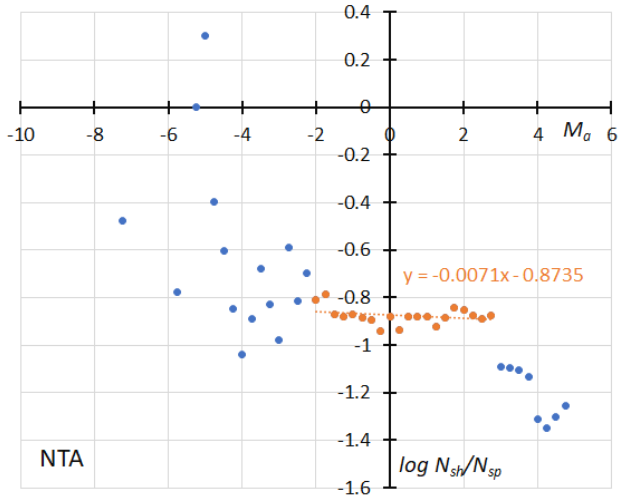

Figure 45 – GMN originally classified NTA meteors. The dotted line indicates the result of the linear regression analysis for the Northern Taurids, between M_a = –2~+2.75, dots on both sides are excluded from the analysis because of the scarcity of the data (see Koseki, 2023, page 162).

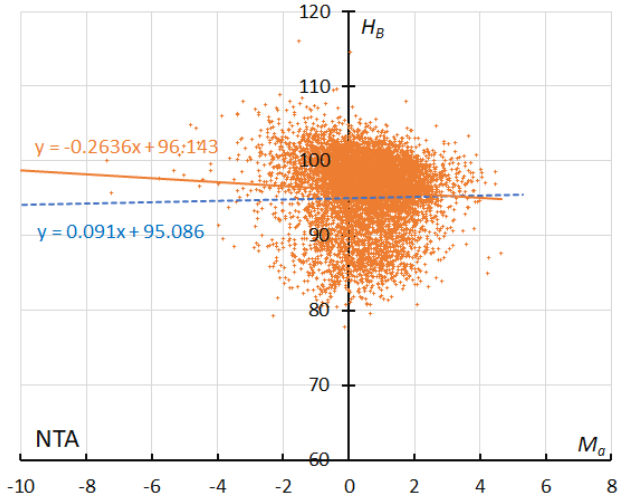

Figure 46 – GMN originally classified NTA meteors. The result of the linear regression for sporadic meteors is shown as a dashed line, that of the Northern Taurids as a solid line (see Koseki, 2023, page 162).

© eMeteorNews

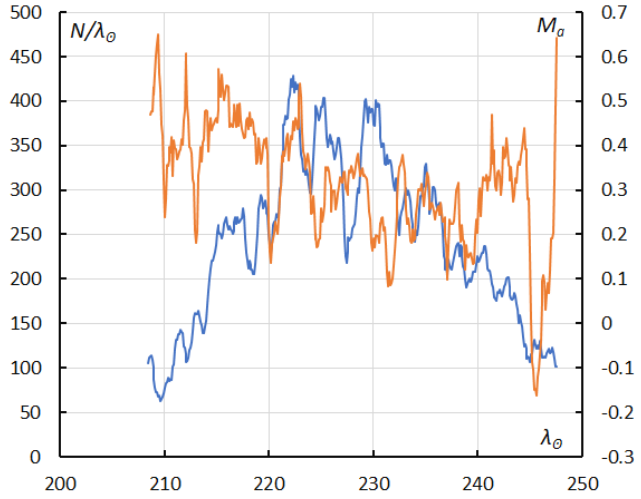

Figure 47 – The sliding mean of the number of the reclassified results of Northern Taurids (solid line, blue) and of the absolute magnitude (solid line, orange) using with 1 solar longitude bin; the number is the total number of orbits collected (see Koseki, 2023, page 162).

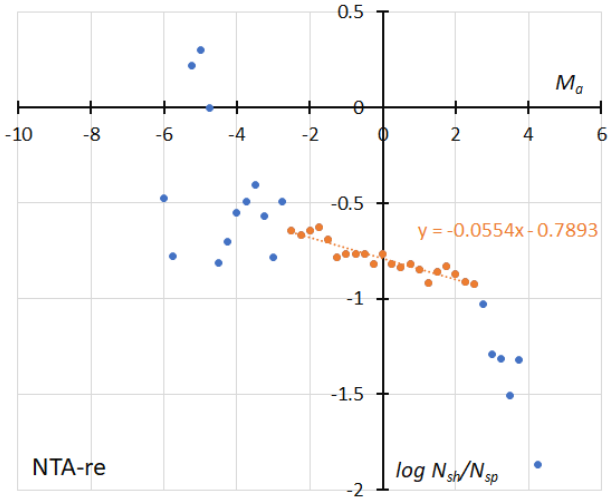

Figure 48 – The dotted line indicates the result of the linear regression analysis for the reclassified results of Northern Taurids, between M_a = –2.5~+2.5, crosses on both sides are excluded from the analysis because of the scarcity of the data (see Koseki, 2023, page 162).

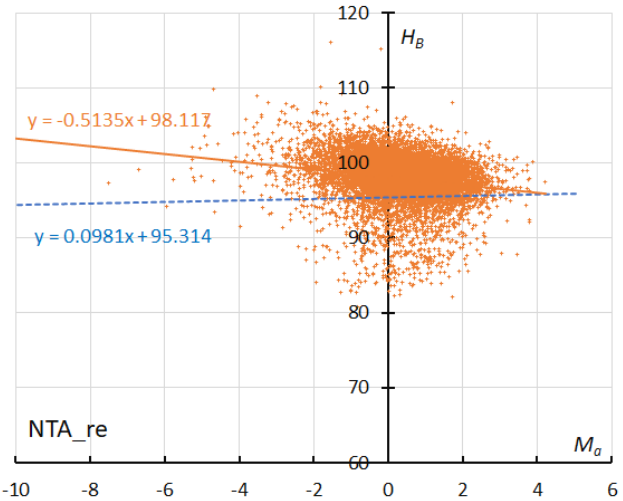

Figure 49 – The result of the linear regression for sporadic meteors is shown as a dashed line, that of the reclassified results of Northern Taurids as a solid line (see Koseki, 2023, page 162).

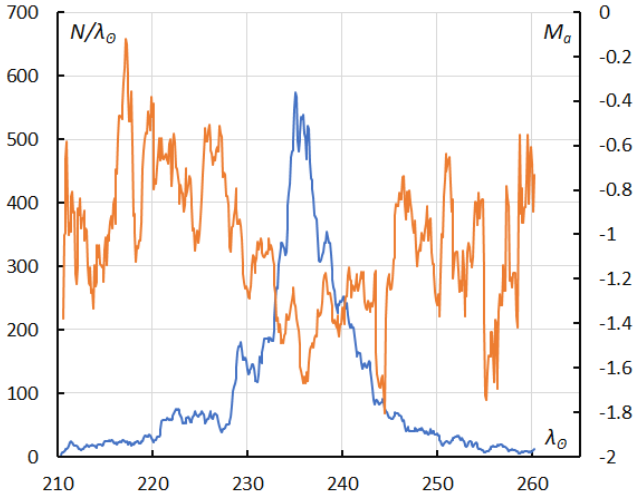

Figure 50 – The sliding mean of the number of Leonids (solid line, blue) and of the absolute magnitude (solid line, orange) using with 1 solar longitude bin; the number is the total number of orbits collected (see Koseki, 2023, page 162).

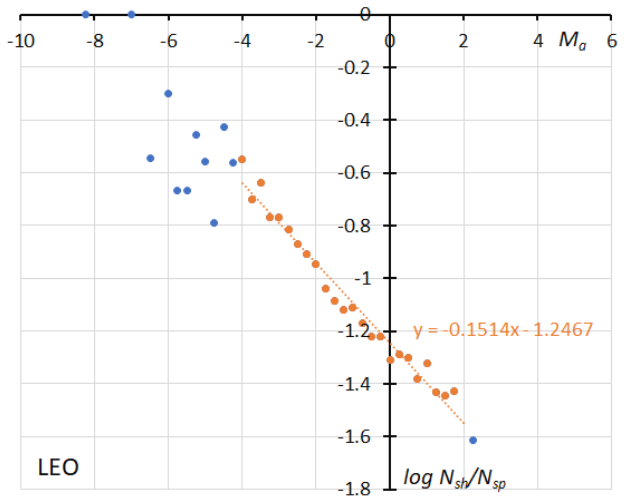

Figure 51 – The dotted line indicates the result of the linear regression analysis for the Leonids, between M_a = –4~+2, crosses on both sides are excluded from the analysis because of the scarcity of the data (see Koseki, 2023, page 163).

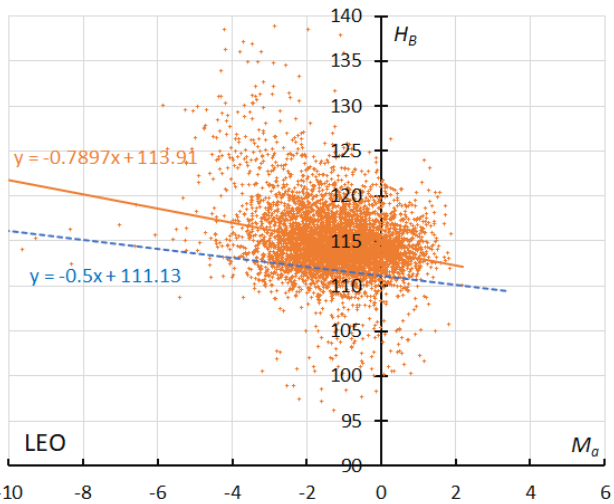

Figure 52 – The result of the linear regression for sporadic meteors is shown as a dashed line, that of Leonids as a solid line (see Koseki, 2023, page 163).

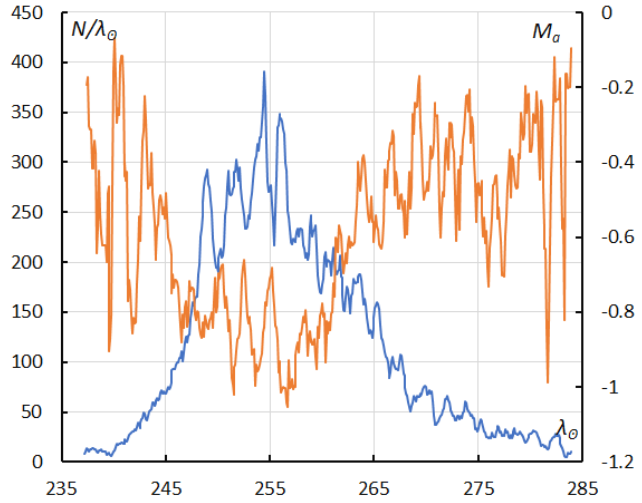

Figure 53 – The sliding mean of the number of sigma Hydrids (solid line, blue) and of the absolute magnitude (solid line, orange) using with 1 solar longitude bin; the number is the total number of orbits collected (see Koseki, 2023, page 163).

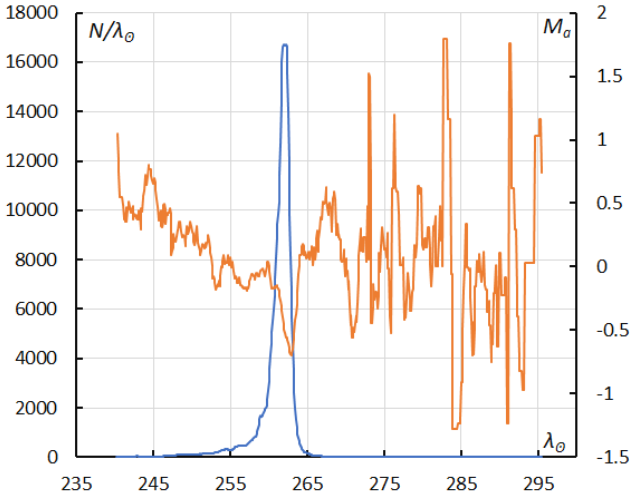

Figure 56 – The sliding mean of the number of Geminids (solid line, blue) and of the absolute magnitude (solid line, orange) using with 1 solar longitude bin; the number is the total number of orbits collected (see Koseki, 2023, page 164).

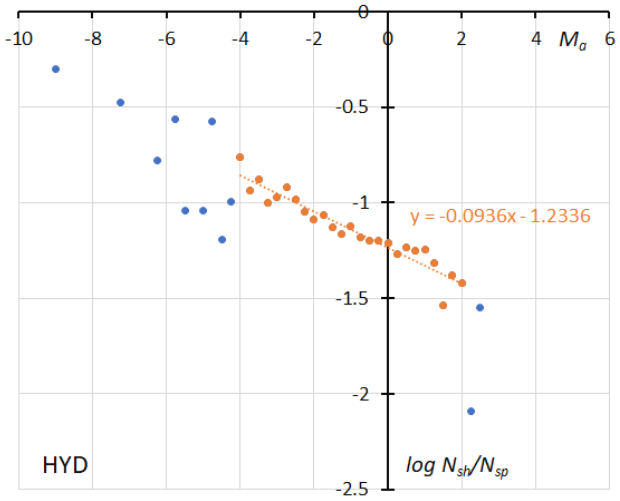

Figure 54 – The dotted line indicates the result of the linear regression analysis for the sigma Hydrids, between M_a = –4~+2, dots on both sides are excluded from the analysis because of the scarcity of the data (see Koseki, 2023, page 163).

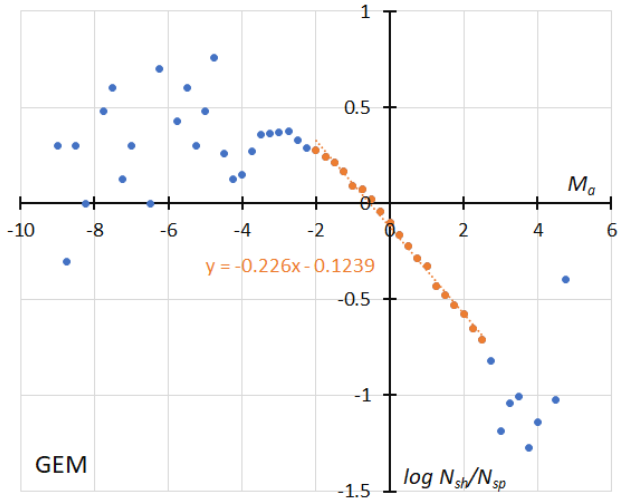

Figure 57 – The dotted line indicates the result of the linear regression analysis for the Geminids, between M_a = –2~+2.5, dotts on both sides are excluded from the analysis because of the scarcity of the data (see Koseki, 2023, page 164).

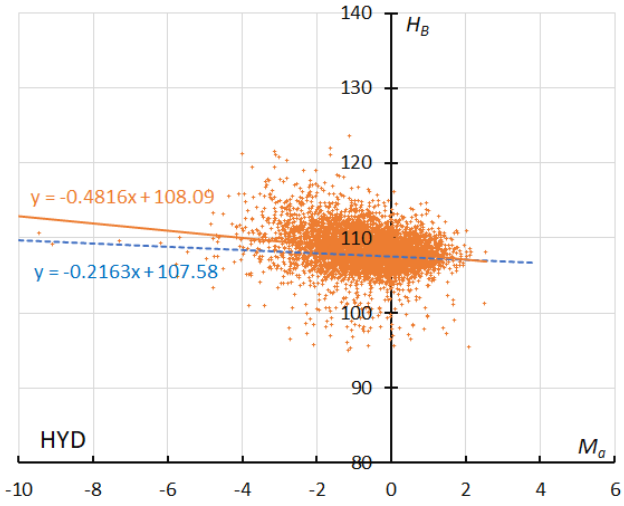

Figure 55 – The result of the linear regression for sporadic meteors is shown as a dashed line, that of the sigma Hydrids as a solid line (see Koseki, 2023, page 163).

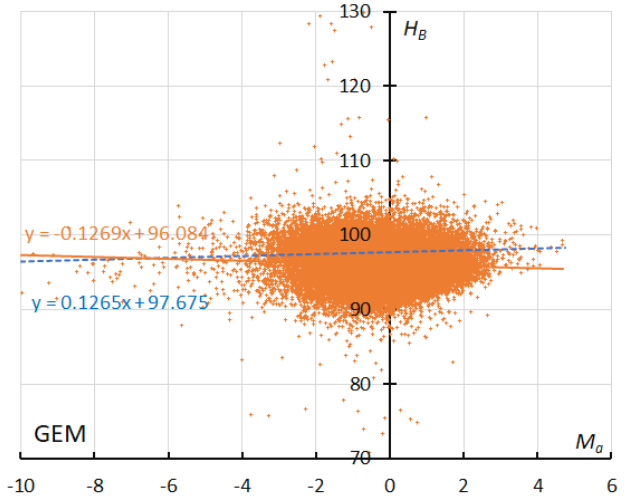

Figure 58 – The result of the linear regression for sporadic meteors is shown as a dashed line, that of the Geminids as a solid line (see Koseki, 2023, page 164).

© eMeteorNews

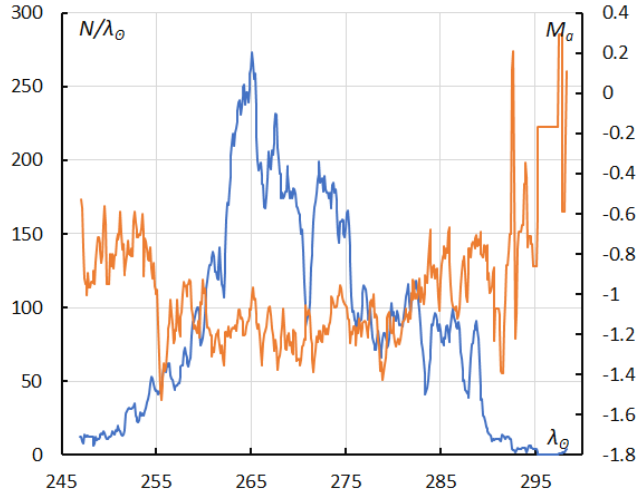

Figure 59 – The sliding mean of the number of Comae Berenicids (solid line, blue) and of the absolute magnitude (solid line, orange) using with 1 solar longitude bin; the number is the total number of orbits collected (see Koseki, 2023, page 164).

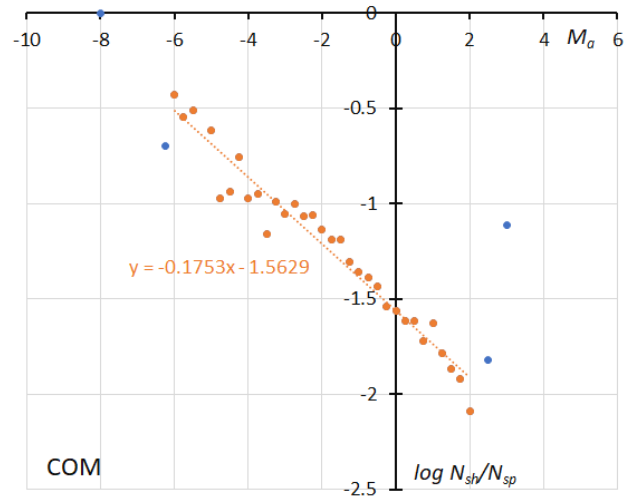

Figure 60 – The dotted line indicates the result of the linear regression analysis for the Comae Berenicids, between M_a = –6~+2, dots on both sides are excluded from the analysis because of the scarcity of the data (see Koseki, 2023, page 164).

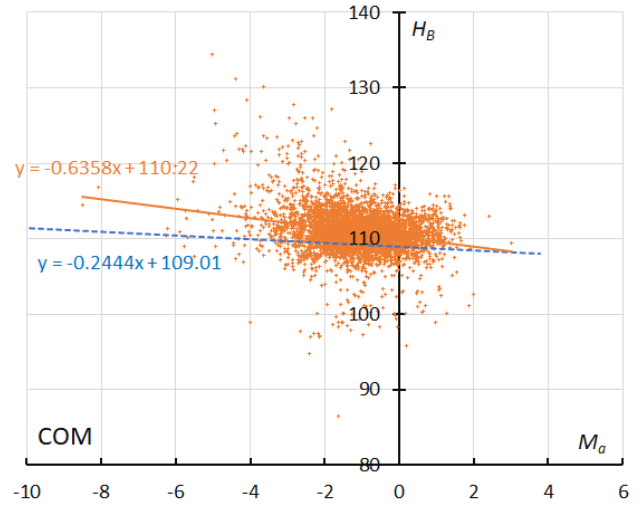

Figure 61 – The result of the linear regression for sporadic meteors is shown as a dashed line, that of the Comae Berenicids as a solid line (see Koseki, 2023, page 165).

Acknowledgments

We sincerely appreciate the Global Meteor Network and SonotaCo net members for their enthusiastic efforts for meteor observations and for making their database public.

References

Jenniskens P., Nénon Q., Gural P. S., Albers J., Haberman B., Johnson B., Morales R., Grigsby B. J., Samuels D., Johannink C. (2016). "CAMS newly detected meteor showers and the sporadic background". *Icarus*, **266**, 384–409.

Koseki M. (2018). "Different definitions make a meteor shower distorted. The views from SonotaCo net and CAMS". *WGN, Journal of the International Meteor Organization*, **46**, 119–135.

Koseki M. (2020). "Confusions in IAUMDC Meteor Shower Database (SD)". *eMetN*, **5**, 93–111.

Koseki M. (2023). "Properties of 14 major meteor showers: magnitude ratio derived from video observations" *eMetN*, **8**, 151–170.

Rendtel J. (2022). "International Meteor Organization - 2023 Meteor Shower Calendar".

SonotaCo (2009). "A meteor shower catalog based on video observations in 2007–2008". *WGN, Journal of the IMO*, **37**, 55–62.

SonotaCo, Uehara S., Sekiguchi T., Fujiwara Y., Maeda K., and Ueda M. (2021). "J14: A Meteor Shower and Cluster". *WGN, Journal of the IMO*, **49**, 76–97.

Vida D., Gural P., Brown P., Campbell-Brown M., Wiegert P. (2019). "Estimating trajectories of meteors: an observational Monte Carlo approach - I. Theory". *Monthly Notices of the Royal Astronomical Society*, **491**, 2688–2705.

Vida D., Gural P., Brown P., Campbell-Brown M., Wiegert P. (2020). "Estimating trajectories of meteors: an observational Monte Carlo approach - II. Results". *Monthly Notices of the Royal Astronomical Society*, **491**, 3996–4011.

Vida D., Šegon D., Gural P. S., Brown P. G., McIntyre M. J., Dijkema T. J., Pavletić L., Kukić P., Mazur M. J., Eschman P., Roggemans P., Merlak A., Zubrović D. (2021). "The Global Meteor Network – Methodology and first results". *Monthly Notices of the Royal Astronomical Society*, **506**, 5046–5074.

A possibly new meteor shower in Sagitta

Damir Šegon[1], Denis Vida[2] and Paul Roggemans[3]

[1] **Astronomical Society Istra Pula, Park Monte Zaro 2, 52100 Pula, Croatia**

[2] **Department of Earth Sciences, University of Western Ontario, London, Ontario, N6A 5B7, Canada**
denis.vida@gmail.com

[3] **Pijnboomstraat 25, 2800 Mechelen, Belgium**
paul.roggemans@gmail.com

A short duration new meteor shower on a long period comet type orbit has been detected during May 2023 by the Global Meteor Network. Meteors belonging to the new shower were observed between 53.93° < λ_O < 54.80° (2023, May 15–16) from a radiant at R.A. = 300° and Decl.= +18° with a geocentric velocity of 59.7 km/s. The new meteor shower has been listed in the Working List of Meteor Showers under the temporary identification M2023-K1.

1 Introduction

A routine visual check of the daily radiant plots of the Global Meteor Network revealed a concentration of radiants about 10° from the gamma Aquiliids (GAQ, #0531) radiant, and visual inspection of plots for the previous and next night revealed that the possibly new shower has been active for only the night of 15–16 May 2023 (*Figure 1*). The initial search through the IAU database has shown this may be a new shower, and a deeper investigation has been made.

2 Method and results

We used the procedure as described for some recent cases of possibly new showers in Bootes and Draco (Šegon et al., 2023). The Southworth–Hawkins dissimilarity criteria D_{SH} has been chosen for the analysis of the new radiant concentration. A first iteration revealed a clear concentration of orbits, as it can be seen on *Figure 2*. The Railey distribution fit pointed at a D_{SH} value of 0.1 as the orbital similarity cutoff (*Figure 3*), which resulted in 15 orbits representing the possibly new meteor shower.

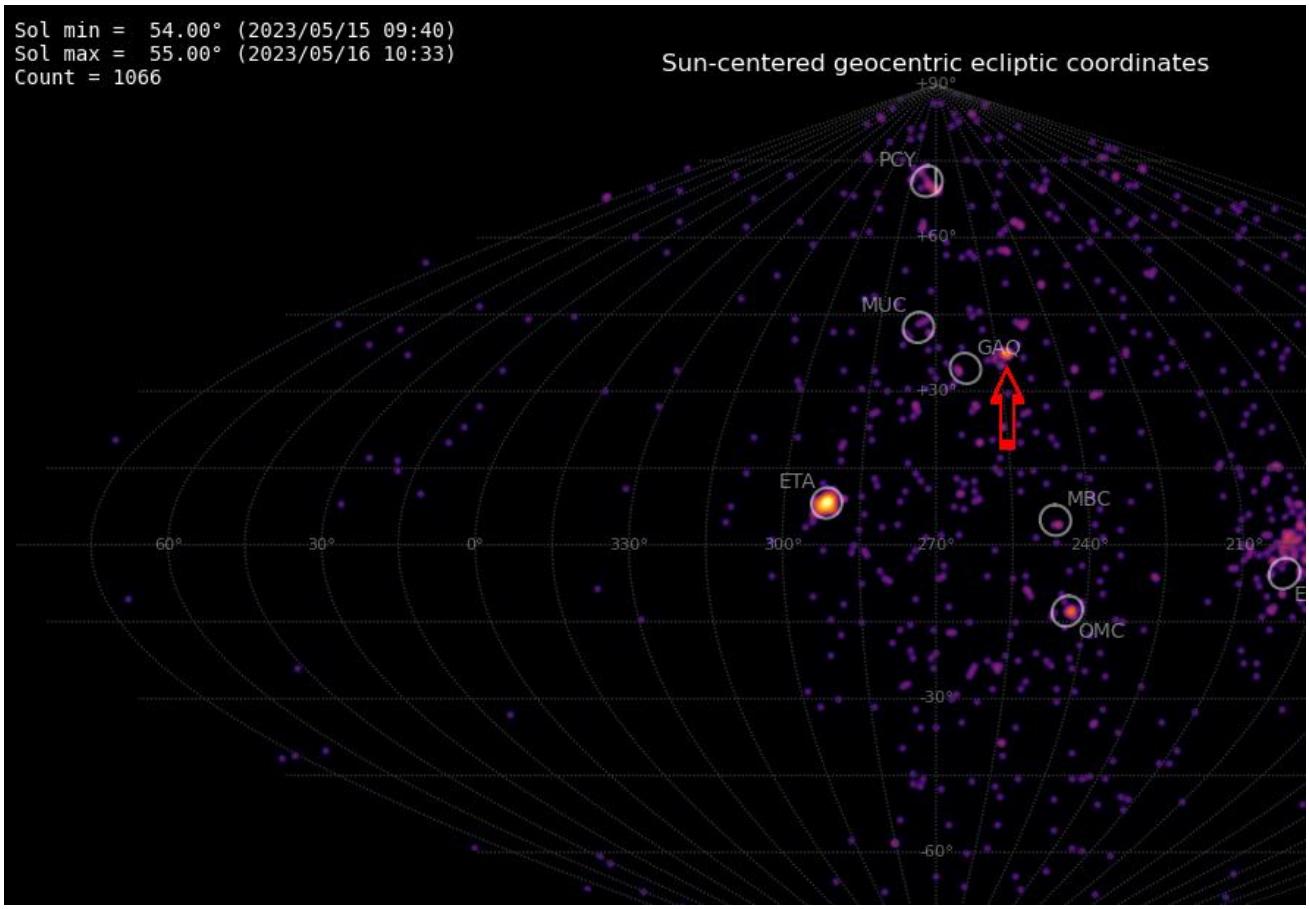

Figure 1 – Radiant plot of the Global Meteor Network data for 2023 May 15–16 in Sun-centered geocentric ecliptic coordinates. The new radiant is visible right (west) of the GAQ radiant and is marked by a red arrow.

 © eMeteorNews

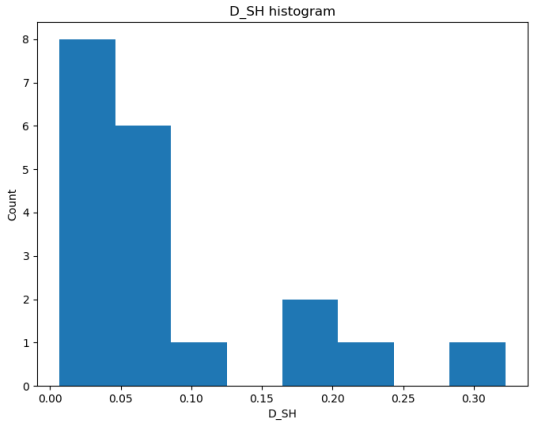

Figure 2 – Histogram of the distribution of the D_{SH} criterion values valid for the final mean orbit.

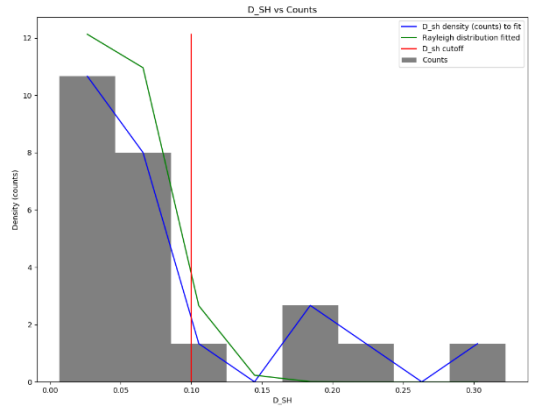

Figure 3 – Rayleigh distribution fit and D_{SH} criterion cutoff.

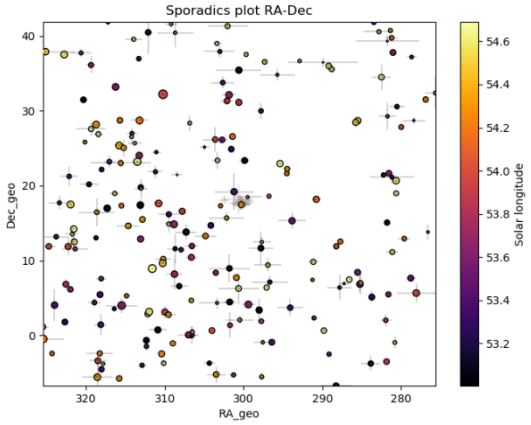

Figure 4 – All non shower meteor radiants in geocentric equatorial coordinates during the shower activity. The pale diamonds represent the new shower radiants plots, error bars represent two sigma values in both coordinates.

The presence of non-shower radiants in the area around the possibly new shower (*Figure 4*) shows the cutoff to be reliable since the density of meteor radiants does not look affected after removing shower members (plotted as pale diamonds). The plot of the shower meteor radiants in equatorial coordinates shows a very compact group, with a standard deviation of the distances from the average radiant position of about a single degree (see *Figure 5*). The *Π–i* diagram shows a compact group of radiants too (*Figure 6*), without any other groups of radiants to be seen.

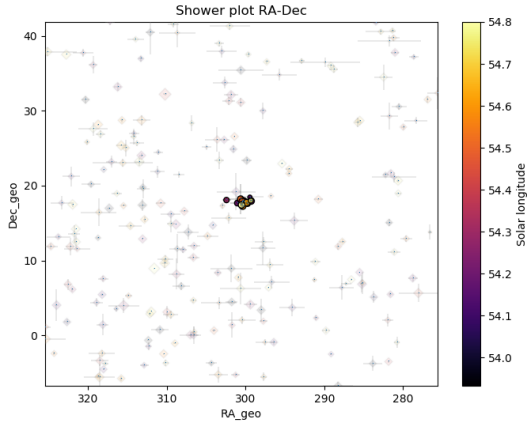

Figure 5 – The reverse of *Figure 4*, now the shower meteors are shown as circles and the non shower meteors as grayed out diamonds. Note that there are no other groups of meteor radiants to be seen in the vicinity of the possibly new meteor shower.

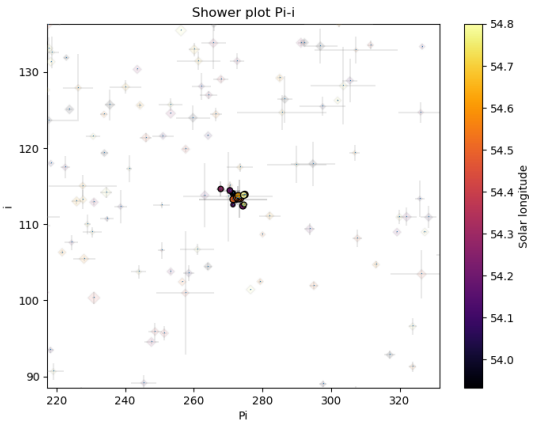

Figure 6 – The diagram of the inclination *i* against longitude of perihelion *Π* shows showing a distinct group of radiants without any other groups to be seen.

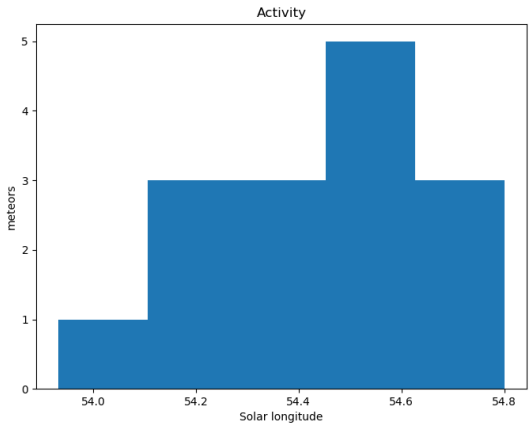

Figure 7 – The activity period with the number of orbits identified as new shower members.

The radiant of the possibly new shower lies in the constellation of Sagitta, near the 5.3-magnitude star 13 Sge. The activity of the shower has been detected between

53.93° and 54.80° of solar longitude (*Figure 7*), however we may round the activity to about one day. Only a single meteor had a positive magnitude, and the overall average brightness was –1.5 with all Sirius-bright meteors. On average, six GMN cameras captured the same event: only four meteors were captured from two locations, and a single one was detected from twenty-one (21) sites.

This case has shown one of the most important characteristics of the Global Meteor Network, namely the value to cover events as they happen all around the globe. The first meteor has been captured from the USA, followed by South Korea, New Zealand, Malaysia, followed by United Kingdom and the Netherlands, Brazil and back to the USA where the last meteor has been captured!

3 New shower or existing shower?

Before making claims that the detected activity qualifies to be listed as a new meteor shower, the known existing meteor showers active around this time from this part of the sky must be checked. The only suspect candidate is the gamma-Aquiliids (GAQ#0531) meteor shower, first reported by Šegon et al. (2014). In geocentric equatorial coordinates as well as in Sun- centered ecliptic geocentric coordinates, the radiant concentrations appear as close but distinct neighbors. As the new shower activity appears later than the GAQ-activity and west of it in radiant position, the off-set in radiant positions cannot be explained by radiant drift. The Tisserand relative to Jupiter proves both GAQ and the new shower are Long Period Comet-type orbits (*Table 1*). The orbits differ mainly by ~10° in inclination and ~26° in longitude of perihelion.

Table 1 – Known neighboring shower, gamma-Aquiliids (GAQ#0531, Shiba, 2023), compared to the new meteor shower, New (a) and New (b) derived by two different methods.

	GAQ	New (a)	New (b)
$\lambda_\odot$ (°)	48.7	54.54	54.5
$\lambda_{\odot b}$ (°)	40.2	53.93	54.2
$\lambda_{\odot e}$ (°)	58.0	54.80	55.5
α_g (°)	304.9	300.3	300.4
δ_g (°)	+14.4	+17.8	+17.8
$\Delta\alpha_g$ (°)	0.97	–	–
$\Delta\delta_g$ (°)	0.24	–	–
v_g (km/s)	62.8	59.7	59.6
λ (°)	311.3	307.2	307.3
$\lambda_g - \lambda_\odot$ (°)	262.7	252.8	252.8
β_g (°)	33.0	37.4	37.5
a (A.U.)	27.5	300.9	79.4
q (A.U.)	0.985	0.903	0.9014
e	0.964	0997	0.989
i (°)	123.7	113.5	113.4
ω (°)	197.7	218.2	218.4
Ω (°)	48.7	54.4	54.5
Π (°)	246.4	272.6	272.9
T_j	–0.49	–0.45	-0.40
N	40	15	9

Further verification of the IAU MDC Working List of Meteor Showers (Jenniskens et al., 2020; Jopek and Kaňuchová, 2014; 2017; Jopek and Jenniskens, 2011; Neslušan et al., 2020) did not reveal any other nearby meteor shower activity.

4 Another search method

Another method has been applied to check this new meteor shower discovery. The starting point here can be any visually spotted concentration of radiant points or any other indication for the occurrence of similar orbits. The method has been described before (Roggemans et al., 2019). The main difference with the method applied in *Section 2* is that three different discrimination criteria are combined in order to have only those orbits which fit different criteria. The D-criteria that we use are these of Southworth and Hawkins (1963), Drummond (1981) and Jopek (1993) combined. Instead of using a cutoff value for the D-criteria these values are considered in different classes with different thresholds of similarity. Depending on the dispersion and the type of orbits, the most appropriate threshold of similarity is selected to locate the best fitting mean orbit as the result of an iterative procedure.

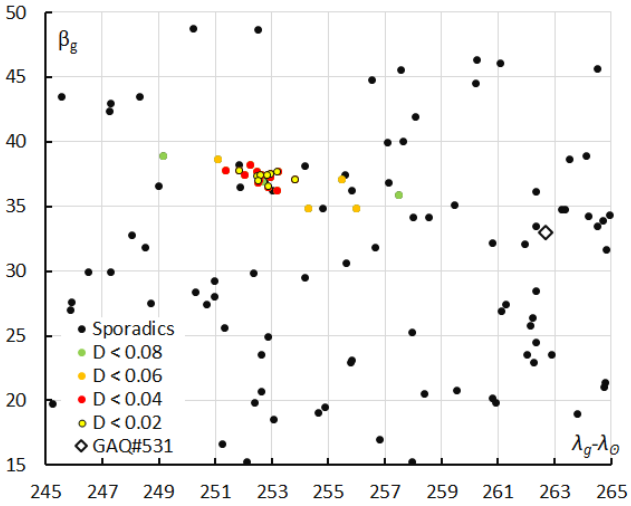

Figure 8 – Radiant plot in geocentric Sun-centered ecliptic coordinates for different similarity thresholds, the radiant of the gamma-Aquiliids (GAQ#0531) is marked as a diamond.

This method detects 45 candidate orbits if we admit $D_D < 0.08$, 30 for $D_D < 0.06$, 20 for $D_D < 0.04$ and 9 for $D_D < 0.02$. The better the similarity, the narrower the observing window. The mean orbit computed according to Jopek et al. (2006) for the orbits selected using the method of Šegon et al. (2023) is listed as New (a) in *Table 1*, the mean orbit for the selection using the method of Roggemans et al. (2019) is listed under New (b). The dispersion in geocentric Sun-centered ecliptic coordinates is displayed in *Figure 8*. The position of the gamma-Aquiliids (GAQ#0531) is shown east (at right) of the new shower.

© eMeteorNews

The concentration of the orbits of the newly discovered meteor shower appears very distinctly in the diagrams of the inclination against the longitude of perihelion (*Figure 9*) and the diagram of the inclination against the perihelion distance (*Figure 10*). In both diagrams the position of the gamma-Aquiliids (GAQ#0531) is marked as a diamond and appears clearly separated from the new meteor shower orbits.

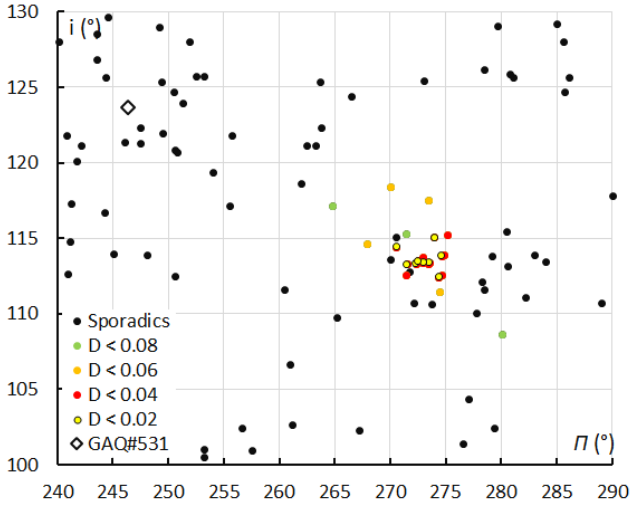

Figure 9 – Diagram of the inclination *i* against the longitude of perihelion *Π*, the radiant of the gamma-Aquiliids (GAQ#0531) is marked as a diamond.

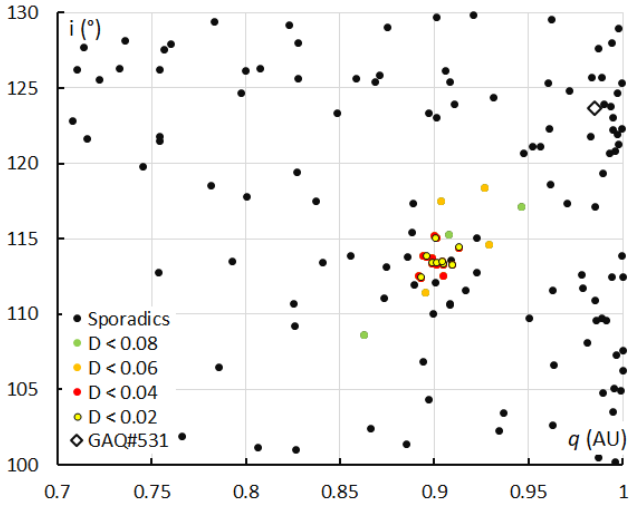

Figure 10 – Diagram of the inclination *i* against the perihelion distance *q*, the radiant of the gamma-Aquiliids (GAQ#0531) is marked as a diamond.

5 Comparing older data and other datasets

Looking up past years orbit data for Global Meteor Network (2018–2022, 722315 orbits), we find 35 orbits with $D_D < 0.08$ and 7 with $D_D < 0.04$, recorded in the period 2020–2022. The SonotaCo net orbit data (2007–2022, 443197 orbits) has 21 orbits with $D_D < 0.08$ and only 3 with $D_D < 0.04$, recorded in different years. EDMOND (2001–2016, 317831 orbits), has 16 orbits with $D_D < 0.08$ and only 2 with $D_D < 0.04$ in different years. The CAMS orbit data (2010–2016, 471582 orbits), has 24 orbits with $D_D < 0.08$ and only 3 with $D_D < 0.04$, recorded in different years between 2012 and 2016.

None of the major video orbit catalogues has previously recorded any trace of some concentration of orbits related to the new meteor shower.

6 Conclusion

A possibly new meteor shower in the constellation of Sagitta active for only about a day, has been found from the results of May 15–16, 2023 observations by Global Meteor Network. The resulting orbit is a typical long period comet one, but no connection to any known comet has been found meaning the parent body of this shower remains unknown. The new meteor shower has been listed in the Working List of Meteor Showers under the temporary identification M2023-K1[3].

Acknowledgment

The authors thank all people who support the Global Meteor Network by contributing meteor camera data or in any other way to help monitoring meteor activity around the clock worldwide. The Global Meteor Network results were obtained thanks to the efforts of the following volunteers: *Adam Mullins, Aden Walker, Adrian Bigland, Adriana Roggemans, Alain Marin, Alan Beech, Alan Maunder, Alan Pevec, Alan Pickwick, Aled Powell, Alejandro Barriuso, Aleksandar Merlak, Alex Bell, Alex Haislip, Alex Hodge, Alex Jeffery, Alex Kichev, Alex McConahay, Alex Pratt, Alex Roig, Alexander Wiedekind-Klein, Alexandre Alves, Alfredo Dal' Ava Júnior, Amy Barron, Anatoly Ijon, Andre Rousseau, Andrea Storani, Andrei Marukhno, Andres Fernandez, Andrew Campbell-Laing, Andrew Challis, Andrew Cooper, Andrew Fiamingo, Andrew Heath, Andrew Moyle, Andrew Washington, Andy Stott, Ange Fox, Angel Sierra, Angélica López Olmos, Ansgar Schmidt, Anthony Hopkinson, Anthony Pitt, Anton Macan, Anton Yanishevskiy, Anzhari Purnomo, Arie Blumenzweig, Arie Verveer, Attila Nemes, Barry Findley, Bart Dessoy, Bela Szomi Kralj, Bernard Côté, Bernard Hagen, Bev M. Ewen-Smith, Bill Cooke, Bill Wallace, Bill Witte, Bob Evans, Bob Greschke, Bob Hufnagel, Bob Marshall, Bob Massey, Bob Zarnke, Brenda Goodwill, Brendan Cooney, Brian Chapman, Brian Murphy, Brian Rowe, Bruno Bonicontro, Callum Potter, Carl Elkins, Carl Mustoe, Carl Panter, Charlie McCormack, Chris Baddiley, Chris Blake, Chris Dakin, Chris George, Chris James, Chris Ramsay, Chris Reichelt, Christian Wanlin, Christine Ord, Christof Zink, Christophe Demeautis, Christopher Coomber, Christopher Curtis, Christopher Tofts, Chuck Goldsmith, Chuck Pullen, Ciaran Tangney, Claude Boivin, Claude Surprenant, Clive Sanders, Colin Graham, Colin Marshall, Colin Nichols, Con Stoitsis, Creina Beaman, Daknam Al-Ahmadi, Damien Lemay, Damien McNamara, Damir Matković, Damir*

[3] https://www.ta3.sk/IAUC22DB/MDC2022/Roje/pojedynczy_obiekt.php?lporz=01710&kodstrumienia=01221

Šegon, Damjan Nemarnik, Dan Klinglesmith, Dan Pye, Daniel Duarte, Daniel J. Grinkevich, Daniela Cardozo Mourão, Danijel Reponj, Danko Kočiš, Dario Zubović, Dave Jones, Dave Mowbray, Dave Newbury, Dave Smith, David Akerman, David Attreed, David Bailey, David Brash, David Castledine, David Hatton, David Leurquin, David Price, David Rankin, David Robinson, David Rollinson, David Strawford, David Taylor, Dean Moore, Denis Bergeron, Denis St-Gelais, Dennis Behan, Derek Poulton, Didier Walliang, Dino Čaljkušić, Dmitrii Rychkov, Dominique Guiot, Don Anderson, Don Hladiuk, Dorian Božičević, Dougal Matthews, Douglas Sloane, Dustin Rego, Dylan O'Donnell, Ed Breuer, Ed Harman, Edgar Mendes Merizio, Edison José Felipe Pérezgómez Álvarez, Edson Valencia Morales, Eduardo Fernandez Del Peloso, Edward Cooper, Ehud Behar, Enrico Pettarin, Enrique Arce, Enrique Chávez Garcilazo, Eric Lopez, Eric Toops, Erwin van Ballegoij, Erwin Harkink, Ewan Richardson, Fabricio Borges, Fernando Dall'Igna, Fernando Jordan, Fernando Requena, Filip Matković, Filip Mezak, Filip Parag, Fiona Cole, Florent Benoit, François Simard, Frank Lyter, Frantisek Bilek, Gaétan Laflamme, Gareth Brown, Gareth Lloyd, Gareth Oakey, Garry Dymond, Gary Parker, Gavin Martin, Gene Mroz, Geoff Scott, Georges Attard, Georgi Momchilov, Germano Soru, Gilton Cavallini, Gordon Hudson, Graeme Hanigan, Graham Stevens, Graham Winstanley, Greg Michael, Gustav Frisholm, Guy Létourneau, Guy Williamson, Hamish Barker, Haris Jeffrey, Harri Kiiskinen, Hartmut Leiting, Heather Petelo, Heriton Rocha, Hervé Lamy, Herve Roche, Holger Pedersen, Horst Meyerdierks, Howard Edin, Hugo González, Iain Drea, Ian Enting Graham, Ian Lauwerys, Ian Parker, Ian Pass, Ian A. Smith, Ian Williams, Ian Hepworth, Igor Duchaj, Igor Henrique, Igor Macuka, Igor Pavletić, Ilya Jankowsky, Ioannis Kedros, Ivan Gašparić, Ivan Sardelić, Ivica Ćiković, Ivica Skokić, Ivo Dijan, Ivo Silvestri, Jacques Masson, Jacques Walliang, Jacqui Thompson, James Davenport, James Farrar, James Scott, James Stanley, Jamie Allen, Jamie Cooper, Jamie McCulloch, Jamie Olver, Jamie Shepherd, Jan Hykel, Jan Wisniewski, Janis Russell, Janusz Powazki, Jason Burns, Jason Charles, Jason Gill, Jason van Hattum, Jason Sanders, Javor Kac, Jay Shaffer, Jean Francois Larouche, Jean Vallieres, Jean-Baptiste Kikwaya, Jean-Louis Naudin, Jean-Marie Jacquart, Jean-Paul Dumoulin, Jean-Philippe Barrilliot, Jeff Holmes, Jeff Huddle, Jeff Wood, Jeremy Taylor, Jessica Richards, Jim Blackhurst, Jim Cheetham, Jim Critchley, Jim Fordice, Jim Gilbert, Jim Rowe, Jim Seargeant, Jochen Vollsted, Jocimar Justino, John W. Briggs, John Drummond, John Hale, John Kmetz, John Maclean, John Savage, John Thurmond, John Tuckett, John Waller, John Wildridge, Jon Bursey, Jonathan Alexis Valdez Aguilar, Jonathan Eames, Jonathan Mackey, Jonathan Whiting, Jonathan Wyatt, Jonathon Kambulow, Jorge Augusto Acosta Bermúdez, Jorge Oliveira, Jose Carballada, Jose Galindo Lopez, José María García, José-Luis Martín, Josip Belas, Josip Krpan, Jost Jahn, Juan Luis Muñoz, Jürgen Dörr, Jürgen Ketterer, Justin Zani, Kath Johnston, Kees Habraken, Keith Maslin, Ken Jamrogowicz, Kevin Gibbs-Wragge, Kevin Morgan, Klaas Jobse, Korado Korlević, Kyle Francis, Lachlan Gilbert, Larry Groom, Laurent Brunetto, Laurie Stanton, Lawrence Saville, Lee Hill, Lev Pustil'Nik, Lisa Holstein, Llewellyn Cupido, Lorna McCalman, Louw Ferreira, Lovro Pavletić, Lubomir Moravek, Lucia Dowling, Luciano Miguel Diniz, Ludger Börgerding, Maciej Reszelsk, Manel Colldecarrera, Marc Corretgé Gilart, Marcelo Domingues, Marcelo Zurita, Marco Verstraaten, Margareta Gumilar, Marián Harnádek, Mark Fairfax, Mark Gatehouse, Mark Haworth, Mark McIntyre, Mark Phillips, Mark Robbins, Mark Spink, Mark Suhovecky, Mark Williams, Marko Šegon, Marthinus Roos, Martin Breukers, Martin Richmond-Hardy, Martin Robinson, Martin Walker, Martin Woodward, Martyn Andrews, Mason McCormack, Matej Mihelčić, Matt Cheselka, Matthew Howarth, Megan Gialluca, Mia Boothroyd, Michael Cook, Michael Mazur, Michael O'Connell, Michel Saint-Laurent, Miguel Diaz Angel, Miguel Preciado, Mike Breimann, Mike Hutchings, Mike Read, Mike Shaw, Milan Kalina, Mirjana Malarić, Muhammad Luqmanul Hakim Muharam, Murray Forbes, Murray Singleton, Murray Thompson, Myron Valenta, Nawaz Mahomed, Ned Smith, Nedeljko Mandić, Neil Graham, Neil Papworth, Neil Waters, Nelson Moreira, Neville Vann, Nial Bruce, Nicholas Hill, Nicholas Ruffier, Nick Howarth, Nick James, Nick Moskovitz, Nick Norman, Nick Primavesi, Nick Quinn, Nick Russel, Nicola Masseroni, Nigel Bubb, Nigel Evans, Nigel Owen, Nikola Gotovac, Nikolay Gusev, Nikos Sioulas, Noah Simmonds, Ollie Eisman, Pablo Canedo, Paraksh Vankawala, Pat Devine, Patrick Franks, Patrick Poitevin, Patrik Kukić, Paul Cox, Paul Dickinson, Paul Haworth, Paul Heelis, Paul Kavanagh, Paul Ludick, Paul Prouse, Paul Pugh, Paul Roche, Paul Roggemans, Paul Stewart, Pedro Augusto Hay Day, Penko Yordanov, Pete Graham, Pete Lynch, Peter G. Brown, Peter Campbell-Burns, Peter Davis, Peter Eschman, Peter Gural, Peter Hallett, Peter Jaquiery, Peter Kent, Peter Lee, Peter McKellar, Peter Meadows, Peter Stewart, Peter Triffitt, Pető Zsolt, Phil James, Philip Gladstone, Philip Norton, Philippe Schaak, Phillip Wilhelm Maximilian Grammerstorf, Pierre Gamache, Pierre de Ponthière, Pierre-Michael Micaletti, Pierre-Yves Pechart, Pieter Dijkema, Predrag Vukovic, Przemek Nagański, Radim Stano, Rajko Sušanj, Raoul van Eijndhoven, Reinhard Kühn, Remi Lacasse, Renato Cássio Poltronieri, René Tardif, Richard Abraham, Richard Bassom, Richard Croy, Richard Davis, Richard Fleet, Richard Hayler, Richard Johnston, Richard Kacerek, Richard Payne, Richard Stevenson, Rick Fischer, Rick Hewett, Rick James, Ricky Bassom, Rob Agar, Rob de Corday Long, Rob Saunders, Robert Longbottom, Robert McCoy, Robert Saint-Jean, Robert D. Steele, Robert Veronneau, Robin Boivin, Robin Earl, Roel Gloudemans, Roger Banks, Roger Morin, Roland Idaczyk, Rolf Carstens, Romulo Jose, Ron James Jr, Roslina Hussain, Russell Jackson, Ryan Frazer, Ryan Harper, Salvador Aguirre, Sam Green, Sam Hemmelgarn, Sarah Tonorio, Scott Kaufmann, Sebastian Klier, Seppe Canonaco, Seraphin Feller, Serge Bergeron, Sergio Mazzi, Simon Cooke-Willis, Simon Holbeche, Simon Maidment, Simon McMillan, Simon Minnican, Simon Parsons, Simon Saunders, Sofia

 © eMeteorNews

Ulrich, Stacey Downton, Stanislav Korotkiy, Stanislav Tkachenko, Stefan Frei, Stephane Zanoni, Stephen Grimes, Steve Berry, Steve Bosley, Steve Carter, Steve Dearden, Steve Homer, Steve Kaufman, Steve Lamb, Steve Rau, Steve Tonkin, Steve Trone, Steve Welch, Steven Shanks, Steven Tilley, Stewart Doyle, Stuart Brett, Stuart Land, Stuart McAndrew, Sylvain Cadieux, Tammo Jan Dijkema, Terry Pundiak, Terry Richardson, Terry Simmich, Thiago Paes, Thomas Blog, Thomas Schmiereck, Thomas Stevenson, Tihomir Jakopčić, Tim Burgess, Tim Claydon, Tim Cooper, Tim Gloudemans, Tim Havens, Tim Polfliet, Tioga Gulon, Tobias Westphal, Tom Warner, Tommy McEwan, Tommy B. Nielsen, Torcuill Torrance, Tosh White, Tracey Snelus, Trevor Clifton, Ubiratan Borges, Urs Wirthmueller, Uwe Glässner, Vasilii Savtchenko, Ventsislav Bodakov, Victor Acciari, Vincent McDermott, Vladimir Jovanović, Waily Harim, Warley Souza, Washington Oliveira, Wenceslao Trujillo, William Perkin, William Schauff, William Stewart, Wullie Mitchell, Yakov Tchenak, Yfore Scott, Yohsuke Akamatsu, Yong-Ik Byun, Yuri Stepanychev, Zané Smit, Zbigniew Krzeminski, Željko Andreić, Zhuoyang Chen, Zoran Dragić, Zoran Knez, Zoran Novak, Asociación de Astronomía de Marina Alta, Costa Blanca Astronomical Society, Perth Observatory Volunteer Group, Royal Astronomical Society of Canada Calgary Centre (list established 2 May 2023).

References

Drummond J. D. (1981). “A test of comet and meteor shower associations”. *Icarus*, **45**, 545–553.

Jopek T. J. (1993). “Remarks on the meteor orbital similarity D-criterion”. *Icarus*, **106**, 603–607.

Jopek T. J., Rudawska R. and Pretka-Ziomek H. (2006). “Calculation of the mean orbit of a meteoroid stream”. *Monthly Notices of the Royal Astronomical Society*, **371**, 1367–1372.

Jopek T. J., Jenniskens P. M. (2011). “The Working Group on Meteor Showers Nomenclature: A History, Current Status and a Call for Contributions”. In, W.J. Cooke, D.E. Moser, B.F. Hardin, and D. Janches, editors, *Meteoroids: The Smallest Solar System Bodies, Proceedings of the Meteoroids Conference* held in Breckenridge, Colorado, USA, May 24-28, 2010. NASA/CP-2011-216469, pages 7–13.

Jopek T. J., Kaňuchová Z. (2014). “Current status of the~IAU MDC Meteor Showers Database”. In, T.J. Jopek, F.J.M. Rietmeijer, J. Watanabe, I.P. Williams, editors, *Meteoroids 2013 Proceedings of the Astronomical Conference* held at A.M. University, Poznan, Poland, Aug. 26-30, 2013, A.M. University Press, pages 353–364.

Jopek T. J., Kaňuchová Z. (2017). “IAU Meteor Data Center-the shower database: A status report”. *Planetary and Space Science*, **143**, 3–6.

Neslušan L., Poručan V., Svoreň J., Jakubík M. (2020). “On the new design of the IAU MDC portal”. *WGN, Journal of the International Meteor Organization*, **48**, 168–169.

Roggemans P., Johannink C. and Campbell-Burns P. (2019a). “October Ursae Majorids (OCU#333)”. *eMetN*, **4**, 55–64.

Šegon D., Gural P., Andreić Ž., Skokić I., Korlević K., Vida D., Novoselnik F. (2014). “New showers from parent body search across several video meteor databases”. *WGN, Journal of the International Meteor Organization*, **42**, 57–64.

Šegon D., Vida D., Roggemans P. (2023). “New meteor shower in Draco”. *eMetN*, **8**, 171–176.

Shiba Y. (2023). Submitted to *WGN, Journal of the International Meteor Organization*.

Southworth R. B. and Hawkins G. S. (1963). “Statistics of meteor streams”. *Smithsonian Contributions to Astrophysics*, **7**, 261–285.

GMN observations of the Crew-5 trunk reentry

Tammo Jan Dijkema[1], Denis Vida[2], Cees Bassa[1], Nick Moskovitz[3] and Peter Eschman[4]

[1] **ASTRON, Oude Hoogeveensedijk 4, 7991 PD, Dwingeloo, The Netherlands**
dijkema@astron.nl, bassa@astron.nl

[2] **Department of Physics and Astronomy, University of Western Ontario, London, Ontario, N6A 3K7, Canada**
dvida@uwo.ca

[3] **Lowell Observatory**
nmosko@lowell.edu

[4] **New Mexico Meteor ArrayAlbuquerque, New Mexico, USA**
peschman@gmail.com

Using the cameras of the Global Meteor Network in Arizona, Colorado and New Mexico we reconstruct the reentry trajectory of the Dragon capsule trunk (Crew-5 flight) which occurred on 2023 April 27 around 08^h52^m UTC. We compare the preliminary trajectory to known orbital information of the object and deduce the moment of rapid reentry.

1 Introduction

On 11 March 2023, four astronauts returned from the International Space Station in the Crew-5 Dragon spacecraft. Shortly before the capsule reentry, it separated from its 37 m^3 trunk. The trunk entered an orbit around Earth, and reentered on 27 April 2023, around 08^h52^m UTC. The reentry of the trunk was well observed by meteor cameras of the Global Meteor Network (GMN) in the American Southwest. We report on these observations and compare the camera-derived trajectory with the last known orbit of the trunk.

2 Observations

The reentry was observed by 21 GMN cameras. All of them had clear skies, allowing accurate astrometric calibration on many stars. The reentry was detected on almost all cameras by the fireball detector and raw video of the reentry was saved. For some parts of the observations, we had to fall back to "FF" files in the 'four-frame format' (Vida et al., 2021) which contain data aggregated over 10 seconds. An overview of the observations is shown in *Figure 2*.

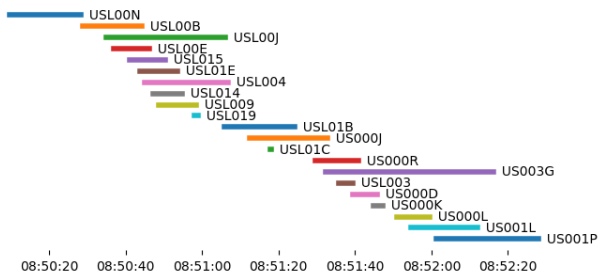

Figure 1 – Cameras contributing over time (UTC).

Figure 1 shows the cameras that observed the reentry over time. Most cameras that observed the event were operated by either the Lowell Observatory or the New Mexico Meteor Array (NMMA).

3 Data reduction

All observations were manually calibrated and the location of the trunk on every video frame was manually picked using the SkyFit2 software (Vida et al., 2021). These picks are available in the Global Fireball Exchange (GFE) format and are part of the accompanying data release (Dijkema et al., 2023).

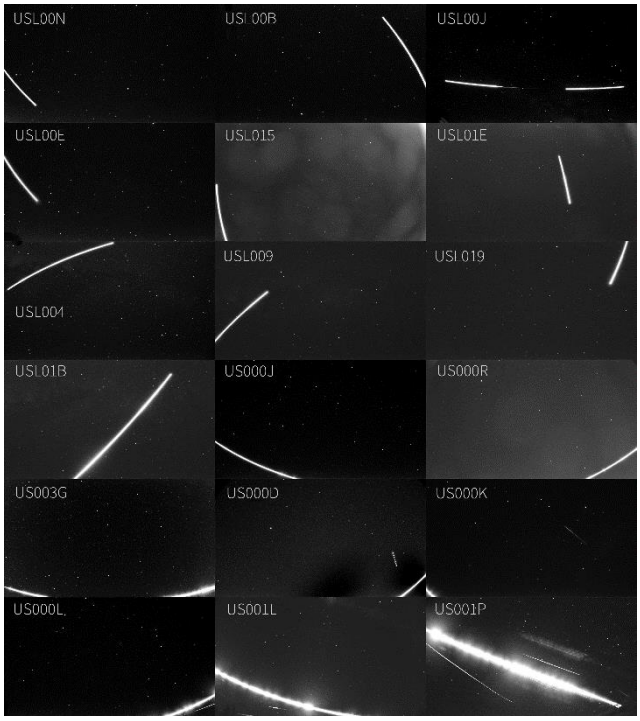

Figure 2 – Co-added images of the camera observations. Note that only portions of the trajectory are shown from some stations for which FF files were available.

 © eMeteorNews

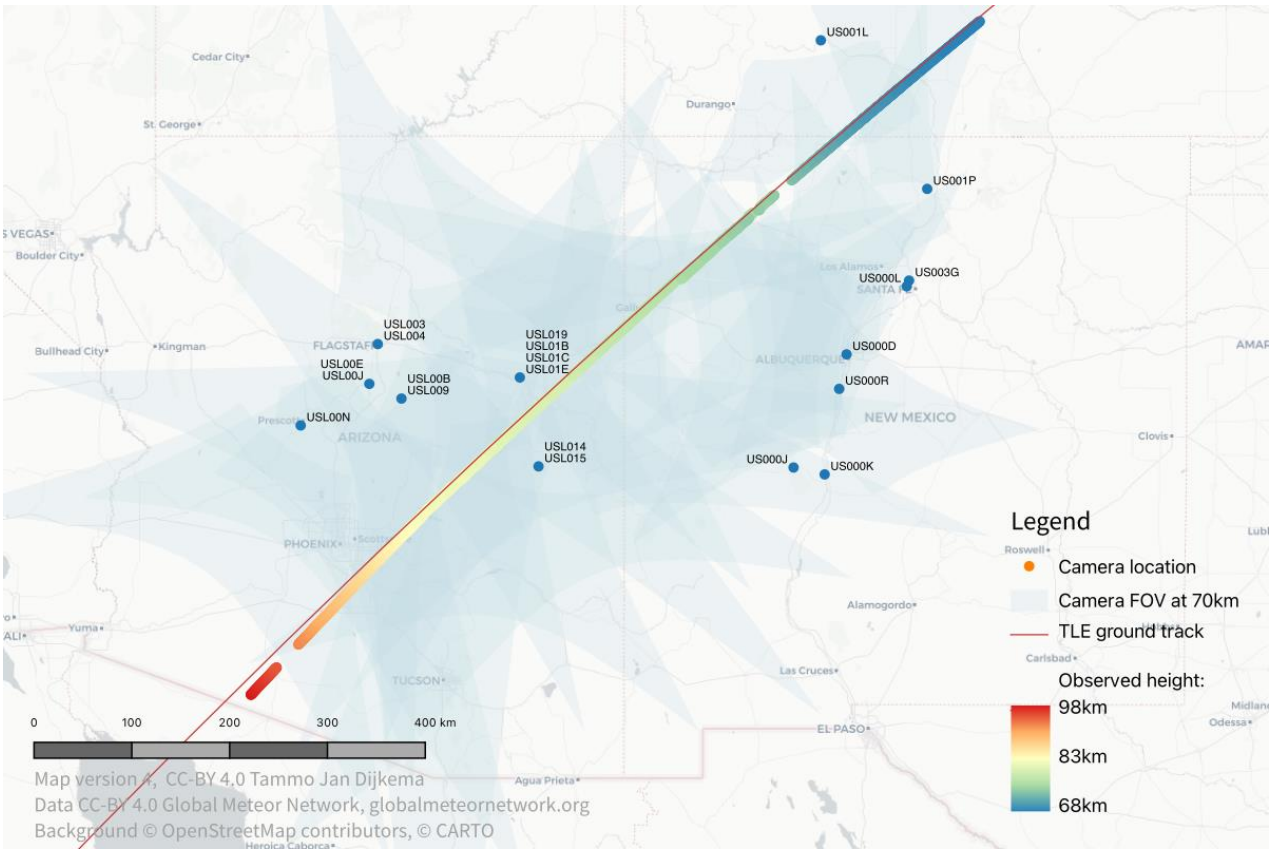

Figure 3 – Ground track of the reentry. The red line shows the ground track of the propagated TLE orbit.

The trajectory was computed piecemeal using the WesternMeteorPyLib (WMPL) trajectory solver (Vida et al., 2019). The solver was developed and tuned for meteors on heliocentric orbits which have a much shorter duration and higher speeds, unlike satellites on geocentric orbits. When used without alterations, the solver will produce an inaccurate trajectory with high deviations from the measurements.

We have worked around the limitations of WMPL by cutting the data into time chunks, where each time chunk is treated as an individual event. This technique introduces some discontinuities in the trajectory, which have been marked in the figures. Essentially, the trajectory solver does not compensate for the lift experienced by the spacecraft which curves the trajectory but assumes that individual pieces of the trajectory are straight lines. The compensation for the trajectory curvature due to gravity was also disabled as the lift significantly reduced the amount of trajectory deviation. The same technique was used previously in the reduction of a StarLink reentry above Spain in February 2022 (Dijkema et al., 2022).

4 Comparison with the last-known orbit

Most commonly, the orbits of satellites are monitored by radar systems such as the US Space Surveillance Network (SSN). The orbital parameters are shared on space-track.org[4] in the form of two-line elements (TLEs). Typically, these orbital elements are updated daily.

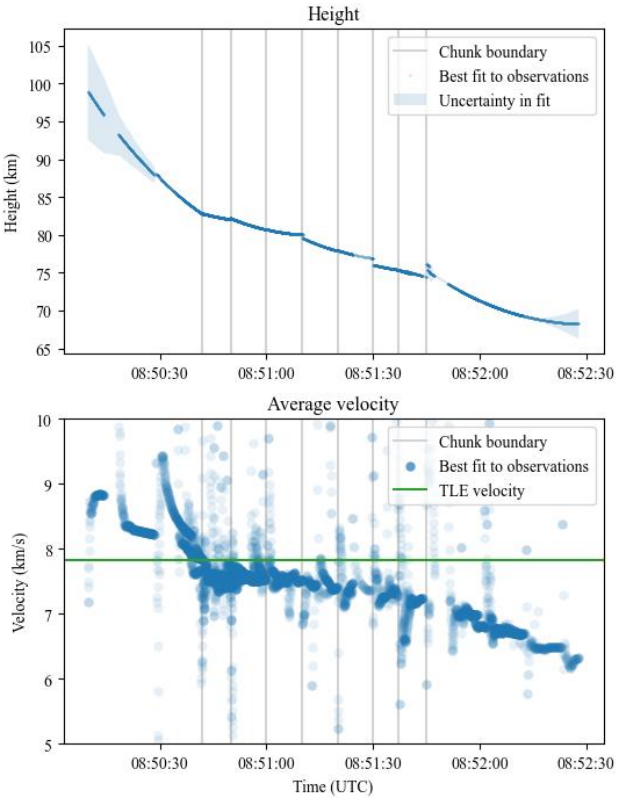

Figure 4 – Top: height vs. time of the observed trajectory. The TLE height is not in the plot, it is at 134 km. Bottom: velocity vs. time our observed trajectory. Fitting errors before around $08^h50^m40^s$ are present as only one camera observed the beginning.

The last known TLE of the Dragon trunk, with a NORAD

[4] https://www.space-track.org (accessed May 9, 2023).

ID 55840, has epoch 2023-04-27T07:40. The epoch is not the time of the radar measurement, but it should be close to it. This means that the orbital parameters were measured using radar observations only hours before the reentry. For an object this close to reentry, the accuracy of the TLE orbit is low.

The ground track of the propagated TLE is shown as a red line in *Figure 3*. It matches our trajectory well. A deviation is visible in the first part of the trajectory which is likely due to the inaccuracy of the meteor observations: only one camera observed the beginning (see *Figure 1*).

Our observations show that the object is ahead of the predicted ground track. At the beginning of our observations, it is ahead of the TLE by about 7 seconds and at the end, it is ahead by about 4 seconds (due to obvious deceleration). It should be noted that there may be a time delay on our observations of about 0.5 seconds.

The main difference between the last known orbit and the observed trajectory is the height. Predicting a suitable 'drag' term in TLEs is notably hard because this term depends on many factors like the orientation of the spacecraft and the solar activity (determining the extent of the atmosphere). The TLE orbit predicts a height of 134 km at the time of the reentry. The observations show (*Figure 4*, top panel) an actual height of around 98 km down to around 68 km (the beginning and end of the trajectory are less accurate).

The TLE orbit predicts an almost constant velocity of 7.8 km/s around the time of the observed reentry. Our observations do not lead to a good velocity fit until $08^{h}50^{m}40^{s}$. From then on, we observed a velocity of 7.6 km/s decreasing to 6.2 km/s (*Figure 4*, bottom panel). The trajectory was not observed in full; the trunk exited the field of view of the last camera before the end.

5 Future work

To improve the trajectory, a trajectory solver could be used which includes the last known orbital information and computes the drag and lift dynamics. From past meteoroid work, a solver that could be considered is that of Sansom et al., 2019. From the spacecraft side, a solver could be used in NASA's General Mission Analysis Tool (Hughes et al., 2017).

6 Conclusion

In this preliminary analysis, we have shown that Global Meteor Network observations of the Crew-5 trunk reentry match the orbit of the Crew-5 trunk well and that meteor camera observations can provide valuable information about the timing, location, height, and dynamics of satellite reentries.

Acknowledgment

We thank all camera operators of the involved cameras for contributing their data: *Thomas Blog*, *Solvay Blomquist*, *Bob Broffel*, *Jim Fordice*, *Matt Francism*, *Megan Gialluca*, *John Glitsos*, *Bob Greschke*, *Sam Hemmelgarn*, *Gene Mroz*, *David Robinson*, *Robert Schottland*, *Jay Shaffer*, *Eric Toops* and *Steve Welch*.

References

Dijkema T. J., Arce E., Carballada J., Martín J. L., and Jordán Sánchez F. (2022). "Global Meteor Network observations of Starlink re-entry 2022-02-10". Zenodo.

Dijkema T. J., Vida D., Moskovitz N., and Eschman P. (2023). "Global Meteor Network observations of Crew-5 Dragon trunk re-entry 2023-04-27". Zenodo.

Hughes S. P., Conway D. J., Parker J. (2017). "Using the general mission analysis tool (GMAT)". NASA Technical Report Server, GSFC-E-DAA-TN39043.

Sansom E. K., Jansen-Sturgeon T., Rutten M. G., Devillepoix H. A., Bland P. A., Howie R. M., ... & Hartig B. A. (2019). "3D meteoroid trajectories". *Icarus*, **321**, 388–406.

Vida D., Šegon D., Gural P. S., Brown P. G., McIntyre M. J., Dijkema T. J., Pavletić L., Kukić Mazur M.J., Eschman P., Roggemans P., Merlak A., Zubrović D. (2021). "The Global Meteor Network – Methodology and first results". *Monthly Notices of the Royal Astronomical Society*, **506**, 5046–5074.

Vida D., Gural P. S., Brown P. G., Campbell-Brown M., and Wiegert P. (2019). "Estimating trajectories of meteors: an observational Monte Carlo approach–I. Theory". *Monthly Notices of the Royal Astronomical Society*, **491**, 2688–2705.

 © eMeteorNews

April 2023 report CAMS-BeNeLux

Carl Johannink

Am Ollenkamp 4, 48599 Gronau, Germany
c.johannink@t-online.de

A summary of the activity of the CAMS-BeNeLux network during the month of April 2023 is presented. This month was good for 9763 multi-station meteors resulting in 2888 orbits.

1 Introduction

Meteor activity in April is still at a low level for northern latitudes. But around April 22nd, we welcome the first well-known yearly meteor shower, since the Quadrantids, in early January: the Lyrids.

2 April 2023 statistics

Weather in April was very unsettled with also temperatures slightly below average values. We could obtain results in 29 out of 30 nights. That seems a fairly good result. But on the other hand, the number of orbits obtained in each of these 29 nights, remained fairly low. This was caused by very different observing conditions across the BeNeLux for most of the time. Only in three nights we could collect more than 200 orbits (April 13–14, 19–20 and 25–26). In 8 nights, we collected less than 10 orbits (including one night without any orbit at all, the first night this month).

CAMS-BeNeLux collected 9763 multi-station meteors this month, resulting in a total of 2888 orbits. 56% of all orbits were captured by more than two stations.

On average 101 cameras were active this month. This number is much higher than last year, since the number of stations grow significantly in the last months.

At least 88 cameras were active every night. When we compare that with the results, this number clearly shows that many stations were very often cloudy for at least a part of the night.

3 Conclusion

Compared to other April months only two years gave a higher number of orbits. This good score is only explained by the larger number of cameras involved in our network.

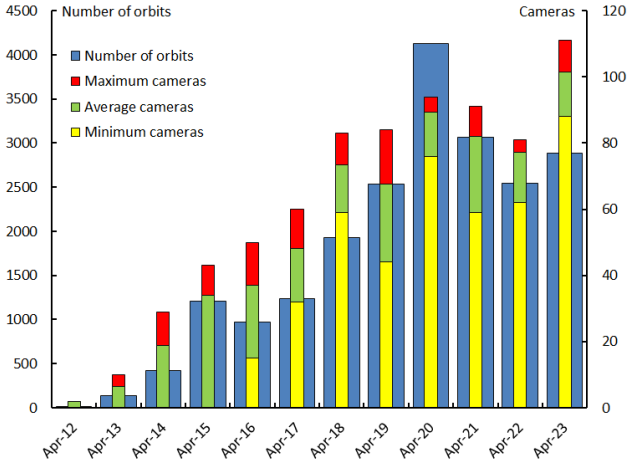

Figure 1 – Comparing April 2023 to previous months of April in the CAMS-BeNeLux history. The blue bars represent the number of orbits, the red bars the maximum number of cameras capturing in a single night, the green bars the average number of cameras capturing per night and the yellow bars the minimum number of cameras.

Table 1 – Number of orbits and active cameras in the BeNeLux during the month of April in the period 2012–2023.

Year	Nights	Orbits	Stations	Max. Cams	Min. Cams	Mean Cams
2012	6	11	4	2		2.0
2013	19	140	9	10		6.5
2014	19	421	12	29		18.8
2015	27	1212	15	43		33.9
2016	26	971	17	50	15	37
2017	28	1235	20	60	32	48.2
2018	27	1929	21	83	59	73.3
2019	29	2538	20	84	44	67.7
2020	29	4128	25	94	76	89.4
2021	28	3061	27	91	59	80.6
2022	27	2543	24	81	62	77.2
2023	29	2888	36	111	88	101.4
Total	294	21077				

© eMeteorNews

Acknowledgement

Many thanks to all participants in the CAMS BeNeLux network for their dedicated efforts. The CAMS BeNeLux team was operated by the following volunteers during the month of April 2023:

Hans Betlem (Woold, Netherlands, Watec 3071, 3072, 3073, 3074, 3075, 3076, 3077 and 3078), *Felix Bettonvil* (Utrecht, Netherlands, Watec 376), *Jean-Marie Biets* (Wilderen, Belgium, Watec 379, 380 and 381), *Ludger Boergerding* (Holdorf, Germany, RMS 3801), *Günther Boerjan* (Assenede, Belgium, RMS 3823), *Martin Breukers* (Hengelo, Netherlands, Watec 320, 321, 322, 323, 324, 325, 326 and 327, RMS 319, 328 and 329), *Seppe Canonaco* (Genk, RMS 3818 and 3819), *Pierre de Ponthiere* (Lesve, Belgium, RMS 3816 and 3826), *Bart Dessoy* (Zoersel, Belgium, Watec 804, 805 and 806), *Tammo Jan Dijkema* (Dwingeloo, Netherlands, RMS 3199), *Isabelle Ansseau*, *Jean-Paul Dumoulin*, *Dominique Guiot* and *Christian Wanlin* (Grapfontaine, Belgium, Watec 814 and 815, RMS 3814 and 3817), *Uwe Glässner* (Langenfeld, Germany, RMS 3800), *Luc Gobin* (Mechelen, Belgium, Watec 3890, 3891, 3892 and 3893), *Tioga Gulon* (Nancy, France, Watec 3900 and 3901), *Robert Haas* (Alphen aan de Rijn, Netherlands, Watec 3160, 3161, 3162, 3163, 3164, 3165, 3166 and 3167), *Robert Haas* (Texel, Netherlands, Watec 811, 812 and 813), *Kees Habraken* (Kattendijke, Netherlands, RMS 3780, 3781, 3782 and 3783), *Klaas Jobse* (Oostkapelle, Netherlands, Watec 3030, 3031, 3032, 3033, 3034, 3035, 3036 and 3037), *Carl Johannink* (Gronau, Germany, Watec 3100, 3101, 3102), *Reinhard Kühn* (Flatzby, Germany, RMS 3802), *Hervé Lamy* (Dourbes, Belgium, Watec 394 and 395, RMS 3825 and 3841), *Hervé Lamy* (Humain, Belgium, RMS 3821 and 3828), *Hervé Lamy* (Ukkel, Belgium, Watec 393 and 817), *Hartmut Leiting* (Solingen, Germany, RMS 3806), *Koen Miskotte* (Ermelo, Netherlands, Watec 3051, 3052, 3053 and 3054), *Pierre-Yves Péchart* (Hagnicourt, France, RMS 3902, 3903, 3904 and 3905), *Eduardo Fernandez del Peloso* (Ludwigshafen, Germany, RMS 3805), *Tim Polfliet* (Gent, Belgium, Watec 396, RMS 3820 and 3840), *Steve Rau* (Oostende, Belgium, RMS 3822), *Steve Rau* (Zillebeke, Belgium, Watec 3850 and 3852, RMS 3851 and 3853), *Martin Richmond-Hardy* (Kirton, England, RMS 3701), *Paul and Adriana Roggemans* (Mechelen, Belgium, RMS 3830 and 3831, Watec 3832, 3833, 3834, 3835, 3836 and 3837), *Jim Rowe* (Eastbourne, Great Britain, RMS 3829), *Philippe Schaack* (Roodt-sur-Syre, Luxemburg, RMS 3952), *Hans Schremmer* (Niederkruechten, Germany, Watec 803), *Erwin van Ballegoij* (Heesh, Netherlands Watec 3148 and 3149), *Andy Washington* (Clapton, England, RMS 3702).

 © eMeteorNews

May 2023 report CAMS-BeNeLux

Carl Johannink

Am Ollenkamp 4, 48599 Gronau, Germany
c.johannink@t-online.de

A summary of the activity of the CAMS-BeNeLux network during the month of May 2023 is presented. This month was good for 9756 multi-station meteors resulting in 2734 orbits.

1 Introduction

Beside the everlasting sporadic activity, this month is well known for one of the greatest meteor showers on the Southern Hemisphere, the eta Aquariids around May 6. Although meteor activity in early May is still at a low level in the BeNeLux, activity from this stream makes observations even in our regions attractive, especially around May 6.

2 May 2023 statistics

The weather in May showed two faces: a very unsettled first half of this month, and a very sunny second half. In 14 nights we could collect more than 100 orbits. No less than 12 of those nights occurred after May 15, which confirm the difference in clear nights in the first and second half of this month.

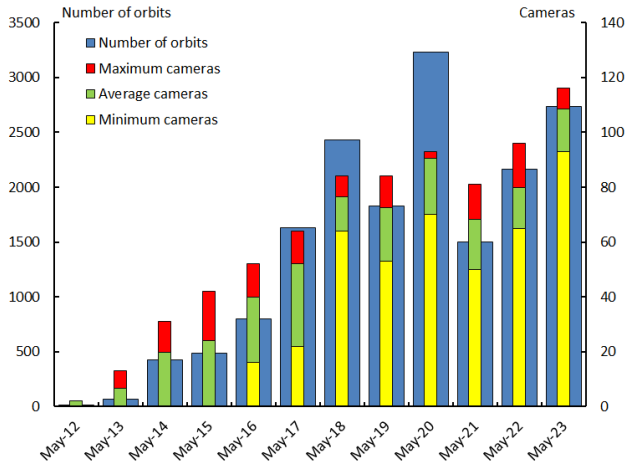

Figure 1 – Comparing May 2023 to previous months of May in the CAMS-BeNeLux history. The blue bars represent the number of orbits, the red bars the maximum number of cameras capturing in a single night, the green bars the average number of cameras capturing per night and the yellow bars the minimum number of cameras.

We could obtain results in 30 out of 31 nights, no orbits for May 8–9 although 6 cameras captured meteors but without triangulations. CAMS-BeNeLux collected 9756 multi-station meteors this month, resulting in a total of 2734 orbits. In these results too, we see a sharp difference for both halves of May: 987 orbits in the first half of May against 1747 orbits in the second half.

Nearly 60% of all orbits were captured by more than two stations, a bit higher than in the last months as a result from the exceptional good conditions in the BeNeLux after May 15.

On average 108 cameras were active this month. This number is much higher than last year, since the number of stations grow significantly in the last months. At least 93 cameras were active every night. Unfortunately, station 3701 isn't active anymore because the operator Martin Richmond-Hardy, passed away early May.

Table 1 – Number of orbits and active cameras in the BeNeLux during the month of May in the period 2012–2023.

Year	Nights	Orbits	Stations	Max. Cams	Min. Cams	Mean Cams
2012	5	13	4	2		2
2013	13	69	9	13		6.8
2014	22	430	13	31		19.7
2015	25	484	15	42		24.2
2016	26	803	17	52	16	39.9
2017	24	1627	19	64	22	52.0
2018	31	2426	21	84	64	76.6
2019	29	1825	20	84	53	72.4
2020	29	3226	24	93	70	90.5
2021	28	1500	25	81	50	68.2
2022	30	2160	28	96	65	79.8
2023	30	2734	36	116	93	108.6
Total	292	17297				

3 Conclusion

Compared to other months of May only one year gave a better score in orbits. May 2020 delivered 3226 orbits. This was one of the sunniest months ever recorded in the BeNeLux with more than 300 hours of sunshine.

As a result we could collect some nights then with more than 200 orbits around the maximum of the eta Aquariids on May 6. Unfortunately, we could only collect a few orbits from this stream in 2023, due to the unsettled weather at that time.

Acknowledgement

Many thanks to all participants in the CAMS BeNeLux network for their dedicated efforts. The CAMS BeNeLux team was operated by the following volunteers during the month of May 2023:

Hans Betlem (Woold, Netherlands, Watec 3071, 3072, 3073, 3074, 3075, 3076, 3077 and 3078), *Felix Bettonvil* (Utrecht, Netherlands, Watec 376), *Jean-Marie Biets* (Wilderen, Belgium, Watec 379, 380 and 381), *Ludger Boergerding* (Holdorf, Germany, RMS 3801), *Günther Boerjan* (Assenede, Belgium, RMS 3823), *Martin Breukers* (Hengelo, Netherlands, Watec 320, 321, 322, 323, 324, 325, 326 and 327, RMS 319, 328 and 329), *Seppe Canonaco* (Genk, RMS 3818 and 3819), *Pierre de Ponthiere* (Lesve, Belgium, RMS 3816 and 3826), *Bart Dessoy* (Zoersel, Belgium, Watec 804, 805 and 806), *Tammo Jan Dijkema* (Dwingeloo, Netherlands, RMS 3199), *Isabelle Ansseau*, *Jean-Paul Dumoulin*, *Dominique Guiot* and *Christian Wanlin* (Grapfontaine, Belgium, Watec 814 and 815, RMS 3814 and 3817), *Uwe Glässner* (Langenfeld, Germany, RMS 3800), *Luc Gobin* (Mechelen, Belgium, Watec 3890, 3891, 3892 and 3893), *Tioga Gulon* (Nancy, France, Watec 3900 and 3901), *Robert Haas* (Alphen aan de Rijn, Netherlands, Watec 3160, 3161, 3162, 3163, 3164, 3165, 3166 and 3167), *Robert Haas* (Texel, Netherlands, Watec 811, 812 and 813), *Kees Habraken* (Kattendijke, Netherlands, RMS 3780, 3781, 3782 and 3783), *Klaas Jobse* (Oostkapelle, Netherlands, Watec 3030, 3031, 3032, 3033, 3034, 3035, 3036 and 3037), *Carl Johannink* (Gronau, Germany, Watec 3100, 3101, 3102), *Reinhard Kühn* (Flatzby, Germany, RMS 3802), *Hervé Lamy* (Dourbes, Belgium, Watec 394 and 395, RMS 3825 and 3841), *Hervé Lamy* (Humain, Belgium, RMS 3821 and 3828), *Hervé Lamy* (Ukkel, Belgium, Watec 393 and 817), *Hartmut Leiting* (Solingen, Germany, RMS 3806), *Koen Miskotte* (Ermelo, Netherlands, Watec 3051, 3052, 3053 and 3054), *Pierre-Yves Péchart* (Hagnicourt, France, RMS 3902, 3903, 3904 and 3905), *Eduardo Fernandez del Peloso* (Ludwigshafen, Germany, RMS 3805), *Tim Polfliet* (Gent, Belgium, Watec 396, RMS 3820 and 3840), *Steve Rau* (Oostende, Belgium, RMS 3822), *Steve Rau* (Zillebeke, Belgium, Watec 3850 and 3852, RMS 3851 and 3853), *Martin Richmond-Hardy* † (Kirton, England, RMS 3701), *Paul and Adriana Roggemans* (Mechelen, Belgium, RMS 3830 and 3831, Watec 3832, 3833, 3834, 3835, 3836 and 3837), *Jim Rowe* (Eastbourne, Great Britain, RMS 3829), *Philippe Schaack* (Roodt-sur-Syre, Luxemburg, RMS 3952), *Hans Schremmer* (Niederkruechten, Germany, Watec 803), *Erwin van Ballegoij* (Heesh, Netherlands Watec 3148 and 3149), *Andy Washington* (Clapton, England, RMS 3702).

 © eMeteorNews

Photographic Lyrid observations on 22 April 2023

Mikhail Maslov

skjeller@yandex.ru

A presentation is given with photographic records obtained during the 2023 Lyrids.

1 Introduction

Here are the results of photographic Lyrid observations on 22 April from 16^h08^m to 21^h00^m UT. The images were taken with a Pentax KP camera and 8.5 mm lens, without guiding. The night was nearly moonless, the session took place under dark rural sky with some light cirrus clouds. In total 22 meteors were detected, 7 LYR and 15 SPO among them. The Lyrid activity was not very high so far, at the half of the sporadic level. Suggesting sporadic ZHR of 10 and taking into account the height of the Lyrid radiant during the night we get the Lyrids ZHR ~ 7.

2 The results

The results are presented in the text form below and in the form of composite images for every hour of observations:

- 16^h08^m–17^h00^m UT – 0 LYR, 5 SPO, Lyrid radiant altitude: 27 degrees, Moon: altitude 2 degrees, phase 7%
- 17^h00^m–18^h00^m UT – 4 LYR, 3 SPO, Lyrid radiant altitude: 35 degrees, Moon: below horizon
- 18^h00^m–19^h00^m UT – 0 LYR, 1 SPO, Lyrid radiant altitude: 44 degrees, Moon: below horizon
- 19^h00^m–20^h00^m UT – 2 LYR, 2 SPO, Lyrid radiant altitude: 52 degrees, Moon: below horizon
- 20^h00^m–21^h00^m UT – 1 LYR, 4 SPO, Lyrid radiant altitude: 60 degrees, Moon: below horizon.

Figure 1 – 20^h00^m–-21^h00^m UT – 1 LYR, 4 SPO, Lyrid radiant altitude: 60 degrees, Moon: below horizon.

Figure 2 – 17^h00^m–18^h00^m UT – 4 LYR, 3 SPO, Lyrid radiant altitude: 35 degrees, Moon: below horizon.

Figure 3 – 18^h00^m–19^h00^m UT – 0 LYR, 1 SPO, Lyrid radiant altitude: 44 degrees, Moon: below horizon.

 © eMeteorNews

Figure 4 – 19^h00^m–20^h00^m UT – 2 LYR, 2 SPO, Lyrid radiant altitude: 52 degrees, Moon: below horizon.

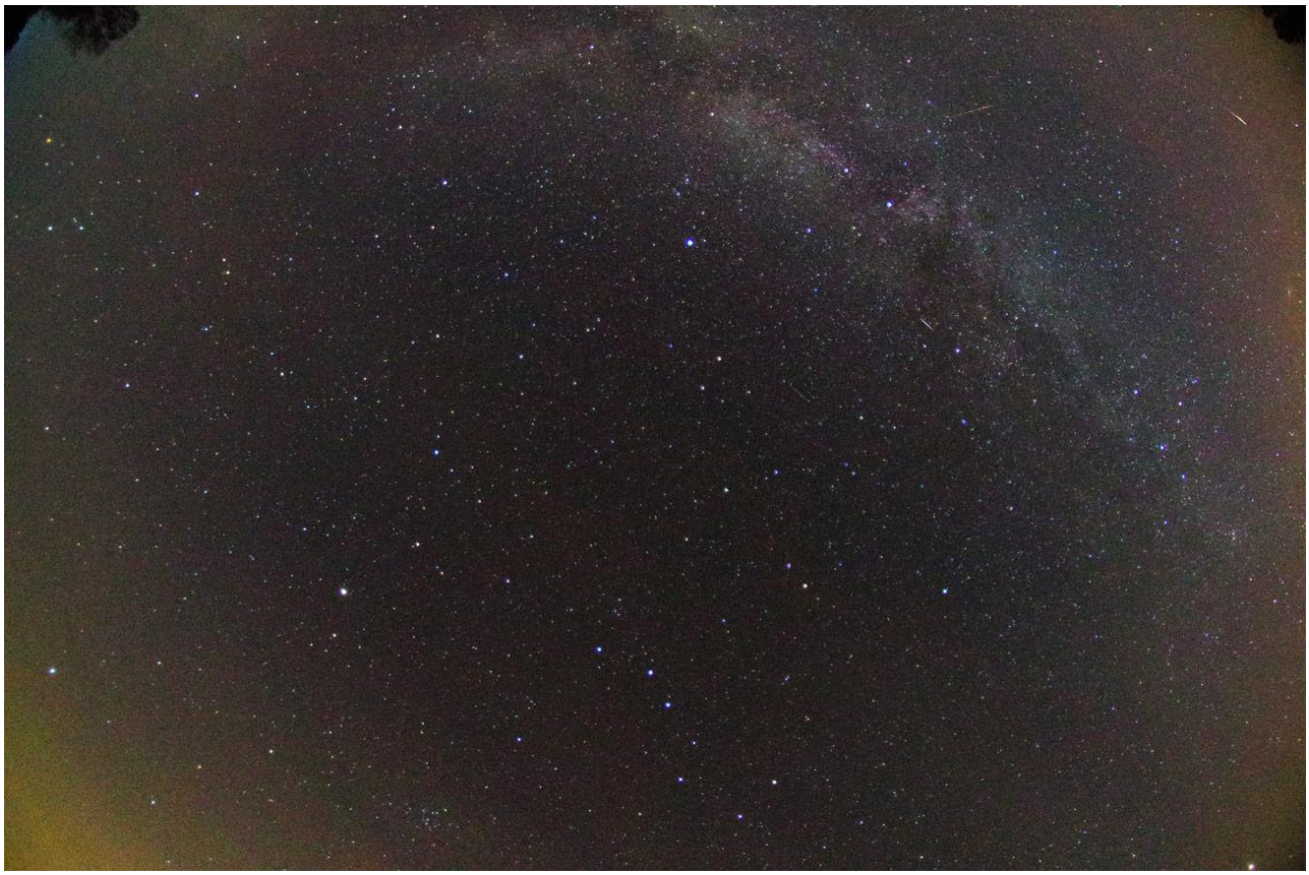

Figure 5 – 20^h00^m–21^h00^m UT – 1 LYR, 4 SPO, Lyrid radiant altitude: 60 degrees, Moon: below horizon.

Radio meteors April 2023

Felix Verbelen

Vereniging voor Sterrenkunde & Volkssterrenwacht MIRA, Grimbergen, Belgium
felix.verbelen@skynet.be

An overview of the radio observations during April 2023 is given.

1 Introduction

The graphs show both the daily totals (*Figure 1 and 2*) and the hourly numbers (*Figure 3 and 4*) of "all" reflections counted automatically, and of manually counted "overdense" reflections, overdense reflections longer than 10 seconds and longer than 1 minute, as observed here at Kampenhout (BE) on the frequency of our VVS-beacon (49.99 MHz) during the month of April 2023.

The hourly numbers, for echoes shorter than 1 minute, are weighted averages derived from:

$$N(h) = \frac{n(h-1)}{4} + \frac{n(h)}{2} + \frac{n(h+1)}{4}$$

Weak to moderate lightning activity was recorded on only 2 days, while local interference and unidentified noise remained low this month. On several days solar noise was however quite strong. A few examples displayed in *Figures 5 to 8*.

Meteor activity was slowly increasing, with a nice outburst of the Lyrids reaching a maximum here on April 23th. As the graphs show, the shower is hardly seen when "all" reflections are considered, but shows up prominently in the graphs of "overdense" reflections. A closer look at the data also reveals a number of fainter showers.

Over the entire month, only 2 reflections longer than 1 minute were observed. Along with some interesting "epsilons" they are included (*Figures 9 to 14*). A lot more "epsilons" are available on request.

In addition to the usual graphs, you will also find the raw counts in cvs-format[5] from which the graphs are derived. The table contains the following columns: day of the month, hour of the day, day + decimals, solar longitude (epoch J2000), counts of "all" reflections, overdense reflections, reflections longer than 10 seconds and reflections longer than 1 minute, the numbers being the observed reflections of the past hour.

[5] https://www.meteornews.net/wp-content/uploads/2023/05/202304_49990_FV_rawcounts.csv

 © eMeteorNews

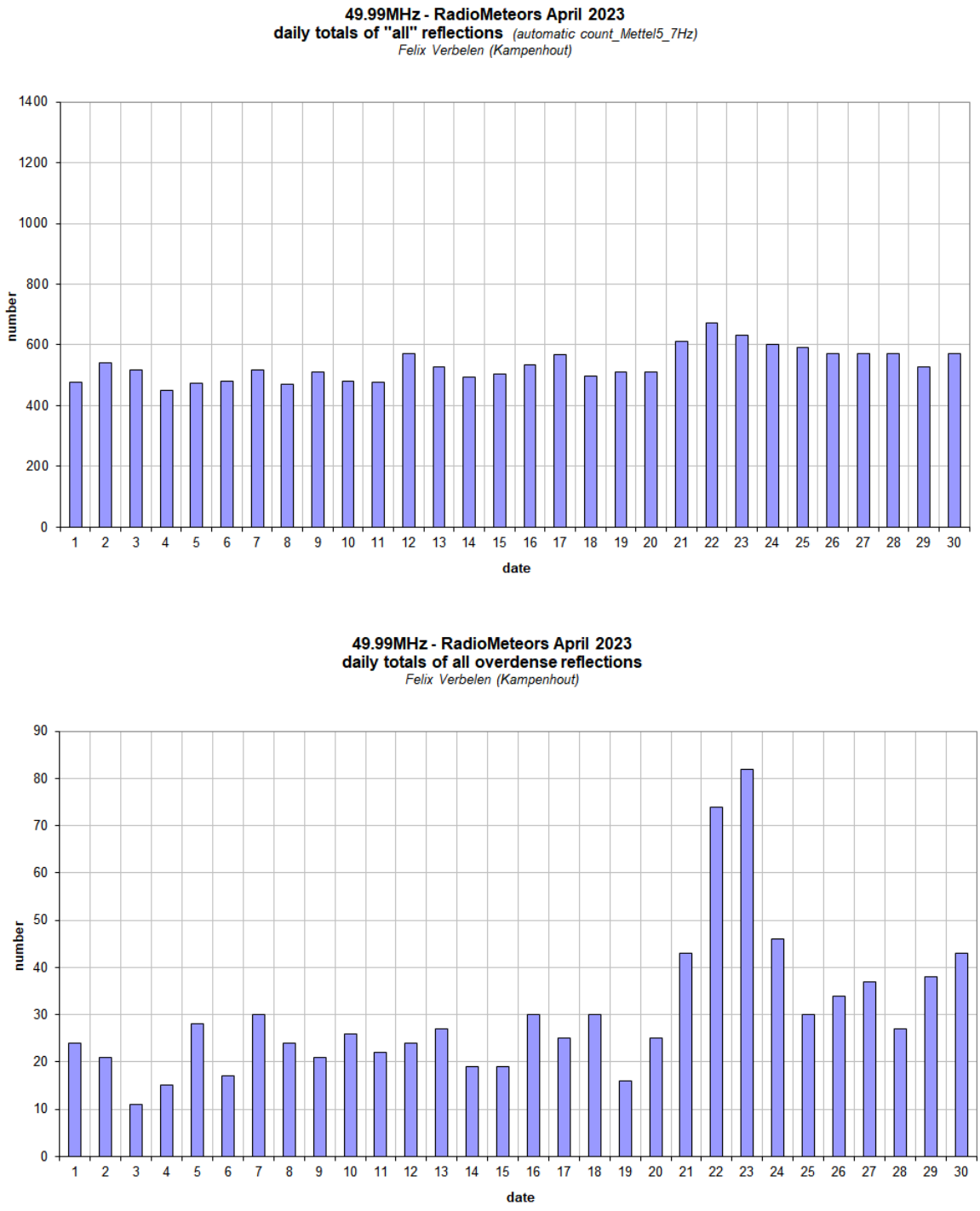

Figure 1 – The daily totals of "all" reflections counted automatically, and of manually counted "overdense" reflections, as observed here at Kampenhout (BE) on the frequency of our VVS-beacon (49.99 MHz) during April 2023.

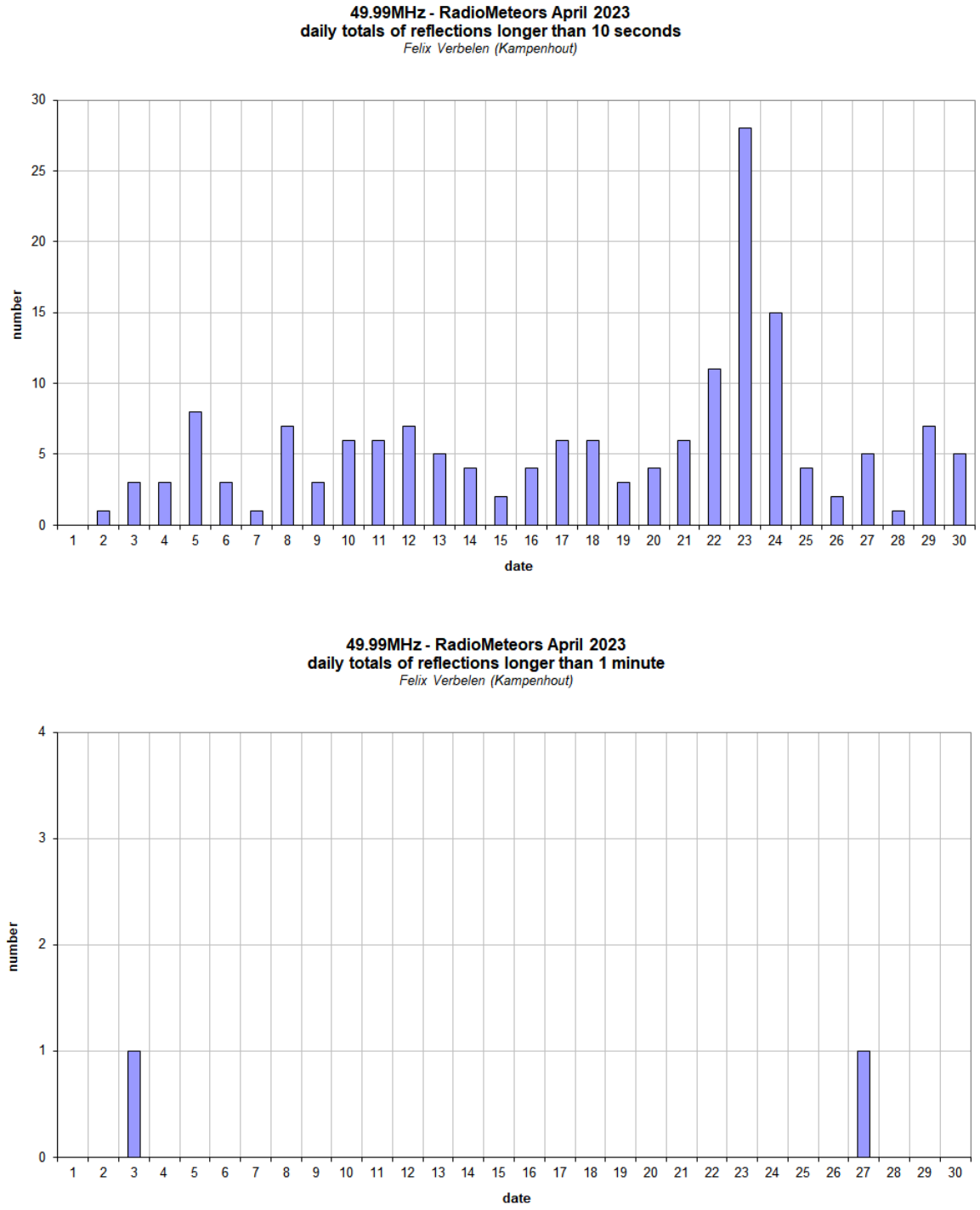

Figure 2 – The daily totals of overdense reflections longer than 10 seconds and longer than 1 minute, as observed here at Kampenhout (BE) on the frequency of our VVS-beacon (49.99 MHz) during April 2023.

 © eMeteorNews

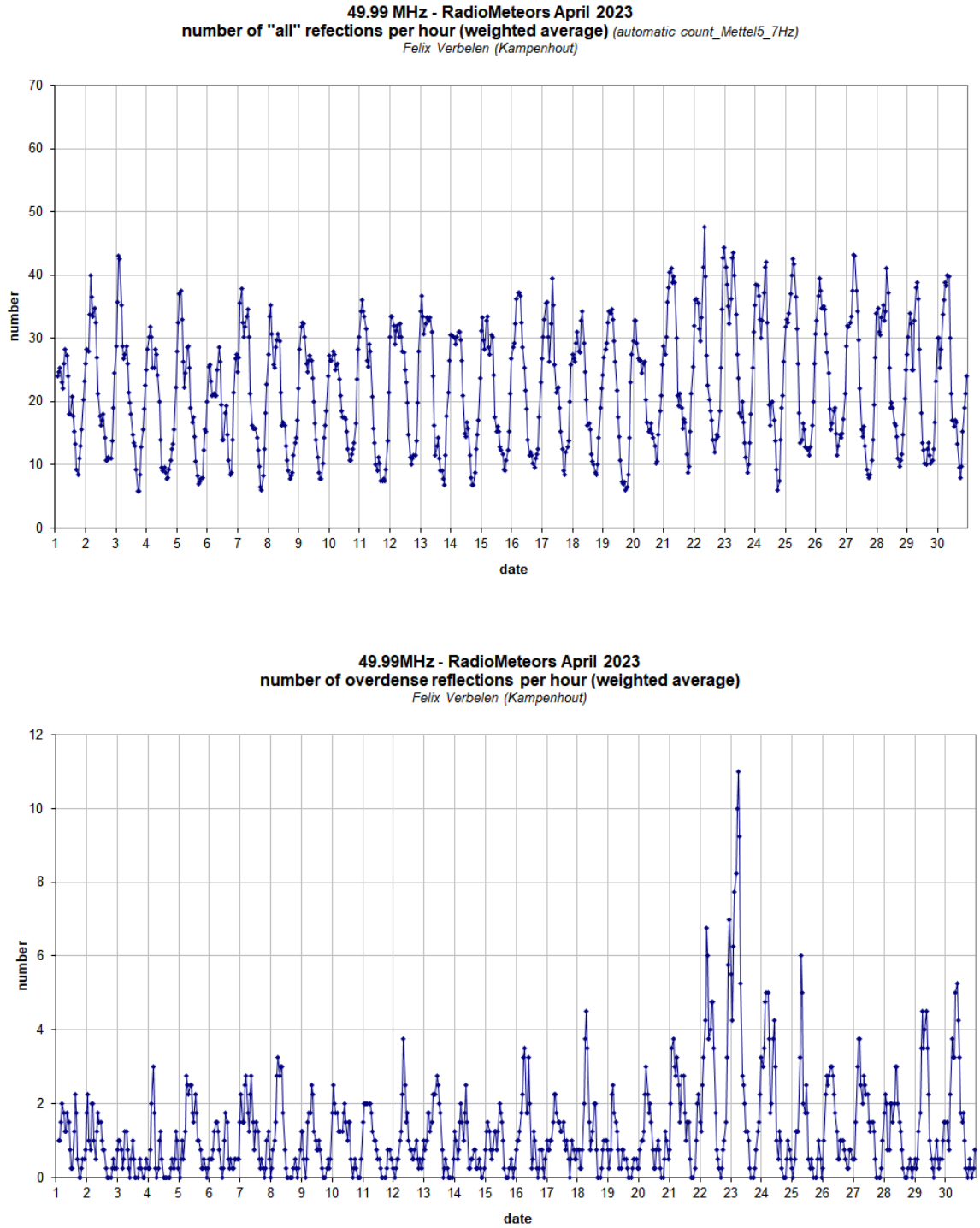

Figure 3 – The hourly numbers of "all" reflections counted automatically, and of manually counted "overdense" reflections, as observed here at Kampenhout (BE) on the frequency of our VVS-beacon (49.99 MHz) during April 2023.

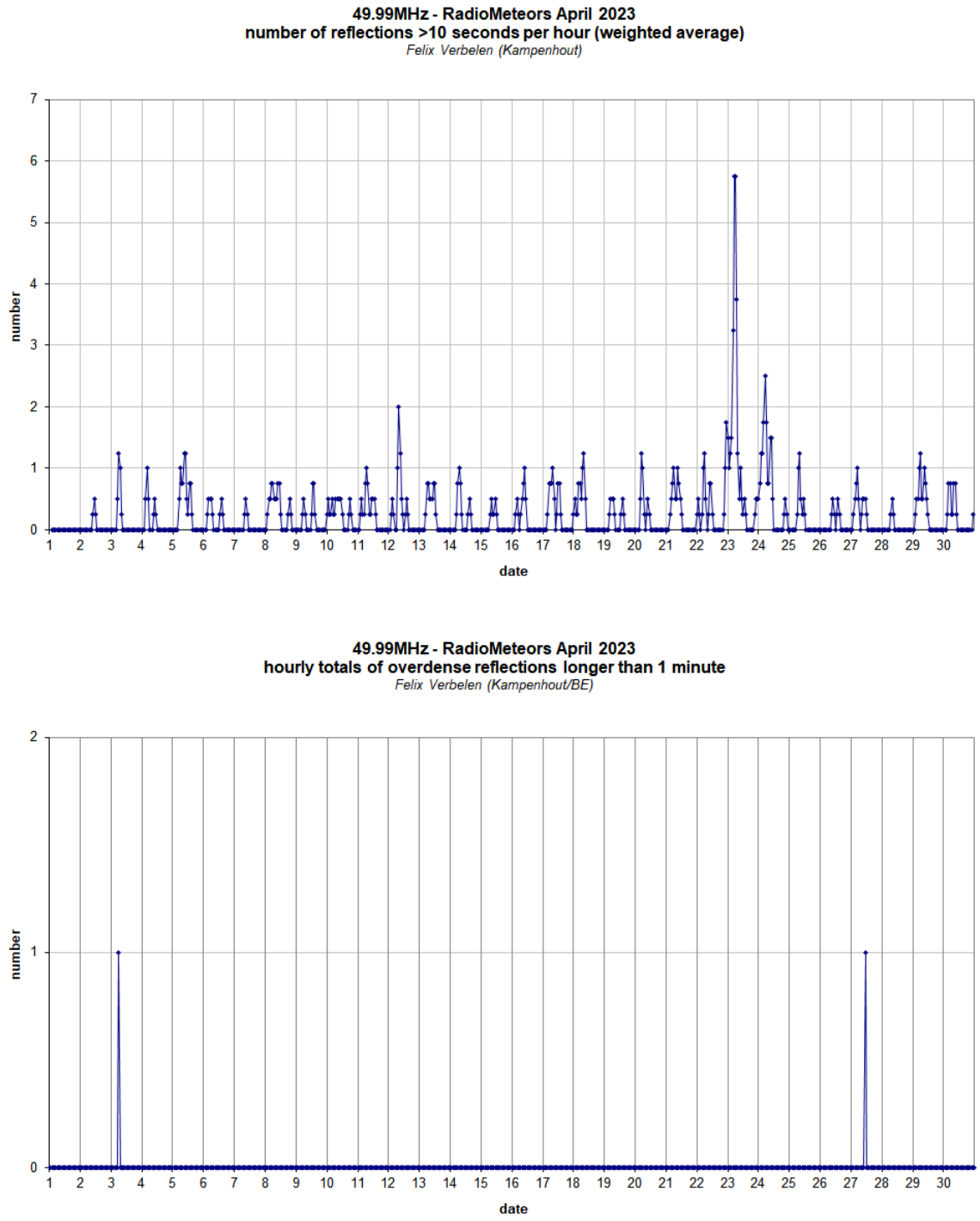

Figure 4 – The hourly numbers of overdense reflections longer than 10 seconds and longer than 1 minute, as observed here at Kampenhout (BE) on the frequency of our VVS-beacon (49.99 MHz) during April 2023.

 © eMeteorNews

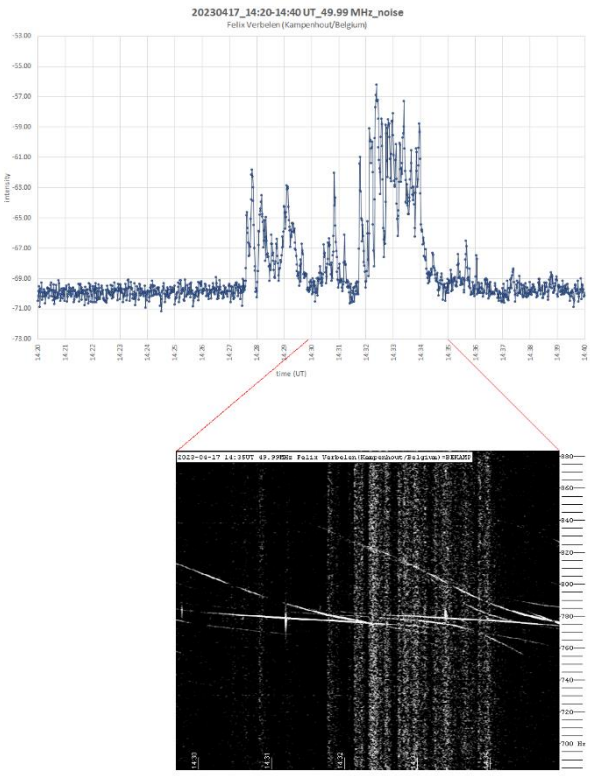

Figure 5 – Solar noise outburst on 17 April 2023.

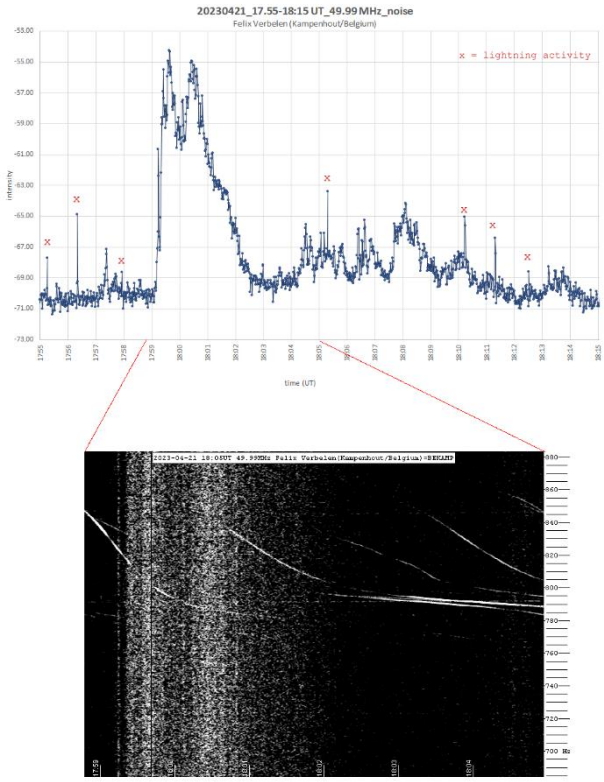

Figure 7 – Solar noise outburst on 21 April 2023.

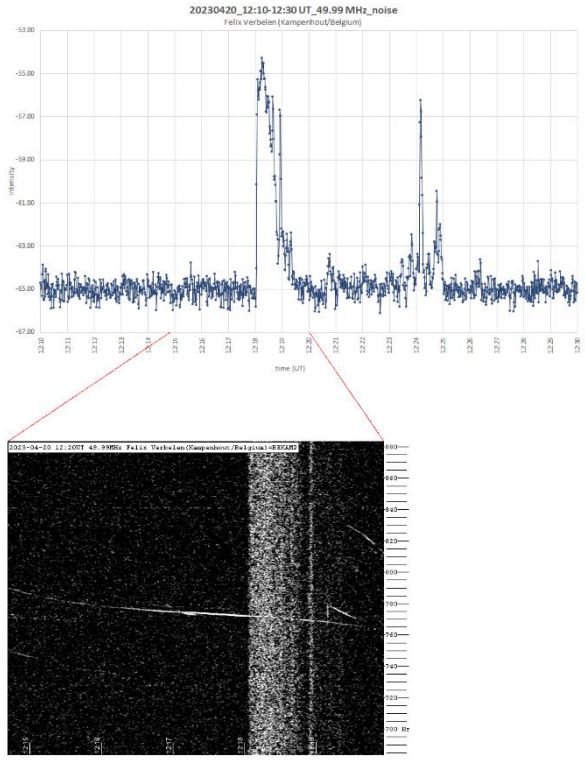

Figure 6 – Solar noise outburst on 20 April 2023.

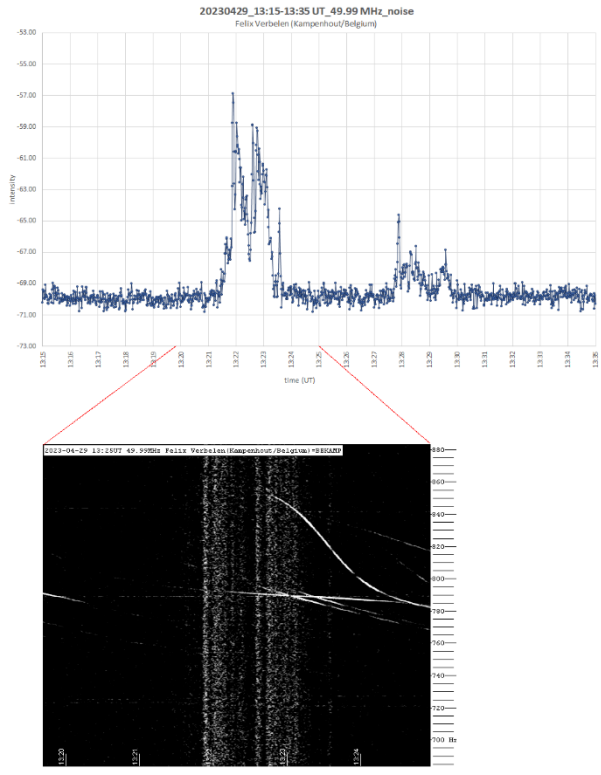

Figure 8 – Solar noise outburst on 17 April 2023.

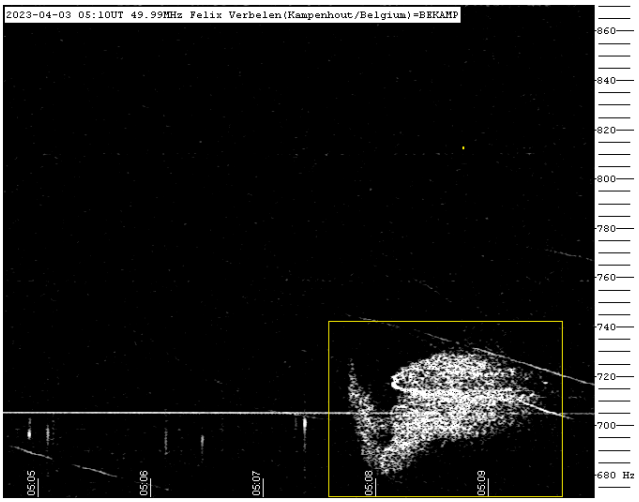

Figure 9 – Meteor echo 3 April 2023, $05^{h}10^{m}$ UT.

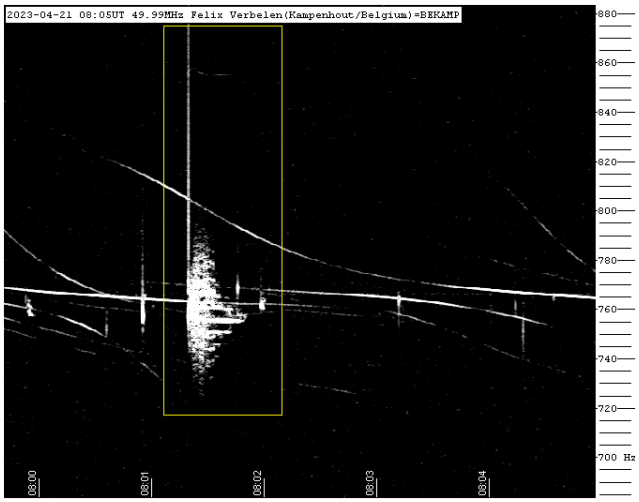

Figure 12 – Meteor echo 21 April 2023, $08^{h}05^{m}$ UT.

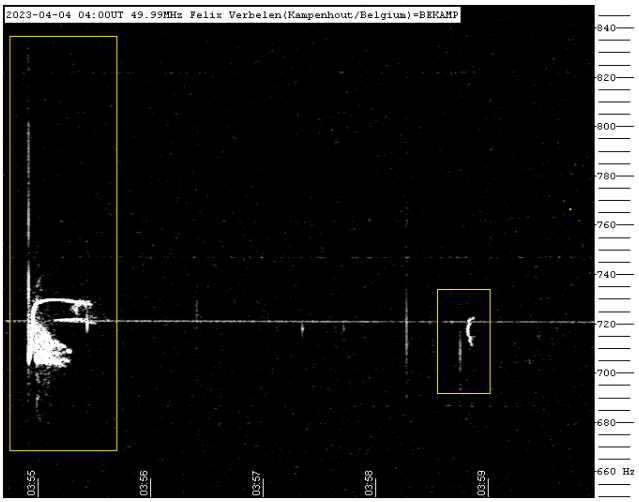

Figure 10 – Meteor echo 4 April 2023, $04^{h}00^{m}$ UT.

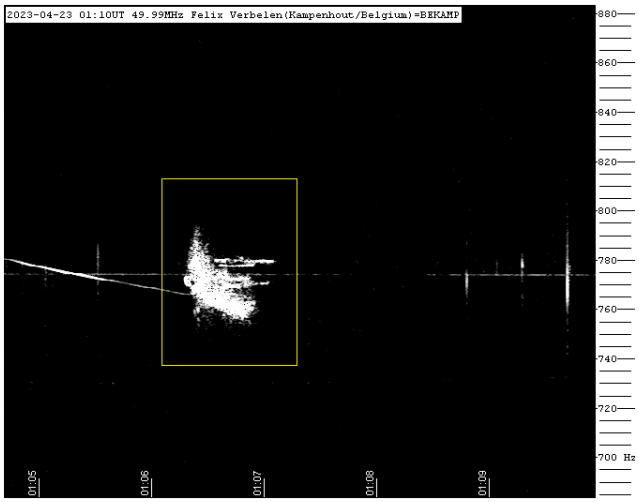

Figure 13 – Meteor echo 23 April 2023, $01^{h}10^{m}$ UT.

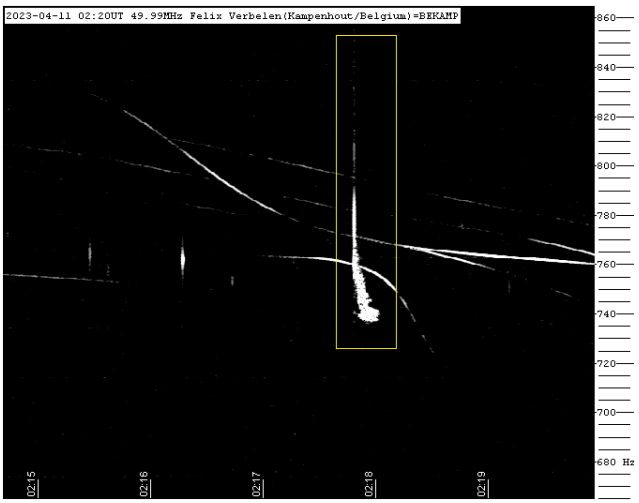

Figure 11 – Meteor echo 11 April 2023, $02^{h}20^{m}$ UT.

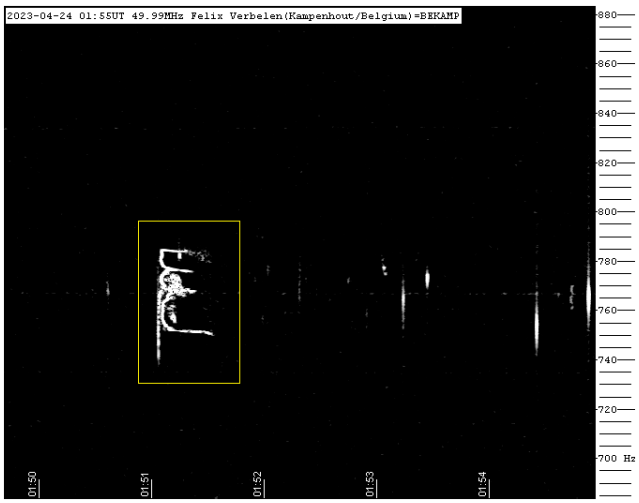

Figure 14 – Meteor echo 24 April 2023, $01^{h}55^{m}$ UT.

© eMeteorNews

Radio meteors May 2023

Felix Verbelen

Vereniging voor Sterrenkunde & Volkssterrenwacht MIRA, Grimbergen, Belgium
felix.verbelen@skynet.be

An overview of the radio observations during May 2023 is given.

1 Introduction

The graphs show both the daily totals (*Figure 1 and 2*) and the hourly numbers (*Figure 3 and 4*) of "all" reflections counted automatically, and of manually counted "overdense" reflections, overdense reflections longer than 10 seconds and longer than 1 minute, as observed here at Kampenhout (BE) on the frequency of our VVS-beacon (49.99 MHz) during the month of May 2023.

The hourly numbers, for echoes shorter than 1 minute, are weighted averages derived from:

$$N(h) = \frac{n(h-1)}{4} + \frac{n(h)}{2} + \frac{n(h+1)}{4}$$

The evolution of the observed meteor activity this month is peculiar which is especially striking in the automatic counts of "all" meteors. On May 13, the number of reflections suddenly drops drastically and remains so on May 14. We see the same on May 22 and 23. Since May 13, the number of reflections remains abnormally low during the day, to show almost normal values during the night.

It was first thought to be a problem with the beacon, but that doesn't seem to be the case. An increased ionization of the D-layer due to the high solar activity could be an explanation, but no direct relationship was found, especially on May 13, 14, 22 and 23. Other causes are still under investigation. The fact is that the low number of reflections was also noticed by other observers of our network.

In the period from May 1 to May 13, lightning activity was recorded on 6 days. It was quite strong on May 4, and on May 5, between 20^h00^m and 21^h00^m UT, the core of a thunderstorm area was directly above the beacon, resulting in many remarkable short reflections (*Figure 7*).

Solar activity produced strong noise almost daily. At our frequency the bursts were mainly of type III and thus relatively short-lived. Some examples are attached (*Figures 5 and 6*).

Especially the eta-Aquariids caused considerable activity in the beginning of the month, which is striking in the counts of the overdense reflections.

Over the entire month, 12 reflections longer than 1 minute were observed. A selection of these is included along with some other interesting "epsilons" (*Figures 8 to 24*). Many more of these are available on request.

In addition to the usual graphs, you will also find the raw counts in cvs-format[6] from which the graphs are derived. The table contains the following columns: day of the month, hour of the day, day + decimals, solar longitude (epoch J2000), counts of "all" reflections, overdense reflections, reflections longer than 10 seconds and reflections longer than 1 minute, the numbers being the observed reflections of the past hour.

[6] https://www.meteornews.net/wp-content/uploads/2023/06/202305_49990_FV_rawcounts.csv

© eMeteorNews

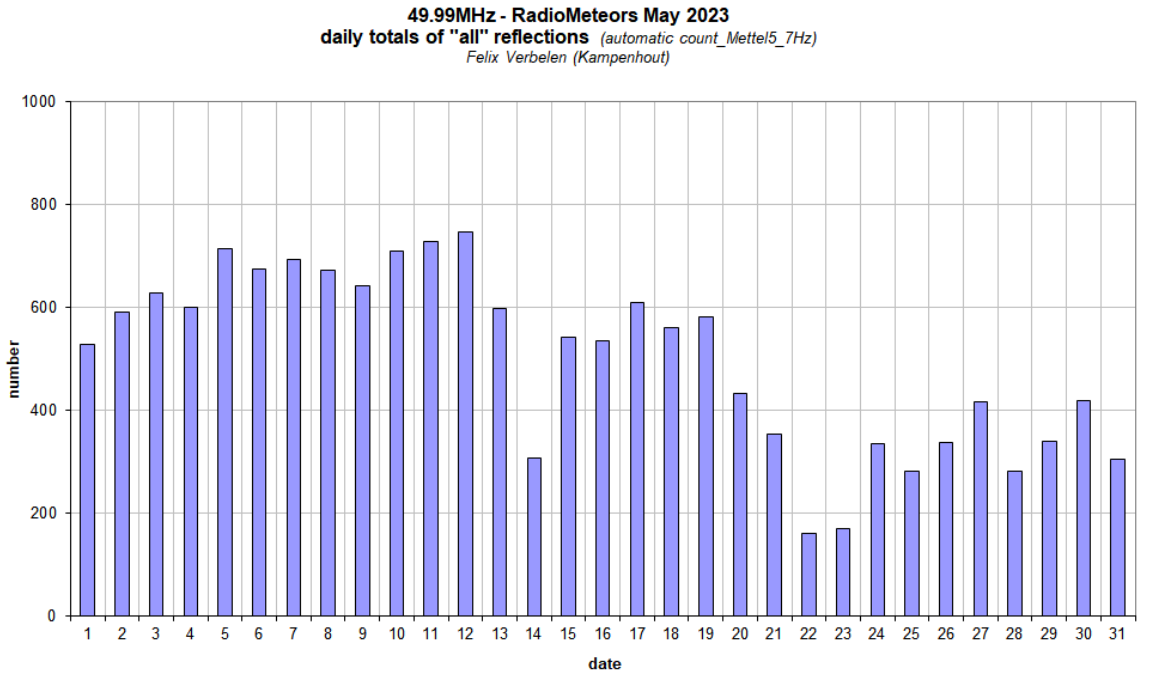

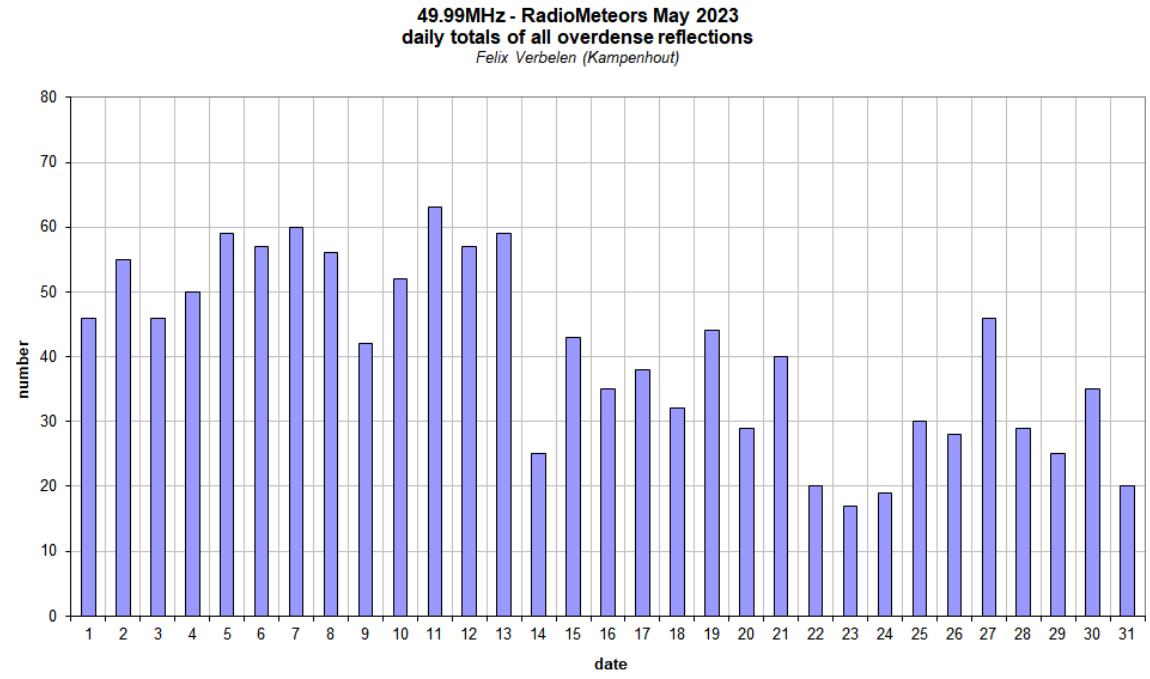

Figure 1 – The daily totals of "all" reflections counted automatically, and of manually counted "overdense" reflections, as observed here at Kampenhout (BE) on the frequency of our VVS-beacon (49.99 MHz) during May 2023.

 © eMeteorNews

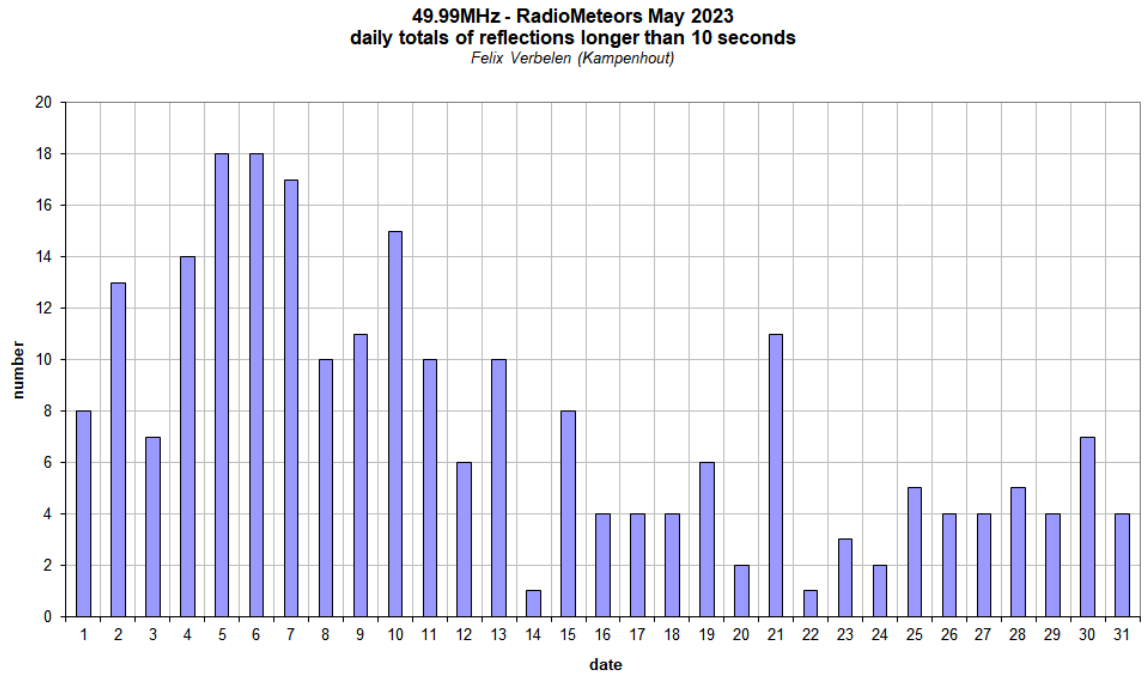

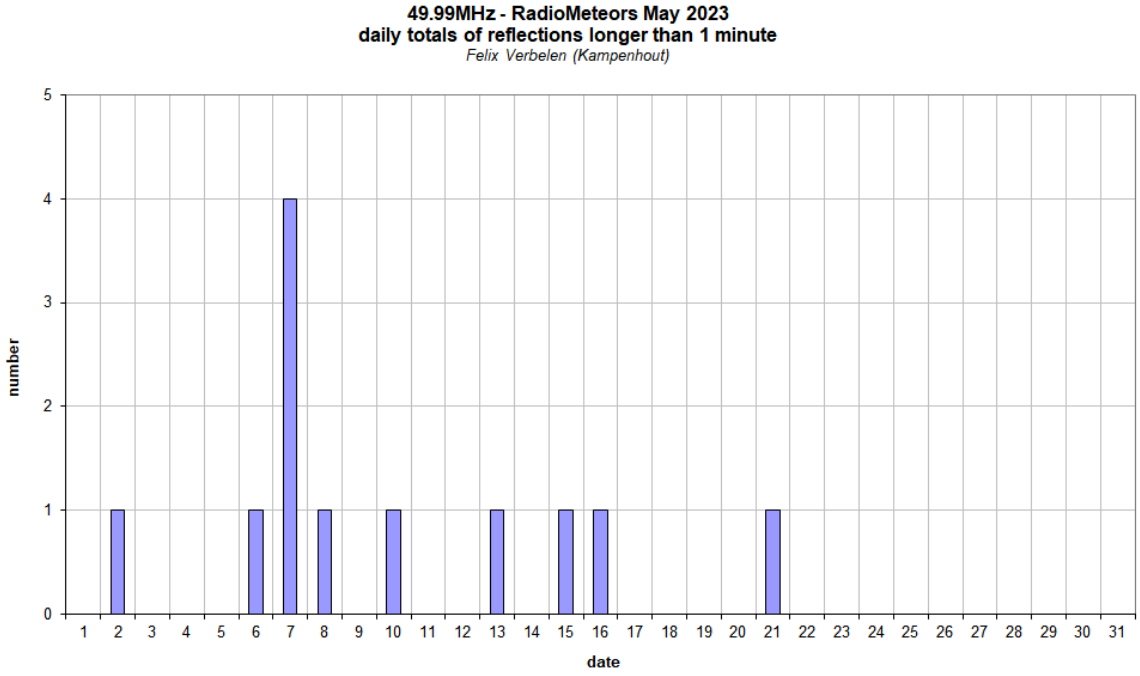

Figure 2 – The daily totals of overdense reflections longer than 10 seconds and longer than 1 minute, as observed here at Kampenhout (BE) on the frequency of our VVS-beacon (49.99 MHz) during May 2023.

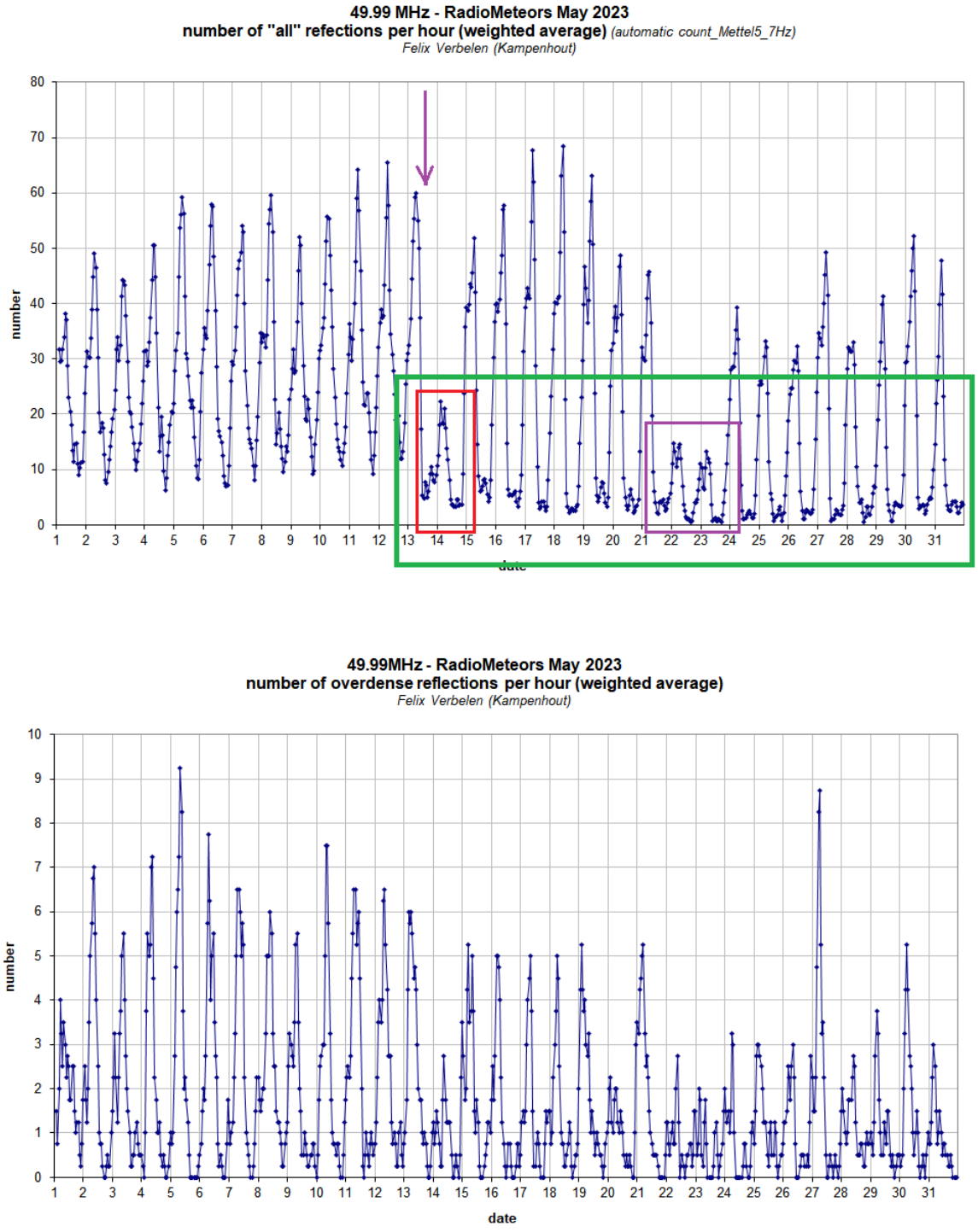

Figure 3 – The hourly numbers of "all" reflections counted automatically, and of manually counted "overdense" reflections, as observed here at Kampenhout (BE) on the frequency of our VVS-beacon (49.99 MHz) during May 2023.

 © eMeteorNews

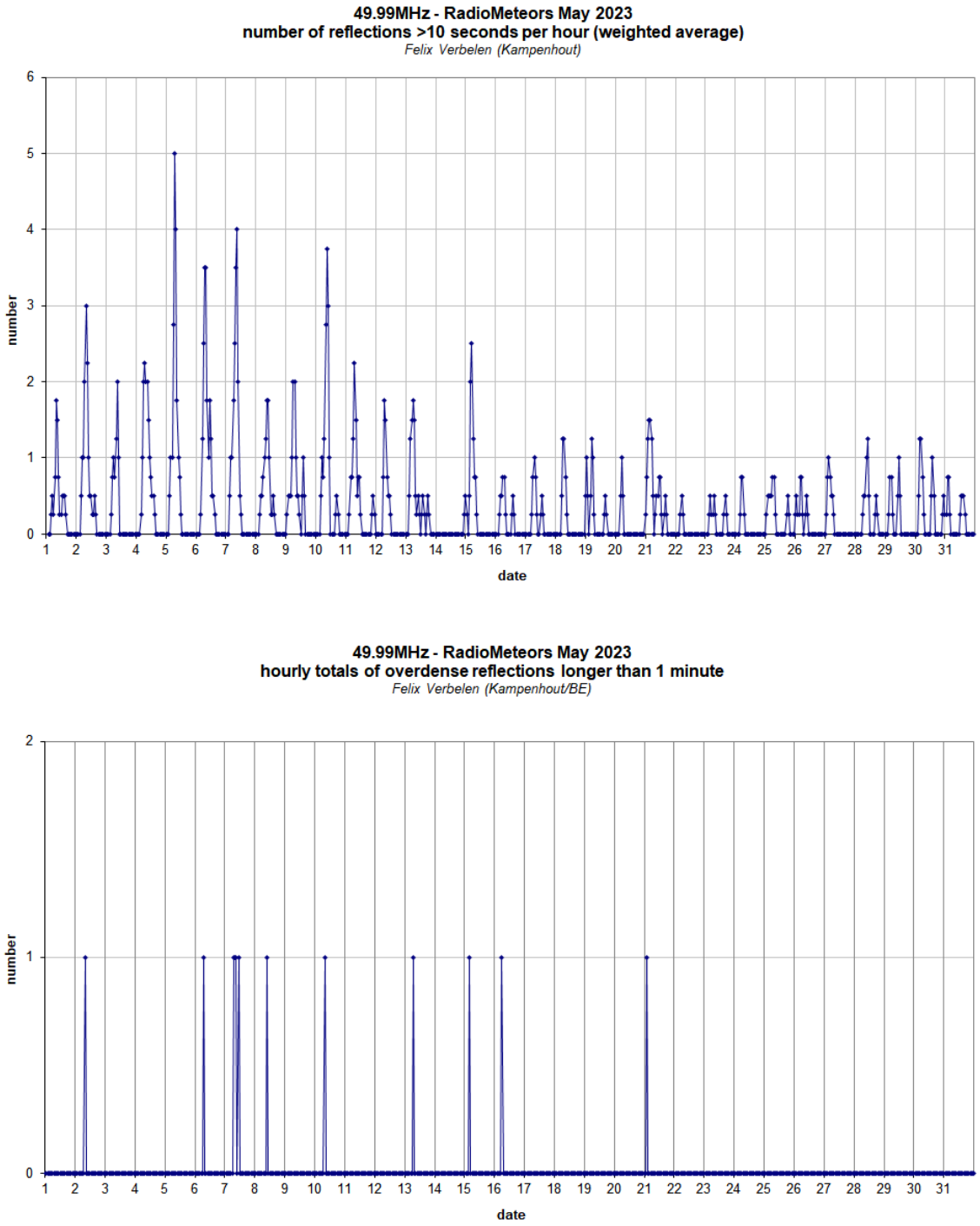

Figure 4 – The hourly numbers of overdense reflections longer than 10 seconds and longer than 1 minute, as observed here at Kampenhout (BE) on the frequency of our VVS-beacon (49.99 MHz) during May 2023.

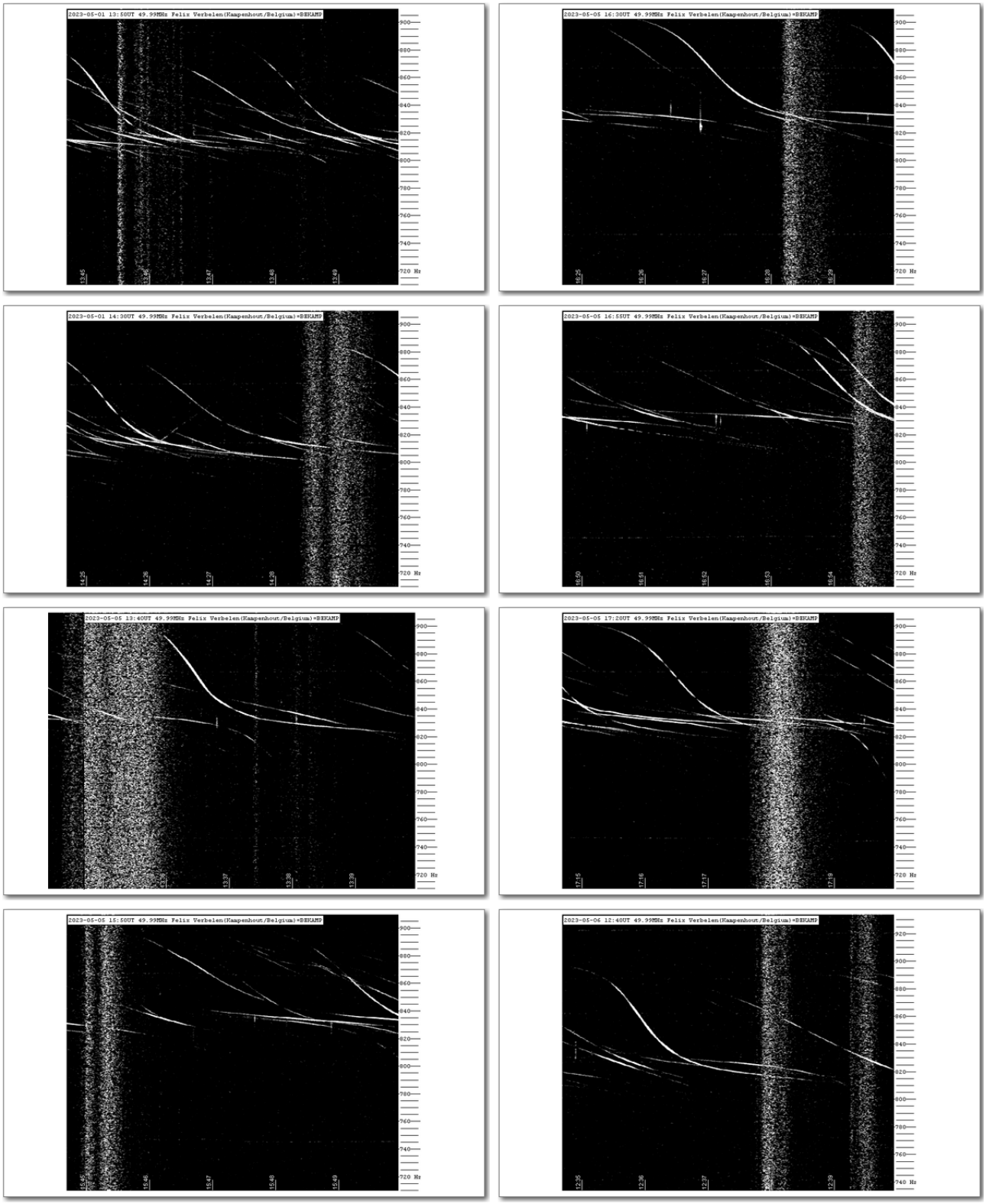

Figure 5 – Solar activity produced strong noise almost daily. At our frequency the bursts were mainly of type III and thus relatively short-lived.

 © eMeteorNews

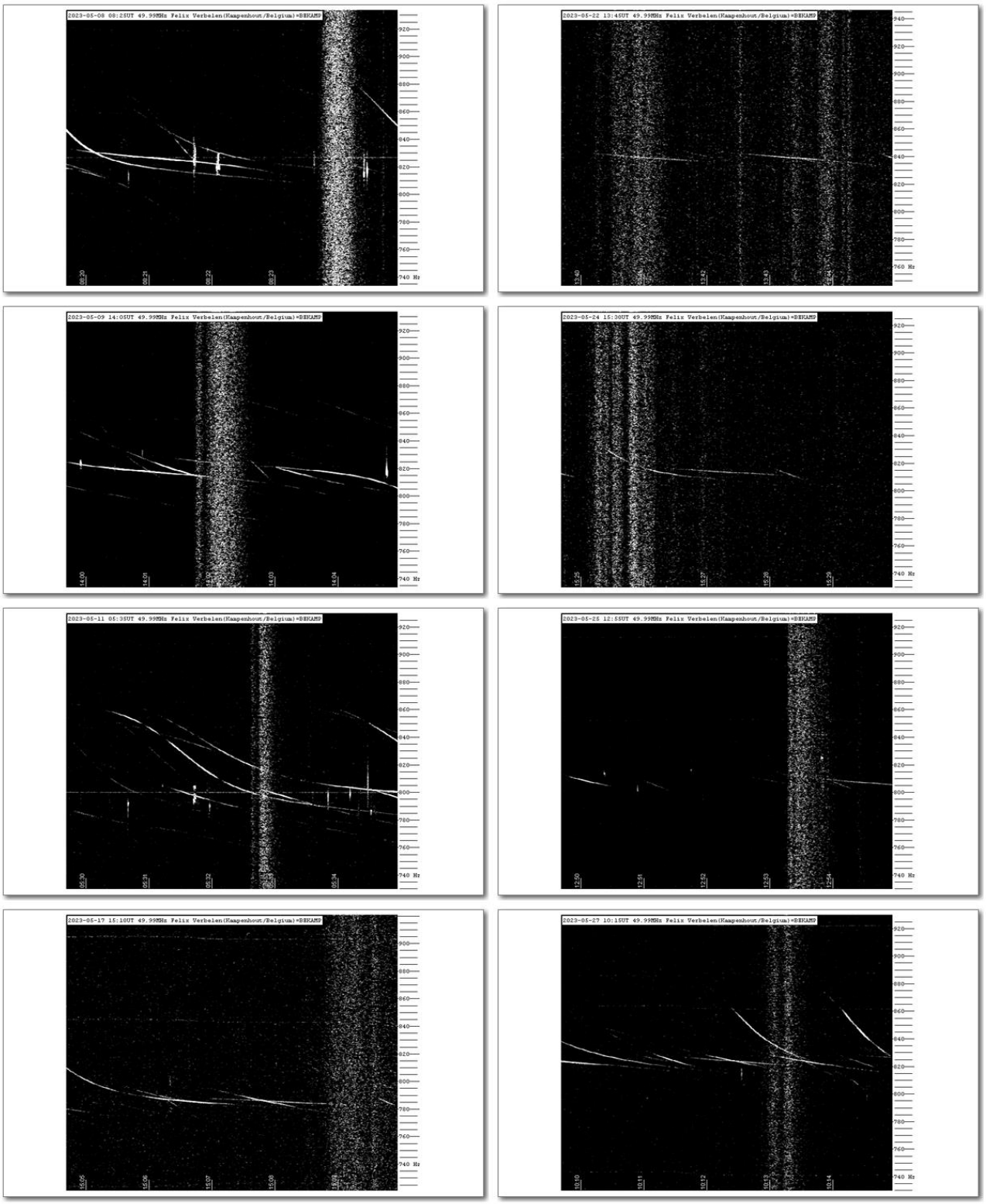

Figure 6 – Solar activity produced strong noise almost daily. At our frequency the bursts were mainly of type III and thus relatively short-lived.

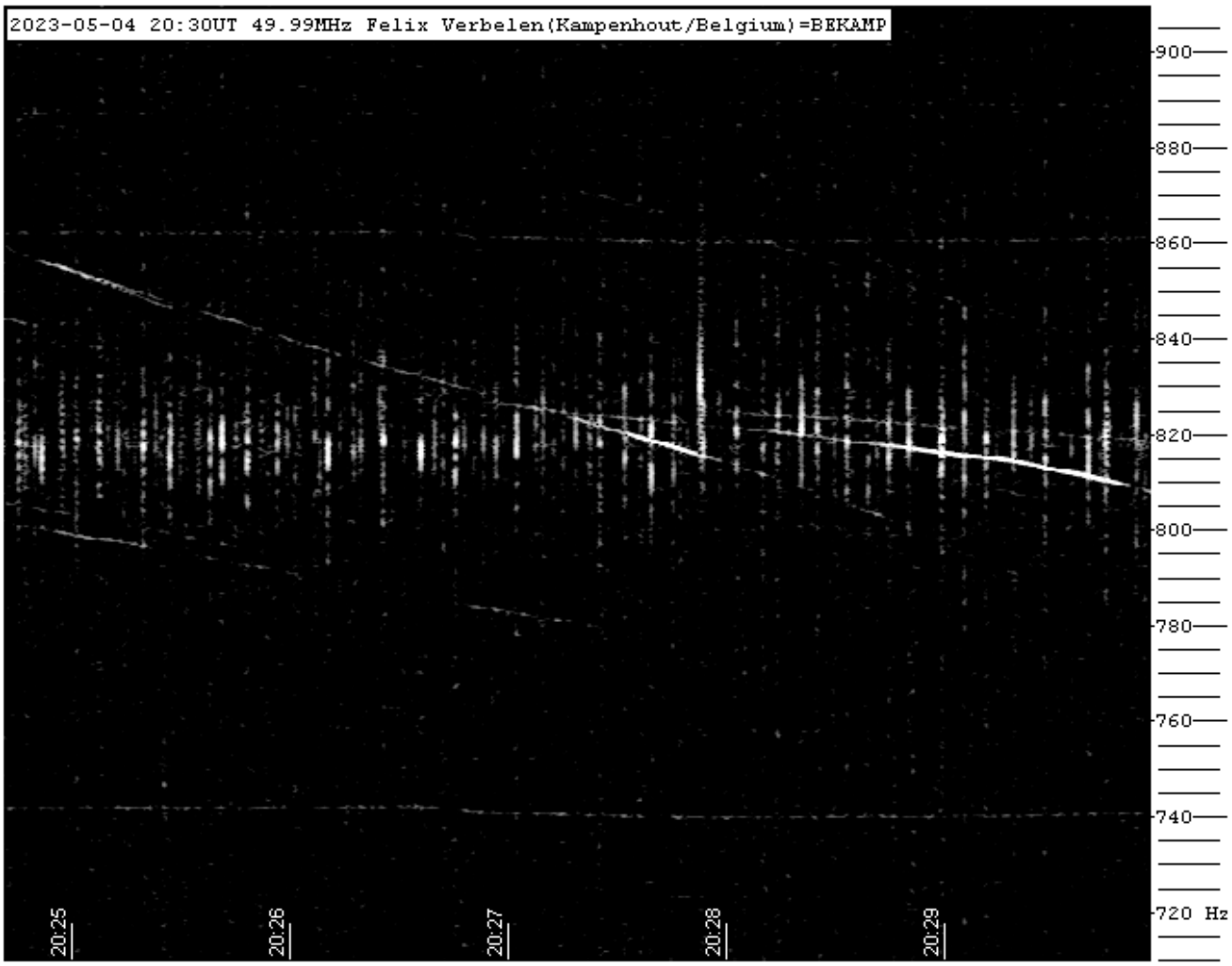

Figure 7 – In the period from May 1 to May 13, lightning activity was recorded on 6 days. It was quite strong on May 4, and on May 5, between 20^h00^m and 21^h00^m UT, the core of a thunderstorm area was directly above the beacon, resulting in many remarkable short reflections.

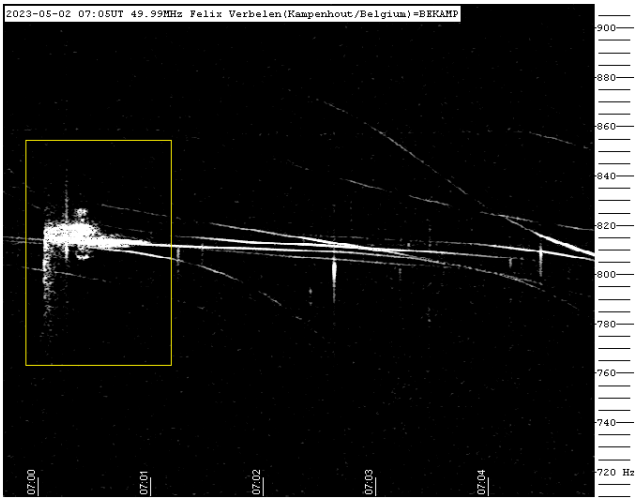

Figure 8 – Meteor echo 2 May 2023, 07^h05^m UT.

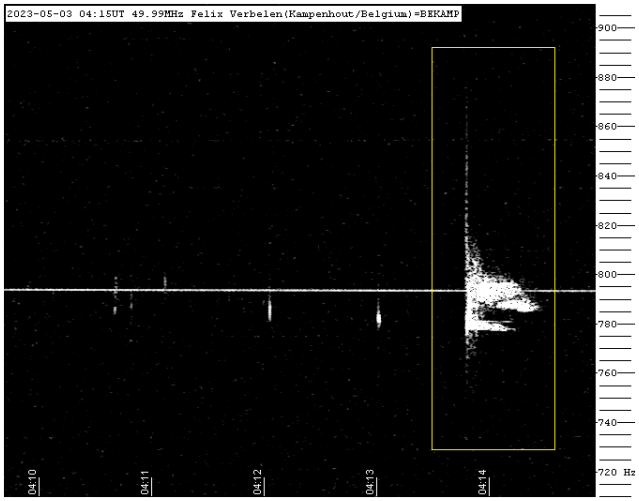

Figure 9 – Meteor echo 3 May 2023, 04^h15^m UT.

 © eMeteorNews

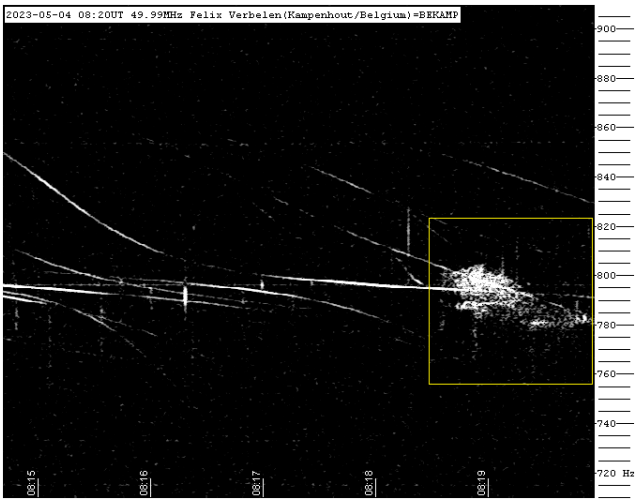

Figure 10 – Meteor echo 4 May 2023, 08^{h}20^{m} UT.

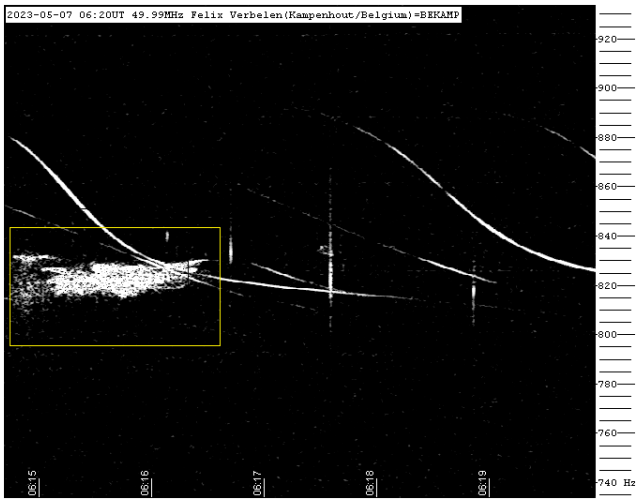

Figure 13 – Meteor echo 7 May 2023, 06^{h}20^{m} UT.

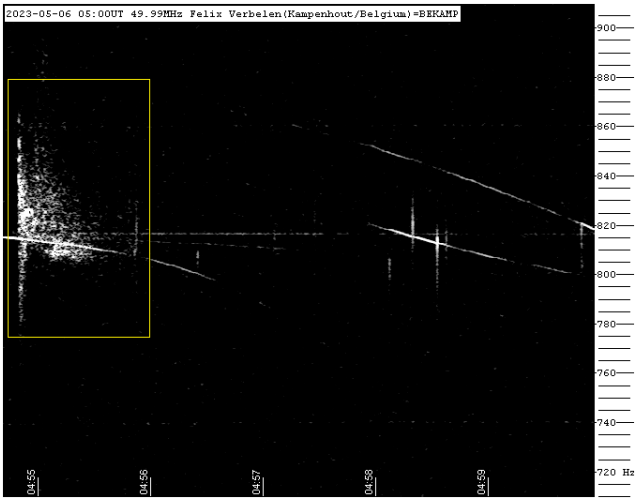

Figure 11 – Meteor echo 6 May 2023, 05^{h}00^{m} UT.

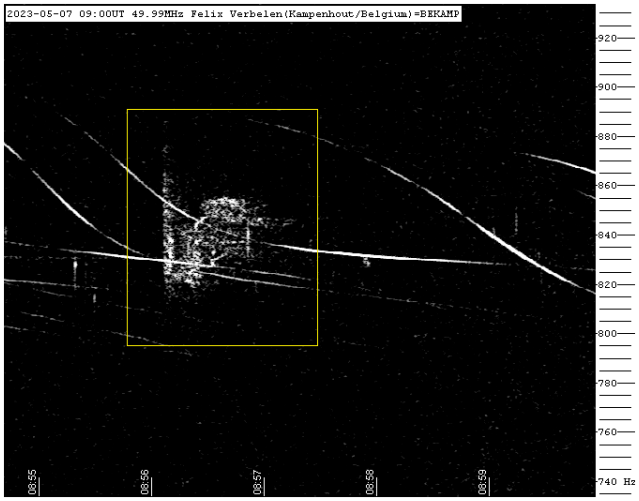

Figure 14 – Meteor echo 7 May 2023, 09^{h}00^{m} UT.

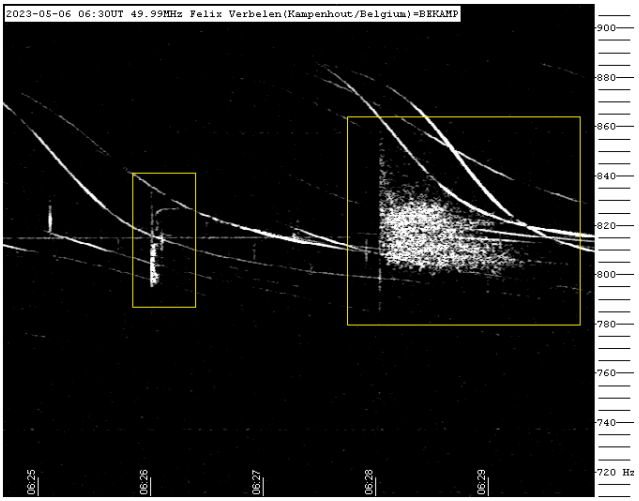

Figure 12 – Meteor echo 6 May 2023, 06^{h}30^{m} UT.

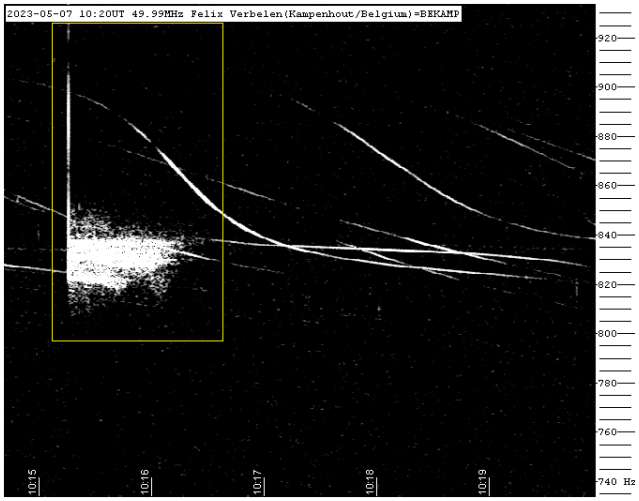

Figure 15 – Meteor echo 7 May 2023, 10^{h}20^{m} UT.

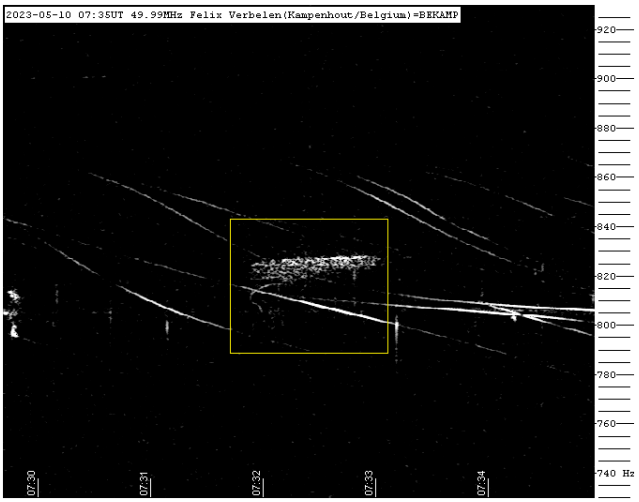

Figure 16 – Meteor echo 10 May 2023, 07^{h}35^{m} UT.

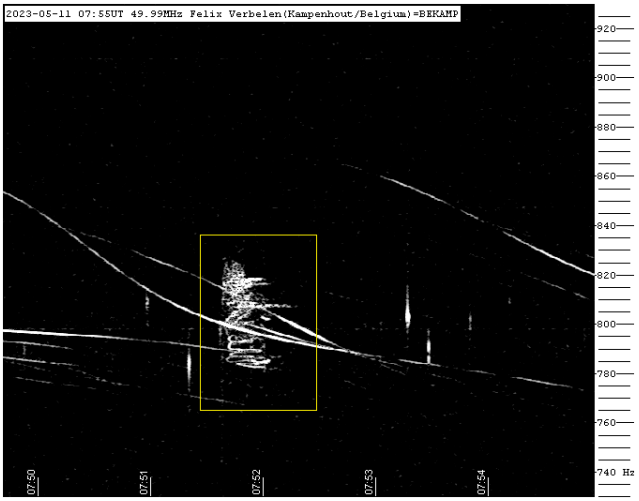

Figure 17 – Meteor echo 11 May 2023, 07^{h}55^{m} UT.

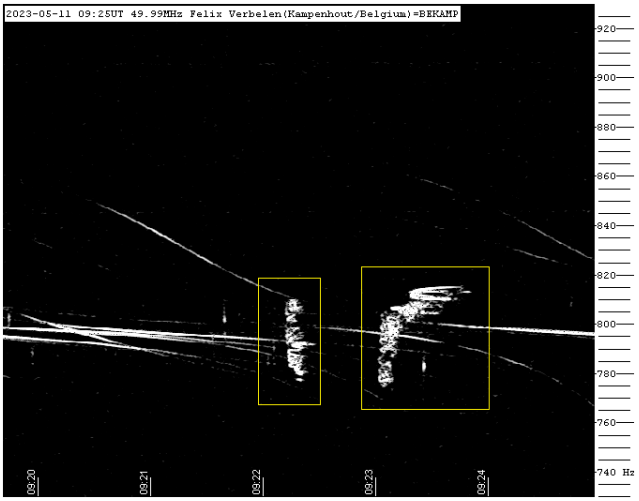

Figure 18 – Meteor echo 11 May 2023, 09^{h}25^{m} UT.

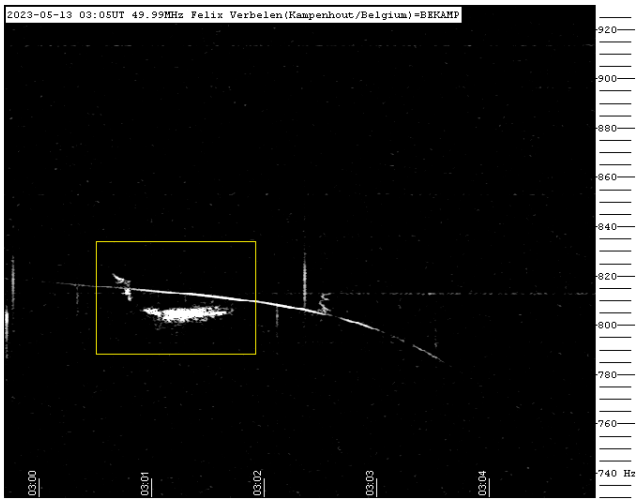

Figure 19 – Meteor echo 13 May 2023, 03^{h}05^{m} UT.

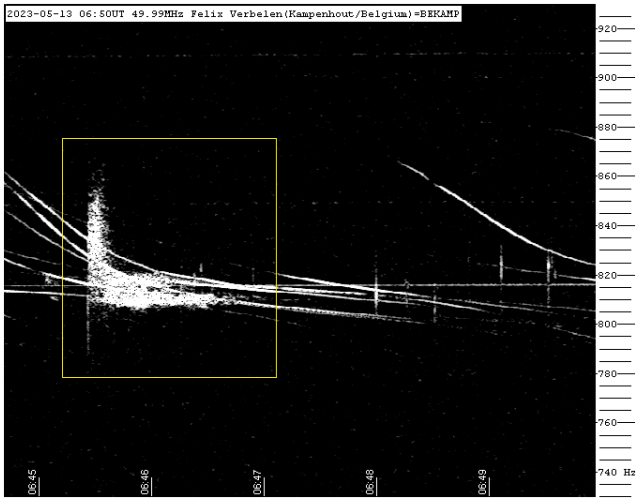

Figure 20 – Meteor echo 13 May 2023, 06^{h}50^{m} UT.

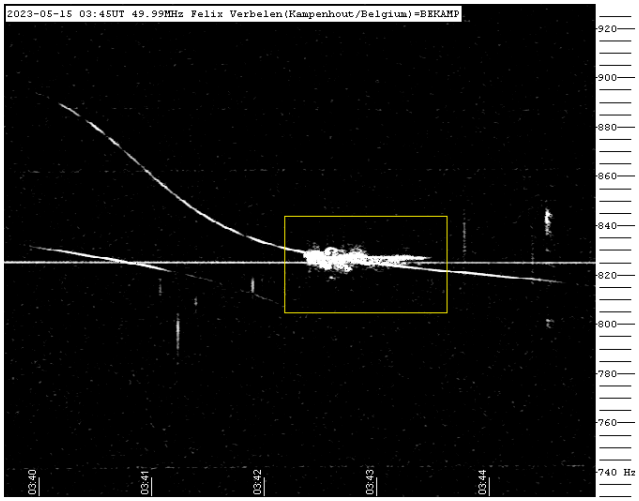

Figure 21 – Meteor echo 15 May 2023, 03^{h}45^{m} UT.

© eMeteorNews

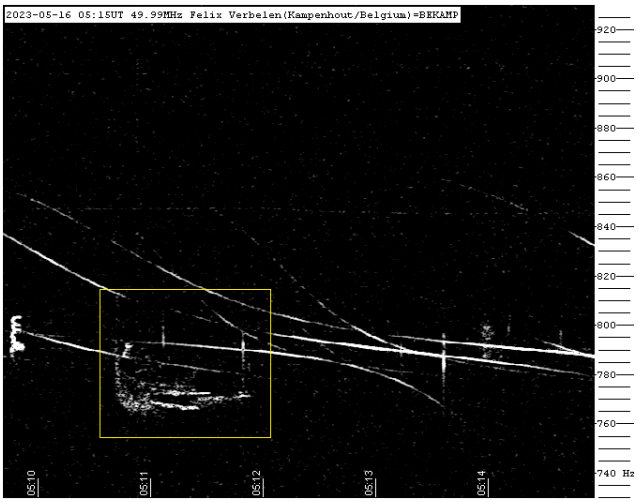

Figure 22 – Meteor echo 16 May 2023, $05^{h}15^{m}$ UT.

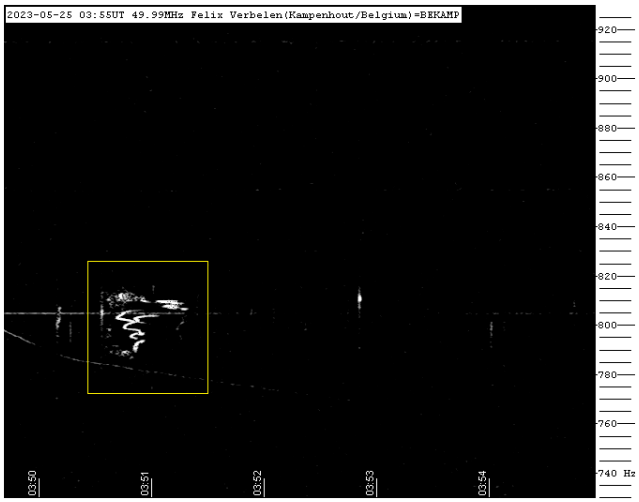

Figure 24 – Meteor echo 25 May 2023, $03^{h}55^{m}$ UT.

Figure 23 – Meteor echo 19 May 2023, $04^{h}05^{m}$ UT.

 © eMeteorNews

The mission of MeteorNews is to offer fast meteor news to a global audience, a swift exchange of information in all fields of active amateur meteor work without editing constraints. MeteorNews is freely available without any fees. To receive a notification: https://www.meteornews.net/newsletter-signup/.

You are welcome to contribute to MeteorNews on a regular or casual basis, if you wish to. Anyone can become an author or editor, send an email to us. For more info read: https://meteornews.net/writing-content-for-emeteornews/

MeteorNews account manager: Richard Kacerek rickzkm@gmail.com.

The running costs for website hosting are covered by a team of sponsors. We want to thank the 2022-2023 sponsors: Anonymous (3x), Mikhail Bidnichenko, Gaetano Brando, TomB, Trevor C, Nigel Cunnington, Richard Glassner, Kevin Heider, Paul Hyde, K. Jamrogowicx, Dave Jones, Richard Kacerek, Richard Lancaster, Joseph Lemaire, Mark McIntyre, Hiroshi Ogawa, Paul Mohan, Stan Nelson, Lubos Neslusan, BillR, Whitham D. Reeve, John Schlin, Ann Schroyens and Denis Vida.

Financial support is still needed and welcome: https://www.justgiving.com/crowdfunding/meteor-news?utm_term=JJBjmJpzV

Contributing to this issue:

- Bassa C.
- Dijkema T. J.
- Eschman P.
- Johannink C.
- Kacerek R.
- Koseki M.
- Maslov M.
- Moskovitz N.
- Roggemans P.
- Šegon D.
- Verbelen F.
- Vida D.

ISSN 2570-4745 Online publication https://meteornews.net

Listed and archived with ADS Abstract Service: https://ui.adsabs.harvard.edu/search/q=eMetN

MeteorNews Publisher:

Valašské Meziříčí Observatory, Vsetínská 78, 75701 Valašské Meziříčí, Czech Republic

Copyright notices © 2023: The copyright of articles submitted to eMeteorNews remains with the authors